

**GUT REGION-SPECIFIC INTERLEUKIN 1 $\beta$  INDUCTION AND  
NLRP3 DOWNREGULATION IN THE MYENTERIC NEURONS OF  
A STREPTOZOTOCIN-INDUCED DIABETIC RAT MODEL**

PhD thesis

**Afnan Mohammad Rashed AL Doghmi**

Supervisor

Dr. Nikolett Bódi

Associate Professor

Doctoral School of Biology

Department of Physiology, Anatomy and Neuroscience

Faculty of Science and Informatics

University of Szeged



2024

Szeged

*Dedication*

*Dedicated to my first teacher; my beloved mother Ameena ALDughmi*

إهداء

إهداء إلى معلمتي الأولى...والدتي الحبيبة أمينة الدغمي

## TABLE OF CONTENTS

<b>ABBREVIATIONS</b> .....	3
<b>1. INTRODUCTION</b> .....	5
1.1. The enteric nervous system: Basic structure and function .....	5
1.2. Morphological classification of enteric neurons .....	6
1.3. Functional and neurochemical classification of enteric neurons .....	8
1.4. Diabetes mellitus .....	10
1.5. Diabetic gastroenteropathy .....	12
1.6. Inflammatory cytokines in type 1 diabetes .....	15
1.6.1. The role of tumour necrosis factor.....	15
1.6.2. The role of interleukin 1 $\beta$ .....	19
1.6.3. The role of inflammasomes .....	22
<b>2. AIMS</b> .....	25
<b>3. MATERIALS AND METHODS</b> .....	27
3.1. Animal models .....	27
3.2. Blood sampling and tissue handling .....	27
3.3. Double-labelling fluorescent immunohistochemistry .....	28
3.4. Post-embedding immunohistochemistry .....	29
3.5. Measurement of tissue and serum interleukin 1 $\beta$ concentrations .....	30
3.6. Bradford protein micromethod for the determination of tissue protein content .....	30
3.7. RNAscope multiplex fluorescent V2 assay .....	31
3.8. Statistical analysis .....	31
<b>4. RESULTS</b> .....	32
4.1. Physiological parameters of experimental animals .....	32
4.1.1. Acute diabetic rat model .....	32
4.1.2. Chronic diabetic rat model .....	32
4.2. Effect of acute and chronic hyperglycaemia on the proportion of interleukin 1 $\beta$ -immunoreactive myenteric neurons .....	33
4.2.1. Acute diabetic rat model .....	33
4.2.2. Chronic diabetic rat model .....	36
4.3. Effect of chronic hyperglycaemia on the proportion of interleukin 1 $\beta$ - immunoreactive nNOS neurons .....	39

4.4.	Effect of chronic hyperglycaemia on the proportion of interleukin 1 $\beta$ -immunoreactive CGRP neurons .....	43
4.5.	Effect of hyperglycaemia on interleukin 1 $\beta$ protein levels .....	46
4.5.1.	Tissue level of interleukin 1 $\beta$ in colonic muscle/myenteric plexus homogenates .....	46
4.5.2.	Levels of interleukin 1 $\beta$ in the pancreatic tissue and serum .....	46
4.6.	Effect of chronic hyperglycaemia on the expression of interleukin 1 $\beta$ mRNA .....	48
4.7.	NLRP3 immunoreactivity and localization in the myenteric neurons .....	53
4.8.	Quantitative evaluation of NLRP3 density within the myenteric ganglia .....	54
4.9.	Effect of chronic hyperglycaemia on the expression of NLRP3 mRNA .....	56
<b>5.</b>	<b>DISCUSSION</b> .....	<b>60</b>
<b>6.</b>	<b>THESIS MAIN FINDINGS</b> .....	<b>69</b>
<b>7.</b>	<b>ACKNOWLEDGMENT</b> .....	<b>70</b>
<b>8.</b>	<b>REFERENCES</b> .....	<b>72</b>
<b>9.</b>	<b>SUMMARY</b> .....	<b>90</b>
<b>10.</b>	<b>ÖSSZEFOGLALÁS</b> .....	<b>94</b>
<b>11.</b>	<b>LIST OF PUBLICATIONS</b> .....	<b>98</b>

## ABBREVIATIONS

ALR	absent in melanoma 2-like receptor
AP-1	activator protein-1
ASC	adaptor protein apoptosis-associated speck-like protein containing a caspase-activation and recruitment domain
ATP	adenosine triphosphate
BIR	baculovirus inhibitor of apoptosis protein repeat
BSA	bovine serum albumin
CARD	caspase-activation and recruitment domain
CGRP	calcitonin gene-related peptide
ChAT	choline acetyltransferase
DAMPs	danger-associated molecular patterns
ELISA	enzyme-linked immunosorbent assay
ENS	enteric nervous system
IL1Ra	interleukin 1 receptor antagonist
IL1RAcP	interleukin 1 receptor-associated protein
IL1RI	interleukin 1 receptor I
IL1 $\beta$	interleukin 1 beta
IPANs	intrinsic primary afferent neurons
IR	immunoreactive
IRAK4	interleukin 1 receptor activated protein kinase 4
JNK	c-Jun N-terminal kinase
LRRs	leucine-rich repeats
MAPK	mitogen-activated protein kinase
MUC-SUBMUC-SP	mucosa-submucosa-submucous plexus
MUSCLE-MP	smooth muscle-myenteric plexus
MYD88	myeloid differentiation primary response 88
NBD	nucleotide-binding domain
NF $\kappa$ B	nuclear factor kappa-light-chain-enhancer of activated B cells
NLR	nucleotide-binding domain and leucine-rich repeat receptor/NOD-like receptor

NLRP3	NOD-, LRR- and pyrin domain-containing protein 3
nNOS	neuronal nitric oxide synthase
NO	nitric oxide
PAMPs	pathogen-associated molecular patterns
PB	phosphate buffer
PIAS1	protein inhibitor of activated signal transducer and activator of transcription 1
PRRs	pattern recognition receptors
PYD	pyrin domain
RNAscope	RNAscope multiplex fluorescent V2 assay
ROS	reactive oxygen species
STZ	streptozotocin
T1D	type 1 diabetes
T2D	type 2 diabetes
TBS	tris(hydroxymethyl)aminomethane-buffered saline
TIR	Toll-and interleukin 1 receptor-like
TLR4	Toll-like receptor 4
TNFR1	tumour necrosis factor receptor 1
TNFR2	tumour necrosis factor receptor 2
TNF $\alpha$	tumour necrosis factor alpha
TRAF6	tumour necrosis factor-associated factor 6

## 1. INTRODUCTION

### 1.1. The enteric nervous system: Basic structure and function

The term “enteric nervous system” (ENS) was first introduced in the early 20<sup>th</sup> century by the British physiologist John N. Langley as one of the three distinct divisions of the autonomic nervous system: sympathetic, parasympathetic, and enteric nervous system (Langley 1921). The ENS refers to the extensive intrinsic neuronal innervations within the gastrointestinal wall, spanning from the oesophagus to the anus (Gabella 1990). Although these neurons have been thought to have originated solely from the neural crest during embryogenesis, new evidence revealed the involvement of cells derived from the endoderm and mesoderm (Brokhman et al. 2019, Subhash et al. 2023). The number of enteric neurons is close to the number of neurons in the spinal cord and therefore corresponds to the size and complexity of the species. For instance, adult humans have 200-600 million neurons in their ENS, while mice enteric neurons are estimated to be around 1.2 million (Furness et al. 2014, Michel et al. 2022). These neurons aggregate together (with the nourishing glial cells) into discrete units that are interconnected by bundles of nerve processes forming ganglionated plexuses. The two main ganglionated plexuses that give rise to the ENS are the myenteric plexus (*Auerbach's* plexus) and the submucous plexus (*Meissner's* plexus). The myenteric plexus lies between the longitudinal and circular smooth muscle layers of the intestinal muscularis externa and mainly regulates gut motility. The submucous plexus is embedded within the submucosa and works as a regulator for secretion, blood flow, and mechanosensory functions (Figure 1, Furness & Costa 1980).

Due to its location within the gastrointestinal layers, the ENS is in constant interaction with different parts of the gastrointestinal tract including gut microbiota (Hyland et al. 2016). Therefore, the ENS has developed a complex system of dynamicity that not only regulates digestive function but also has key roles in regulating the immune system through the communication with gut microbiota. The ENS also communicates with the central nervous system through the vagus nerve and together with the gut microbiota form the so-called microbiota-gut-brain axis (Carabotti et al. 2015). However, the ENS is able form neural circuits that can still function even in the absence of central innervations (De Giorgio et al. 1996). This is due to the presence of intrinsic primary afferent neurons (IPANs) that can sense the physical and chemical states in the gut lumen. IPANs transduce gut stimuli into other sensory, motor, and interneurons to exert their

response function, forming an independent neural microcircuit of the gut which is referred to as the second brain (Furness 2000, Avetisyan et al. 2015). Within this neural microcircuit, diverse populations of neurons exist that differ in their morphology, neurochemical phenotypes, and consequently their function (Wood 1994, Furness 2000, Hansen 2003). The percentage of the different neuronal populations also varies from one intestinal segment to another in health as well as in different pathological conditions (Bo et al. 1999, Bódi et al. 2019, Bagyánszki & Bódi 2023).

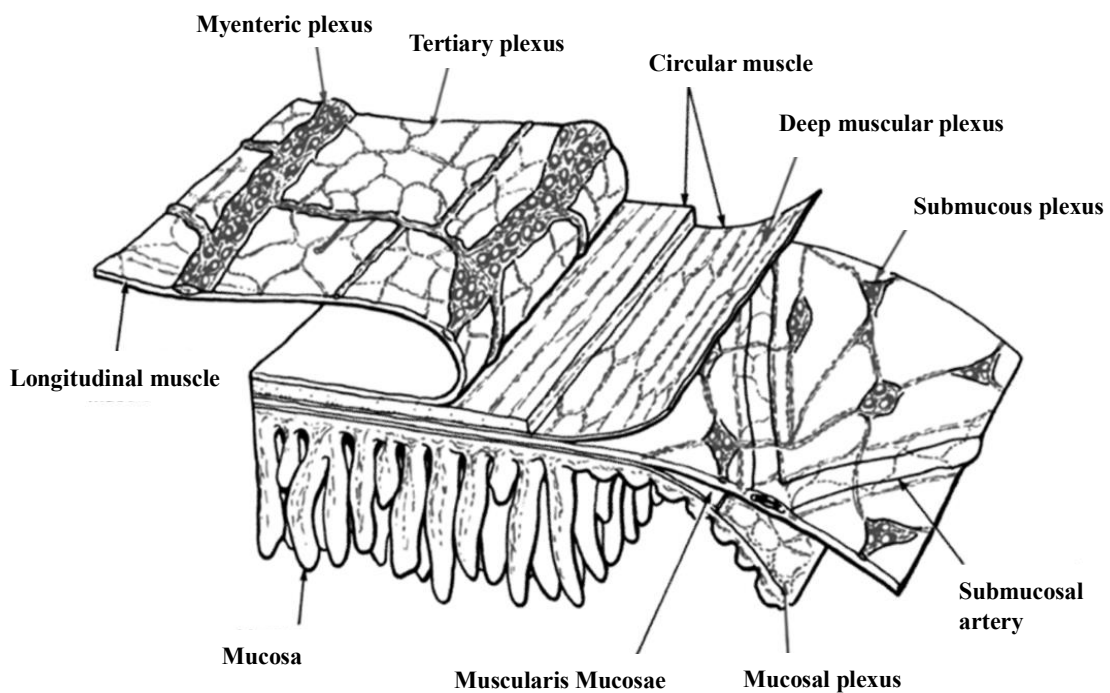


**Figure 1. Enteric ganglia within the gut layers.** The main ganglionated plexuses are myenteric and submucous plexuses. The myenteric ganglia are larger and contain more neurons compared to those in the submucosa (Furness & Costa 1980).

## 1.2. Morphological classification of enteric neurons

Contemporary classification of enteric neurons based on their morphology relies significantly on the contribution of Alexander Dogiel (Dogiel 1895, 1896, 1899). In his work, he observed the different structural characteristics of neurons such as neuronal soma size and shape, dendritic number and size, axonal number, as well as the direction of projections, and used these to classify enteric neurons into three types, known as; Dogiel type I, II, and III (Figure 2, Dogiel 1899). Over the last three decades, many scientists refined and advanced these classifications to extend beyond Dogiel's earlier

work, however, his main classification still encompasses many neurons to date (Furness 2000).

*Dogiel type I neurons* are multidendritic, uniaxonal with flattened, stellate, or angular soma (Figure 2, black arrowhead). These neurons were further subcategorized based on their dendritic shapes into stubby, spiny, or hairy (Brehmer 2021). Apparently, this category contains a variety of functional types such as excitatory and inhibitory motor neurons as well as interneurons (Brehmer et al. 1999).

*Dogiel type II neurons* are multiaxonal with large oval or round soma. This type can have dendritic or adendritic form (Figure 2, asterisk refers to adendritic form). Neurons of the adendritic form have similar projections in pig, guinea pig, and rat small intestine myenteric plexus. One of the axons extends into the mucosa, while the others run circumferentially within secondary strands of the myenteric plexus. These neurons are largely considered to be IPANs (Brehmer et al. 1999).

*Dogiel type III neurons* were described as uniaxonal with long dendrites that are radially arranged which branch and end within the ganglion of origin (Figure 2, white arrowhead). “Tapering” dendrites describes their arrangement where they become thinner towards their ending. In pig small intestine, some type III neurons were found to be intrinsic or intestinofugal interneurons (Brehmer et al. 1999) and others were nitrergic neurons (Timmermans et al. 1994, Brehmer & Stach 1996). Due to these variations in the function of enteric neurons within the same morphological category among different species, neurochemical phenotypes of neurons are indispensable to identify the neurons’ function (Brehmer et al. 1999).

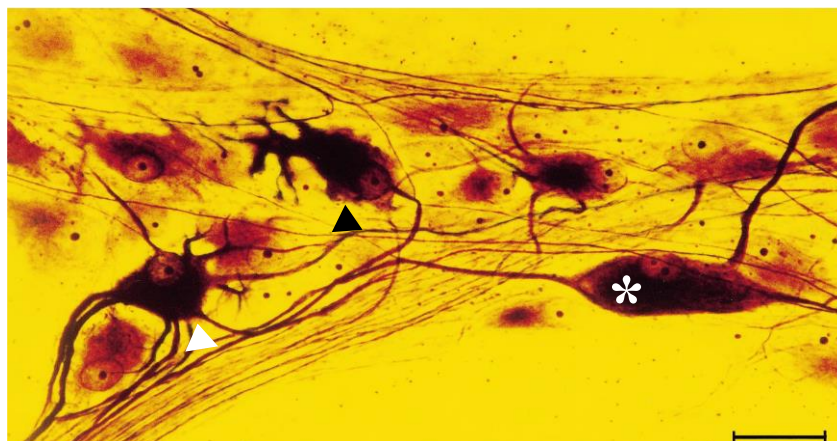


**Figure 2. Representative micrograph of a myenteric ganglion from pig jejunum with silver impregnation displaying different Dogiel types neurons.** The strongly impregnated (*black-brown stained*) neurons represent Dogiel type I neuron (black arrowhead), adendritic Dogiel type II neuron (asterisk), and Dogiel type III neuron (white arrowhead). Scale bar: 50  $\mu$ m (Brehmer et al. 1999).

### 1.3. Functional and neurochemical classification of enteric neurons

There are three main functional types of enteric neurons within the ENS: motor, sensory, and interneurons. The different functional types of neurons usually possess distinct neurochemical coding which determines their main neurotransmitters (Figure 3, Furness 2000, Rao & Gershon 2016).

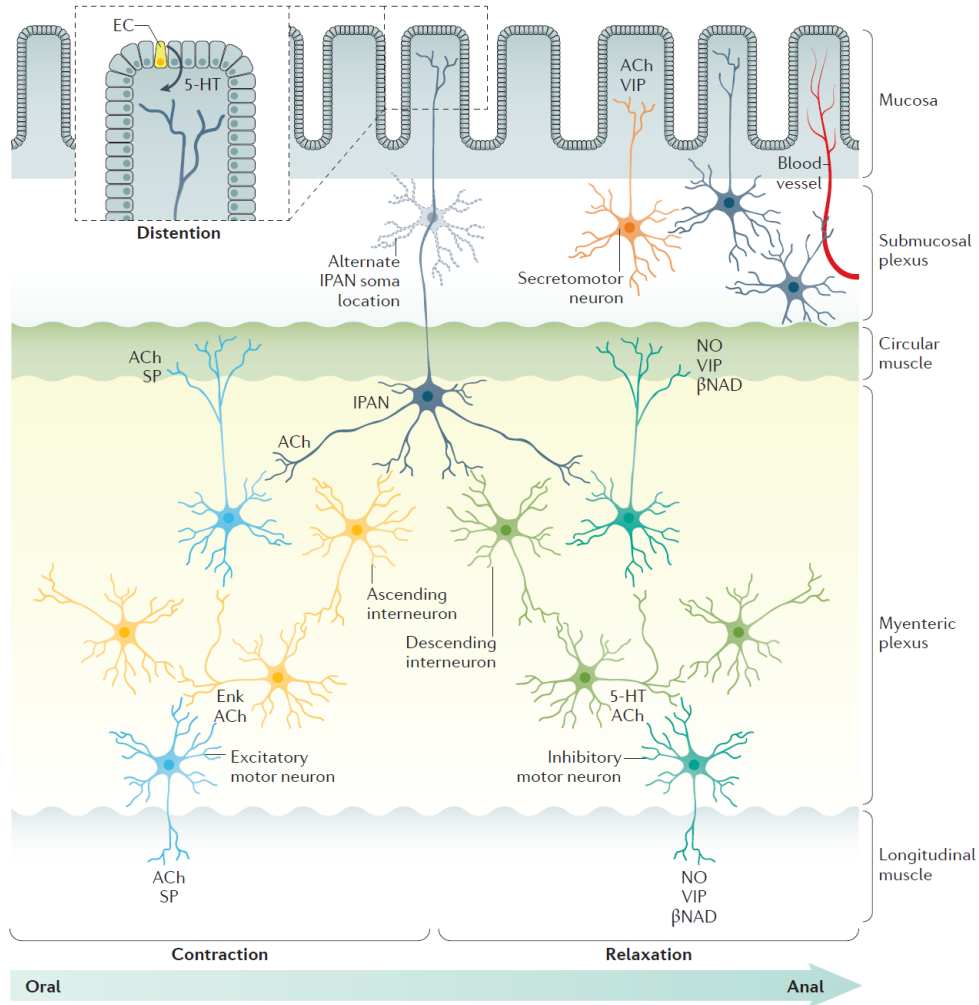


**Figure 3. Functional types of enteric neurons required during peristalsis.** Luminal distention triggers direct activation of mechanoreceptors in the mucosal axons of intrinsic primary afferent neurons (IPANs), as well as indirect activation of IPANs through serotonin (5-HT) release by enterochromaffin cells (ECs). IPANs in turn activate ascending and descending interneurons, resulting in the stimulation of excitatory and inhibitory motor neurons, respectively. Motor neurons cause oral contraction and anal relaxation of intestinal smooth muscle, resulting in the propulsion of luminal contents into the proximal-distal direction. ACh refers to neurons that contain acetylcholine. SP refers to neurons that contain substance P. Enk refers to enkephalin-expressing ascending interneurons. NO and VIP indicate inhibitory motor neurons secreting nitric oxide and vasoactive intestinal peptide.  $\beta$ NAD refers to inhibitory motor neurons secreting the purine,  $\beta$ -nicotinamide adenine dinucleotide. Secretomotor and vasomotor neurons of the submucosal plexus secrete ACh or VIP (Rao & Gershon 2016).

Cumulative research based on the guinea pig and mice ENS identified and classified different functional types of enteric motor neurons that control gut motility and secretomotor function. These include excitatory and inhibitory muscle motor neurons, secretomotor/vasodilator motor neurons, secretomotor non-vasodilator motor neurons, and motor neurons innervating enteroendocrine cells (Furness 2000, Bagyánszki et al. 2012). Excitatory motor neurons are present along the gut axis and innervate both longitudinal and circular muscle layers. These neurons are immunoreactive to choline acetyltransferase (ChAT) and to tachykinins such as substance P and neurokinin A. On the other hand, inhibitory motor neurons encode for neuronal nitric oxide synthase (nNOS) enzyme which produces nitric oxide (NO) to relax smooth muscle cells. Other co-transmitters existing in the inhibitory motor neurons include vasoactive intestinal peptide, pituitary adenylate cyclase-activating peptide, gamma-aminobutyric acid, and adenosine triphosphate (Furness 2000). The different combinations of these co-transmitters give rise to different neuronal subpopulations in the ENS. Although NO is considered as the main neurotransmitter in the inhibitory motor neurons, studies of nNOS blockade or NO scavenging showed only partial blockade in this type of neurons (Furness 2000).

Sensory reflexes within the gut are mediated via extrinsic and intrinsic afferent neurons. From the two types of extrinsic primary afferent neurons, one has cell body in the dorsal root ganglia, while the other one is located in the vagal sensory ganglia and both project to the gut. Cell bodies of intrinsic afferent neurons are situated within the ENS and represent intestinofugal neurons and IPANs (Furness et al. 2004). IPANs relay physiological stimuli including mechanical and chemical changes from the gut lumen to the surrounding neurons within the ENS (Furness et al. 2004). IPANs are multi-axonal with oval or round soma and therefore they are morphologically classified as Dogiel type II neurons. This type of neuron exists in both myenteric and submucous plexuses, with some of the IPANs in the myenteric plexus having their axons projecting to the lumen in addition to the projections existing between the two plexuses. This explains their role as core transducers in different gastrointestinal reflexes across the different layers of the gut. Most of the myenteric IPANs were found to be immunoreactive for both calcitonin and calcitonin-gene related peptide (CGRP), a marker for sensory neurons (Sayegh & Ritter 2003, Mitsui 2009, Hibberd et al. 2022). CGRP exist in two isoforms,  $\alpha$ -CGRP and  $\beta$ -CGRP, which are found in the central and the peripheral nervous systems, respectively

(Russell et al. 2014). As a neurotransmitter, CGRP mediates intrinsic motility reflexes and was found to be involved in immune regulatory mechanisms (Grider 1994, Wu et al. 2022). On the other hand, IPANs present in the submucous plexus of rat colon are negative to CGRP but immunoreactive to substance P and calretinin (Mitsui 2010). Additionally, the majority of submucous IPANs are also immunoreactive to neurokinin-1 receptor and about half of them are immunoreactive to prostaglandin EP<sub>3</sub> receptor (Mitsui 2010). Other types of sensory neurons with Dogiel type I morphology have been observed to be mechanosensory neurons in the distal colon of guinea pig (Spencer & Smith 2004).

Interneurons are key components of the ENS and function as intermediaries between sensory and motor neurons and can have either oral (ascending) or aboral (descending) projections (Costa et al. 1996, Furness 2000). Ascending interneurons are found in the myenteric plexus and classified as Dogiel type I neurons. In the guinea pig small intestine, ascending interneurons use acetylcholine in their synaptic neurotransmission but are also immunoreactive to calretinin, substance P, neurofilament, and enkephalin (Brookes 2001). On the other hand, descending interneurons vary more in function, neurochemistry, and morphology. In addition to ChAT, they are found to be immunoreactive for nNOS and vasoactive intestinal peptide, somatostatin, or serotonin, indicating that local reflexes of descending interneurons are not completely cholinergic (Furness 2006). Descending interneurons that are immunoreactive to serotonin participate in descending excitatory reflexes, while nNOS-immunoreactive interneurons are associated with descending inhibitory reflexes (Furness 2000, 2012).

#### **1.4. Diabetes mellitus**

Diabetes mellitus refers to a chronic, glucose metabolic disorder accompanied by long-lasting hyperglycaemia (Harreiter & Roden 2019). Diabetes is classified mainly into type 1, type 2, and gestational diabetes. Type 1 diabetes (T1D) is an autoimmune disease in which autoreactive T cells specifically target the insulin-producing  $\beta$  cells in the islets of Langerhans (Gillespie 2006). The destruction of  $\beta$  cells leads to a lack of insulin production which results in hyperglycaemia. In type 2 diabetes (T2D), hyperglycaemia develops due to either insufficient insulin production or insulin resistance. The latter is more common and can be the result of a state of metabolic syndrome. On the other hand, gestational diabetes refers to hyperglycaemia that develops during pregnancy that may or may not resolve after pregnancy (Nolan 2011).

Chronic hyperglycaemia commonly leads to short-term manifestations and the progression of long-term complications (Harreiter & Roden 2019). Short-term manifestations include polyuria, increased thirst and hunger, and sudden weight loss. Prolonged hyperglycaemia may develop microvascular and macrovascular complications. Microvascular complications occur when hyperglycaemia affects small blood vessels supplying the eyes, kidney, and peripheral nerves which result in retinopathy, nephropathy, and neuropathy, respectively (Horton & Barrett 2021). Peripheral neuropathy commonly affects patients with chronic diabetes and can be in the form of numbness, paraesthesia, pain in the distal lower extremities, or a combination of these. Diminished nociception is the most detrimental form of peripheral neuropathy due to the risk of developing foot ulcer which could require amputation if left untreated (Peltier et al. 2014). Macrovascular complications arise from atherosclerosis and hypercoagulation which increase the risk of developing different cardiovascular disease, coronary artery disease, cerebrovascular disease, and stroke (Fowler 2008).

The mechanisms underpinning the pathological effects of hyperglycaemia involve a significant increase in oxidative stress and the activation of pro-inflammatory cascades (Maritim et al. 2003, Alexandraki et al. 2008). Precisely, high glucose levels activate metabolic pathways involved in mitochondrial production of reactive oxygen species (ROS), such as hexosamine, polyol, protein kinase C, and advanced glycation end products pathways (Figure 4, Sandireddy et al. 2014). Released advanced glycation end products bind to their receptor leading to the production of ROS and the activation of pro-inflammatory pathways. Eventually, this mediates endothelial or neuronal inflammation which may later progress into apoptotic or necrotic cell death (Figure 4, Sandireddy et al. 2014). These processes may vary among the different types of diabetes and depending on the presence of any predisposing genetic or environmental factors. For instance, in T2D endothelial dysfunction is aggravated by the presence of dyslipidaemia where low-density lipoprotein is a target for oxidation and occlusion of blood vessels leading to atherosclerosis (Fowler 2008, Katakami 2018). In T1D, mitochondrial DNA released from the pancreas due to  $\beta$ -cell death was found to contribute to endothelial damage through the activation of inflammasomes (Pereira et al. 2020).

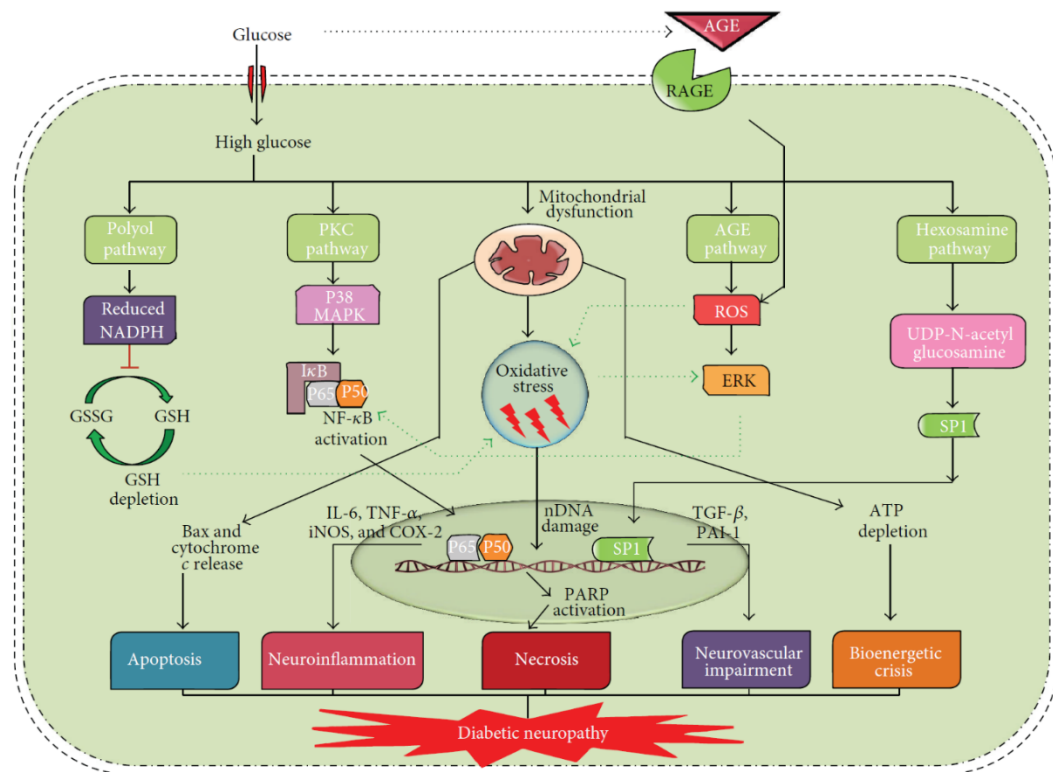


**Figure 4. Pathways involved in hyperglycaemia-induced diabetic neuropathy.** Hyperglycaemia activates several metabolic pathways including polyol, PKC, AGE, and hexosamine pathways. These are integrated through hyperglycaemia-mediated mitochondrial ROS production. Oxidative stress and these classical pathways in combination activate transcription factors such as NF- $\kappa$ B and SP-1, which lead to neuroinflammation and vascular impairment. (PKC: protein kinase, NF- $\kappa$ B: nuclear factor kappa enhancer of B cells, AGE: advanced glycation end products, ROS: reactive oxygen species, SP-1: specialty protein-1, ERK: extracellular related kinase, TNF $\alpha$ : tumour necrosis factor  $\alpha$ , IL-6: interleukin-6, iNOS: inducible nitric oxide synthase, COX-2: cyclooxygenase-2, TGF- $\beta$ : transforming growth factor- $\beta$ , PAI-1: plasminogen activator inhibitor-1, RAGE: receptor of advanced glycation end products, MAPK: mitogen-activated protein kinase, NADPH: nicotinamide adenine dinucleotide phosphate, GSSG: glutathione disulfide, GSH: glutathione, PARP: Poly-adenosine diphosphate ribose polymerase, ATP: adenosine triphosphate) (Sandireddy et al. 2014).

### 1.5. Diabetic gastroenteropathy

Diabetic patients commonly suffer from gastrointestinal symptoms that decrease the quality of life even under controlled glycaemic conditions (Yarandi & Srinivasan 2014). These symptoms are mostly related to dysfunction in gut motility and include nausea, bloating, gastroparesis, abdominal pain, diarrhoea and constipation (Figure 5, Yarandi & Srinivasan 2014).

In the oesophagus, aberrant peristaltic movement and dysfunction of the lower oesophageal sphincter were reported in diabetic patients consequently leading to delayed oesophageal motility and gastro-oesophageal reflux disease, respectively (Kinekawa et al. 2001, Nishida et al. 2004).

In the stomach, early stages of diabetes are likely to be associated with rapid gastric emptying compared to delayed gastric emptying and gastroparesis reported at later stages (Takahashi 2003, Camilleri 2007, Choi et al. 2007). Other gastric symptoms suffered by diabetic patients are early satiety and dyspepsia which are attributed to impaired relaxation of gastric fundus (Samsom et al. 1998, Yarandi & Srinivasan 2014). Regarding the intestinal tract, both constipation and diarrhoea are reported and the exact effect of diabetes on the function of the small and large intestines is still under investigation (Figure 5, Yarandi & Srinivasan 2014).

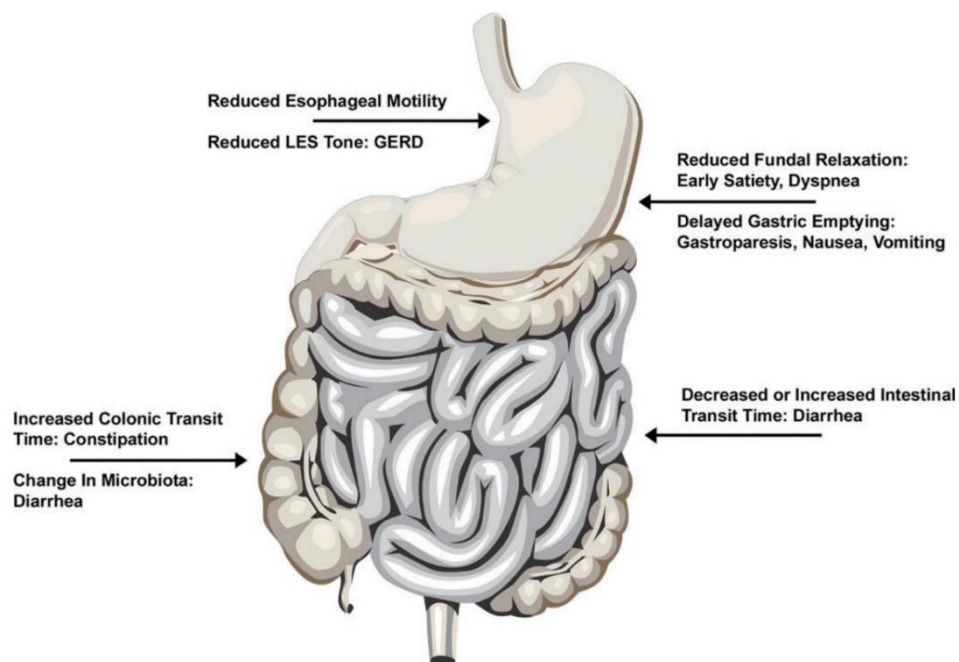


**Figure 5. Gastrointestinal dysfunction under diabetic conditions.** Diabetes can have detrimental consequences on all parts of the gastrointestinal tract most of which are related to motility. GERD: gastro-esophageal reflux disease, LES: lower esophageal sphincter (Yarandi & Srinivasan 2014).

The pathogenesis of these intestinal dysmotility symptoms is very compact and multifactorial in which the ENS is highly affected and occupies a central target that interacts with the surrounding microenvironment, gut microbiota, intestinal immune system, and blood circulation (Figure 5, Yarandi & Srinivasan 2014). Specifically, the myenteric plexus innervating the intestinal smooth muscle layers is severely affected under diabetes compared to the submucous plexus (Izbéki et al. 2008, Miller et al. 2008).

Hyperglycaemia affects the distinct populations of neurons differently; some myenteric neurons undergo degeneration, others change their neurochemical coding, while some neurons stay intact (Chandrasekharan & Srinivasan 2007). This highlights the importance of distinct neuronal subpopulations under diabetic changes. Since bowel

motility is the most deteriorated function, research has focused on studying the changes in the enteric motor neurons under diabetes. It is well demonstrated that inhibitory motor neurons are more severely affected by diabetes than excitatory neurons (Chandrasekharan & Srinivasan 2007).

However, these changes were inconsistent along the intestinal tract. For instance, in a chronic diabetic rat model, myenteric nitrergic neurons (inhibitory motor or interneurons) are degenerated in the jejunum, ileum, and colon, while presumably they only had undergone neurochemical changes in the duodenum manifested by a reduction in the nitrergic neuronal number without any change in the total neuronal number (Izbéki et al. 2008). Moreover, nitrergic neuronal remodelling itself can affect gastrointestinal motility patterns by disrupting the ratio between excitatory and inhibitory neurons within the ENS (Chandrasekharan & Srinivasan 2007). Therefore, the molecular mechanisms behind myenteric nitrergic neuronal degeneration or remodelling under hyperglycaemic conditions have received special attention in the last three decades (Cellek 2004, Chandrasekharan & Srinivasan 2007, Izbéki et al. 2008, Bódi & Bagyánszki 2020).

Intestinal segment-specific factors in the neuronal environment fundamentally determine the diabetic fate of enteric neurons (Figure 6, Bagyánszki & Bódi 2023). It is well demonstrated that chronic hyperglycaemia induces oxidative stress through the ROS production the imbalance between pro- and anti-oxidative mechanisms which ultimately lead to the induction of inflammatory cytokines in the enteric neurons and their microenvironment (Chandrakumar et al. 2017, Malik et al. 2018, Bódi et al. 2021). Moreover, it has been shown that the compositions of luminal and mucosa-associated gut microbiota are altered under diabetic conditions in a region-specific manner (Wirth et al. 2014, Malik et al. 2018, Wirth et al. 2021). The invasion of pathogenic bacteria together with disrupted intestinal barrier, contribute to the activation of pro-inflammatory mediators in the mucosa which is seen under hyperglycaemia (Thaiss et al. 2018). These changes can be sensed and transduced to the neurons in the submucous and myenteric plexuses through IPANs (McVey Neufeld et al. 2015). Moreover, the activation of enteric glia under these conditions gives further mechanisms by which the neuro-immune interplay takes place (Figure 6, Luo et al. 2018, Bagyánszki & Bódi 2023).

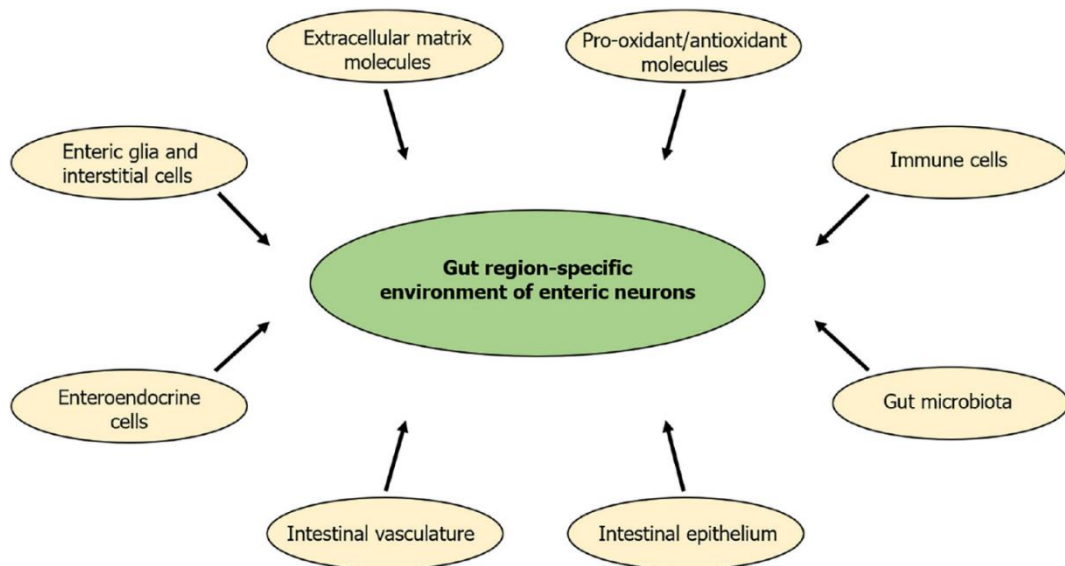


**Figure 6. Key elements that determine the gut region-specific neuronal microenvironment.** The enteric neurons are surrounded by a rich and dynamic microenvironment that encompasses various types of cells including enteric glial cells, interstitial cells of Cajal, intestinal vasculature and epithelium, enteroendocrine cells, intestinal microbiota, and immune cells together with the critical balance of pro-oxidants and antioxidants and extracellular matrix molecules leading to a strictly regional environment of enteric neurons under diabetic conditions (Bagyánszki & Bódi 2023).

## 1.6. Inflammatory cytokines in type 1 diabetes

Cytokines are a broad category of glycoproteins with small molecular weight (< 30kDa) which generally mediate interactions between cells of the immune system. These include interferons, interleukins, the chemokine family, mesenchymal growth factors, the tumour necrosis factor family and adipokines (Dinarello 2007). In T1D, inflammatory cytokines are key players in pancreatic autoimmune inflammation and  $\beta$ -cell destruction, and also contribute to diabetic gastrointestinal manifestations such as enteric neuropathy and motility disturbances, (Butkowski & Jelinek 2017, Malik et al. 2018). Diabetes-related enteric neuropathy may be a result of the upregulation of pro-inflammatory cytokines during diabetes. However, inflammatory cytokines may exhibit non-inflammatory roles on neurons such as exerting neurotrophic effects, inducing neuroplasticity, as well as altering neuronal excitability (Schäfers & Sorkin 2008, Gougeon et al. 2013).

### 1.6.1. The role of tumour necrosis factor $\alpha$

Tumour necrosis factor  $\alpha$  (TNF $\alpha$ ) is a potent cytokine that can trigger a variety of pro-inflammatory responses (MacEwan 2002a). It is mainly produced by activated macrophages and T lymphocytes but can be also expressed by other cell types including enteric neurons (Gougeon et al. 2013). TNF $\alpha$  belongs to TNF receptor superfamily of

ligands that are primarily expressed as membrane proteins which can be cleaved and secreted into soluble forms. TNF $\alpha$  mediates its effect through two cell surface receptors: TNF receptor I (TNFR1) and TNF receptor II (TNFR2). TNFR1 contributes to inflammation, neurodegeneration, and cell death, while TNFR2 is involved in cell regeneration, survival, and neuroprotection (MacEwan 2002b). Therefore, the cellular response exerted by TNF $\alpha$  may vary depending on the tissue and cell type. The transcriptional induction of TNF $\alpha$  is controlled by some transcription factors including activator protein-1 (AP-1), protein inhibitor of activated signal transducer and activator of transcription-1 (PIAS1), nuclear factor kappa-light-chain-enhancer of activated B cells (NF $\kappa$ B), and organic cation transporter-1 (El-Tahan et al. 2016). Hence, the production of TNF $\alpha$  can be induced by inflammatory cascades that activate AP-1 and NF $\kappa$ B pathway such as the activation of Toll-like receptor 4 (TLR4) by lipopolysaccharides and TNF $\alpha$  receptors activation (Means et al. 2000, El-Tahan et al. 2016). Additionally, TNF $\alpha$  can affect glucose and lipid metabolism and interfere with insulin receptor signalling. It can increase non-insulin dependent glucose transport by inducing the synthesis of the glucose transporter GLUT-1 and decrease insulin stimulated glucose transport leading to insulin resistance (Peraldi & Spiegelman 1998).

In T1D, TNF $\alpha$  is implicated in the early destruction of  $\beta$  cells and thus contributes to the disease development (Christen et al. 2001). Moreover, serum levels of TNF $\alpha$  were increased in T1D compared to controls (Qiao et al. 2017). The overproduction of TNF $\alpha$  might mediate the diabetes-related tissue changes through the activation of inducible NOS and the release of NO (McDaniel et al. 1996, Madrigal et al. 2002, Khaloo et al. 2020). TNF $\alpha$  was found to be neurotrophic for enteric neurons in an *in vitro* rat co-culture model (Gougeon et al. 2013). On the other hand, it was shown to induce neurotoxicity and cell apoptosis through glutamate production in cultures of primary human foetal neurons and rat cortical neurons (Ye et al. 2013). Moreover, TNF- $\alpha$  differentially modulated ion channels of nociceptive neurons in rat dorsal root ganglion (Czeschik et al. 2008). These varying effects of TNF $\alpha$  on the different types of neurons may have significance in the background of gut region-dependent myenteric neuropathy in diabetes. Therefore, our research group has investigated the distribution of TNF $\alpha$  in the myenteric neurons and their environment in the different intestinal segments in a T1D rat model (Bódi et al. 2021). In this study, TNF $\alpha$  expression was mapped by fluorescent immunohistochemistry and quantitative immunogold electron microscopy in the myenteric ganglia of duodenum,

ileum, and colon (Figure 7, Bódi et al. 2021). Tissue TNF $\alpha$  levels were measured by enzyme-linked immunosorbent assay (ELISA) in muscle/myenteric plexus-containing (MUSCLE-MP) and mucosa/submucosa/submucous plexus-containing (MUC-SUBMUC-SP) tissue homogenates. We observed an increasing density of TNF $\alpha$ -labelling gold particles in myenteric ganglia from proximal to distal segments and TNF $\alpha$  tissue levels were much more elevated in MUSCLE-MP homogenates than in MUC-SUBMUC-SP samples in healthy controls. In the diabetics, the number of TNF $\alpha$  gold labels was significantly increased in the duodenum, decreased in the colon, and remained unchanged in the ileal ganglia, while insulin did not prevent these diabetes-related TNF $\alpha$  changes. TNF $\alpha$  tissue concentration was also increased in MUSCLE-MP homogenates of diabetic duodenum, while decreased in MUC-SUBMUC-SP samples of diabetic ileum and colon. These findings support that T1D has region-specific and intestinal layer-dependent effects on TNF $\alpha$  expression, contributing to the regional damage of myenteric neurons and their intestinal milieu (Bódi et al. 2021).

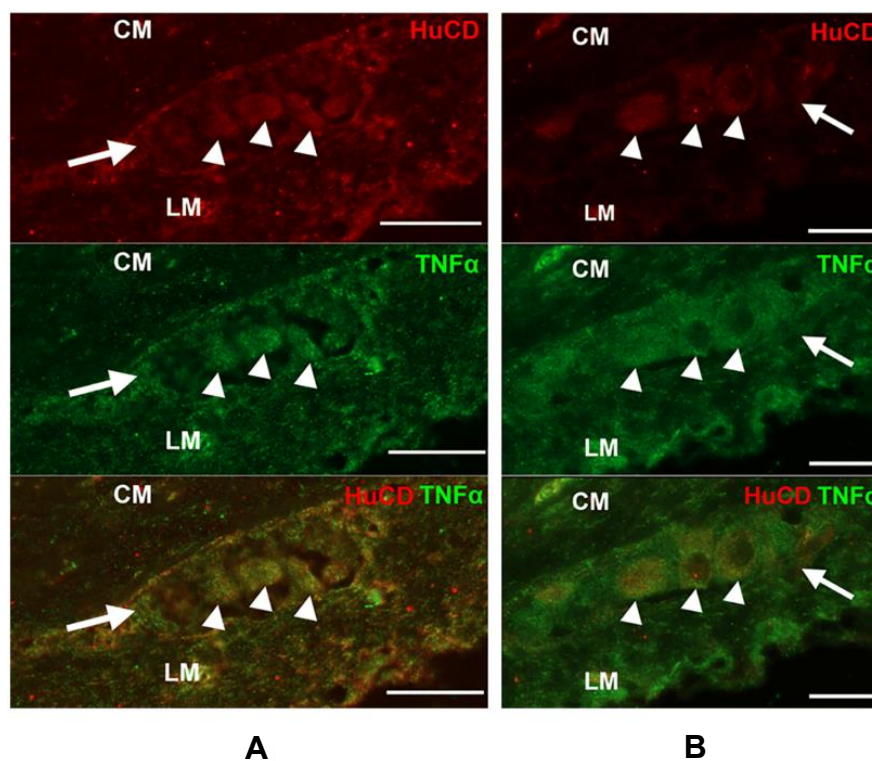


**Figure 7. Representative micrographs of myenteric ganglia from the duodenum of control (A) and diabetic (B) rats after TNF $\alpha$ -HuC/HuD double-labelling fluorescent immunohistochemistry. (LM: longitudinal smooth muscle layer, CM: circular smooth muscle layer, arrow: myenteric ganglia; arrowheads: myenteric neurons. Scale bar: 20  $\mu$ m) (Bódi et al. 2021).**

Since TNF $\alpha$  can have a dual role in cell degeneration or survival depending on the type of activated TNFR, we followed our investigations by studying the expression of TNFR1 and TNFR2 in myenteric ganglia and their environment using the same animal model (Figure 8, Barta et al. 2023). A distinct region-dependent TNFRs expression was revealed in controls. The density of TNFR1 was the lowest, while TNFR2 density was the highest in duodenal ganglia. Moreover, a decreased TNFRs expression from proximal to distal segments was observed in MUSCLE-MP homogenates. In diabetics, the TNFR2 density was substantially decreased in the myenteric ganglia of the duodenum, while no significant changes in TNFR1 density were observed. In diabetic MUSCLE-MP homogenates, both TNFRs levels were significantly decreased in the duodenum, which affected the ratio of TNFR2:TNFR1 in both the ganglia and their muscular environment. These findings highlight that TNFR2 is specifically altered in the duodenal myenteric ganglia of diabetic rats (Barta et al. 2023).

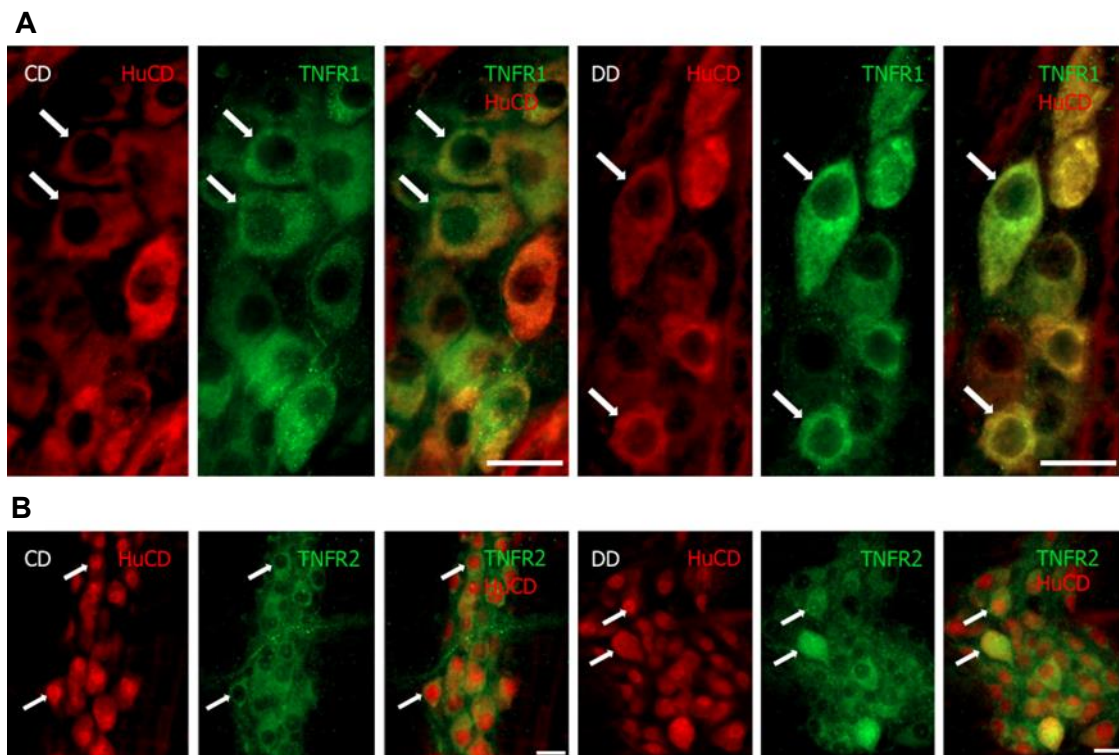


**Figure 8.** Representative micrographs of myenteric ganglia from the duodenum of control and diabetic rats after TNFR1-HuC/HuD (A) or TNFR2-HuC/HuD (B) double-labelling fluorescent immunohistochemistry. (CD: control duodenum; DD: diabetic duodenum, arrows indicate myenteric neurons, Scale bar: 20  $\mu$ m) (Barta et al. 2023).

### 1.6.2. The role of interleukin 1 $\beta$

The pro-inflammatory cytokine interleukin 1 $\beta$  (IL1 $\beta$ ) is a key mediator of the host-defence response to infection and injury (Fitzgerald & Luke 2000). IL1 $\beta$  belongs to the IL1 family of cytokines and is expressed by the *IL1B* gene located within the IL1 genes cluster on chromosome 2 in humans (Taylor et al. 2002). The two isoforms of IL1 protein: IL1 $\alpha$  and IL1 $\beta$ , share 26% of sequence homology and display similar biological signalling pathways. IL1 $\beta$  is typically produced and released by cells in the innate immune system such as activated macrophages and monocytes. However, variety of other cell types were found to express and produce this cytokine including synoviocytes, fibroblasts, endothelial cells, epithelial cells, as well as neurons and glial cells (Ren & Dubner 2008, Ren & Torres 2009).

Inflammatory signalling processes leading to the activation of NF $\kappa$ B pathway result in the expression of IL1 $\beta$ . This includes TNF $\alpha$  signalling pathway, activation of TLR4, as well as the binding of extracellular IL1 $\alpha$  and IL1 $\beta$  itself to the membrane-bound receptor IL1 receptor I (IL1RI) (Weber et al. 2010). IL1 $\beta$  is expressed and produced initially as an inactive 31 kDa pro-protein (pro-IL1 $\beta$ ) which requires the catalytic activation by caspase-1 into an active IL1 $\beta$  cytokine. Active IL1 $\beta$  can be secreted to the extracellular matrix and bind to the extracellular domain of the IL1RI. Upon binding, IL1RI undergoes ligand-induced conformational change which recruits interleukin 1 receptor-associated protein (IL1RAcP) and through the conserved cytosolic Toll-and IL1R-like (TIR) domains, the intracellular signalling proteins Myeloid differentiation primary response 88 (MYD88) and interleukin 1 receptor activated protein kinase 4 (IRAK4) are assembled to initiate signal transduction (Figure 9, Weber et al. 2010, Arranz et al. 2017). Autophosphorylation of IRAK4 will subsequently phosphorylate IRAK1 and IRAK2, which recruits the oligomerization and assembly of TNF-associated factor 6 (TRAF6). This complex of TRAF6 is responsible for the downstream activation of NF $\kappa$ B, c-Jun N-terminal kinase (JNK), p38 Mitogen-activated protein kinase (MAPK) pathways, and extracellular signal-regulated kinases (ERK). The activation of these signalling pathways induces the expression of several gene products involved in inflammatory responses, such as cyclooxygenase-2, IL-6, IL-8, as well as IL1 $\beta$  itself (Weber et al. 2010). Moreover, IL1 $\beta$  can also bind to IL1RII, a decoy receptor which lacks the TIR intracellular domain resulting in a blocked IL1 $\beta$  action. A naturally produced IL1R antagonist (IL1Ra) also exists which competes with IL1 $\alpha$  and IL1 $\beta$  over IL1RI (Figure 9,

Arranz et al. 2017, Boraschi et al. 2018, Migliorini et al. 2020). Another mechanism for the negative regulation of IL1 $\beta$  is the ubiquitylation of pro-IL1 $\beta$  which limits its access by caspase-1 and targets it for proteasomal degradation (Vijayaraj et al. 2021).

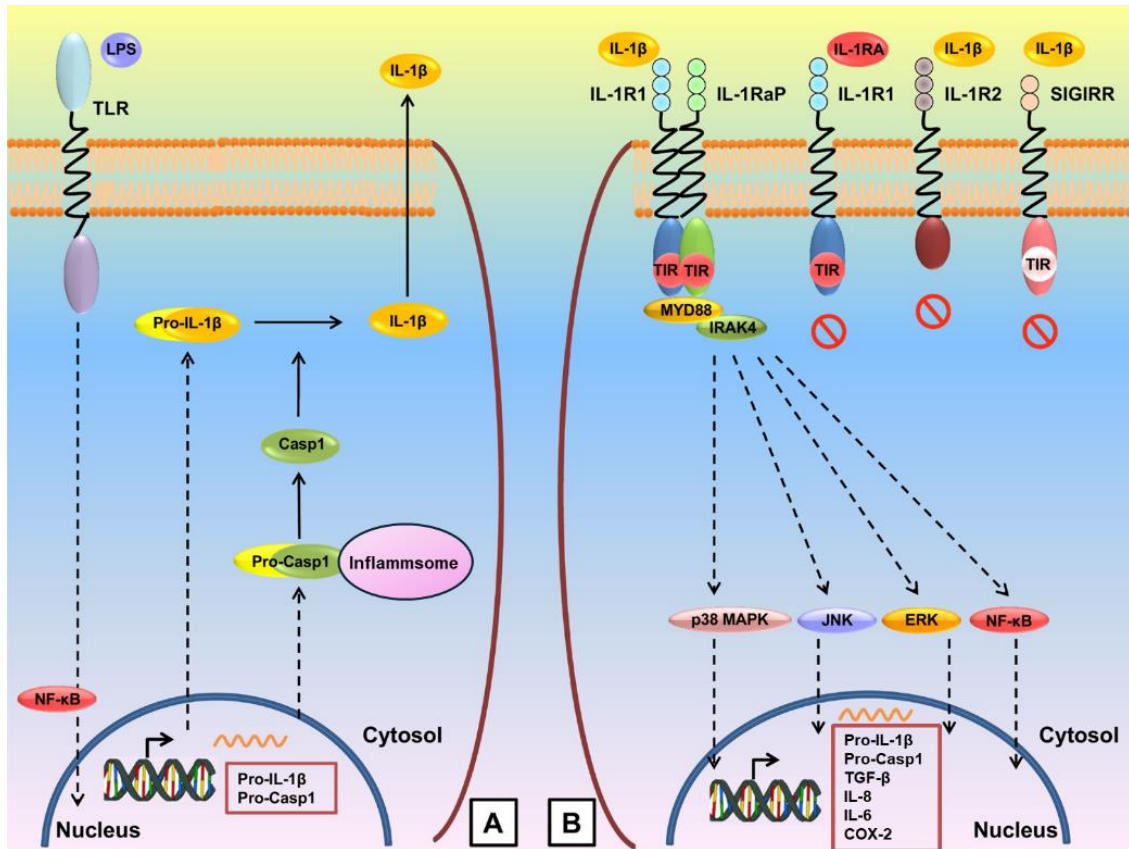


**Figure 9. Activation and signal transduction of interleukin 1 $\beta$ .** A) Pathogenic LPS recognized by TLR, activates a cascade of events that lead to the activation of the transcription factor NF- $\kappa$ B which induces the expression of pro-inflammatory genes including *IL1B* and *CASP1*. IL-1 $\beta$  is initially produced as a pro-IL-1 $\beta$ , which is enzymatically cleaved and activated by Casp1. Pro-casp1 is activated to Casp1 inside an inflammasome complex. B) Secreted IL-1 $\beta$  binds to IL-1R1 and triggers a signalling cascade, which involves p38 MAPK, JNK, ERK and NF- $\kappa$ B activation that result in the expression of genes responsible for immune cell functional activation, survival responses, and cell fate. Negative regulation of IL-1 $\beta$  signalling occurs through competitive binding of IL-1Ra to IL-1R1 and IL-1 $\beta$  binding to IL-1R2 or SIGIRR. (LPS: lipopolysaccharide, TLR: toll-like receptors, NF- $\kappa$ B: nuclear factor kappa-light-chain-enhancer of activated B cells, IL: interleukin, Casp1: caspase 1, IL-1Ra: IL-1 receptor antagonist, IL-1R: IL-1 receptor, IL-1RAP: IL-1 receptor accessory protein, TIR: toll-IL-1 receptor, SIGIRR: single immunoglobulin and TIR domain containing, MYD88: myeloid differentiation primary response 88, IRAK4: IL-1 receptor associated kinase 4, MAPK: mitogen-activated protein kinases, JNK: c-Jun N-terminal kinases, ERK: extracellular signal-regulated kinases, NF- $\kappa$ B: nuclear factor kappa-light-chain-enhancer of activated B cells, TGF- $\beta$ : transforming growth factor  $\beta$ , COX-2: cyclooxygenase-2) (modified from Arranz et al. 2017).

Many studies have demonstrated the role of IL1 $\beta$  in the progression of diseases including Alzheimer's disease, depression, cardiovascular diseases, diabetes, as well as inflammatory bowel disease (Dinarello 2018). However, the importance of IL1 $\beta$  extends beyond its roles in regulating immune responses and contributing to autoinflammatory diseases. Indeed, IL1 $\beta$  was found to be involved in mediating some physiological processes such as sleep, temperature, memory, nociception, and glucose homeostasis (Dinarello 1996, Dror et al. 2017, Lima 2023). The involvement of IL1 $\beta$  in glucose metabolism and homeostasis could explain the crucial role of this cytokine during metabolic diseases such as T1D and insulin resistance.

Studies have shown that IL1 $\beta$  synergically with interferon  $\gamma$  induced apoptosis of pancreatic  $\beta$ -cells. Moreover, animal models of T1D demonstrated the expression of IL1 $\beta$  early in the development of the disease and its high circulating levels may be indicative for the development of T1D or T2D. Therefore, the use of pharmacological antagonists of IL1 $\beta$  was initiated and have shown to improve glycaemic levels and  $\beta$  cell function in diabetic patients (Mandrup-Poulsen et al. 2010).

In the gastrointestinal tract, researchers proved the importance of IL1 $\beta$  in maintaining intestinal homeostasis through the regulation of T helper 17 cells under steady-state conditions. However, excessive levels of IL1 $\beta$  were associated with disrupting the mucosal barrier and the perturbation of microbial compositions (McEntee et al. 2019). Furthermore, administration of IL1 $\beta$  was found to increase intestinal tight junction permeability through the reduction of intestinal epithelial occludin mRNA both *in vitro* and *in vivo* (Rawat et al. 2020). In the ENS, *in vitro* studies revealed that both IL1 $\beta$  and TNF $\alpha$  are neurotrophic for enteric neurons and could induce axonal growth in those neurons surviving after inflammation (Gougeon et al. 2013). Others also demonstrated the ability of IL1 $\beta$  to activate some neuronal populations in the guinea pig ileum and colon. Those IL1 $\beta$ -responsive neurons were found to be mostly immunoreactive to nNOS and enkephalin (Tjwa et al. 2003). This could postulate a role for IL1 $\beta$  in the hyperglycaemia-induced myenteric nitrenergic neuropathy in T1D. Moreover, due to its close involvement with cyclooxygenase-2 signalling pathway, a possible role for IL1 $\beta$  in amplifying pain hypersensitivity via CGRP-immunoreactive neurons is not unforeseen (Neeb et al. 2011, Gui et al. 2016, Stemkowski et al. 2021).

### 1.6.3. The role of inflammasomes

Inflammasomes are large cytosolic multiprotein complexes that are formed to arbitrate host response to cellular damage or infection. Once assembled, an inflammasome complex triggers the proteolytic conversion of procaspase-1 into active caspase-1, which in turn catalyses the cleavage of pro-IL1 $\beta$  and pro-IL18 into active IL1 $\beta$  and IL18, respectively (Martinon et al. 2002, He et al. 2016). The assembly of inflammasomes requires three components of molecules: sensor, adaptor, and effector. In the first step, cytosolic pathogen-associated molecular patterns (PAMPs) or danger-associated molecular patterns (DAMPs) are recognized by pattern recognition receptors (PRRs) like nucleotide-binding domain and leucine-rich repeat receptor/ NOD-like receptor (NLR) or absent in melanoma 2 (AIM2)-like receptor (ALR). Through interactions between the pyrin domains (PYD-PYD), ALRs or NLRs activate, oligomerize and nucleate the adaptor protein apoptosis-associated speck-like protein containing a caspase-activation and recruitment domain (CARD) (ASC). Procaspase-1 is then recruited and bound to ASC through CARD-CARD recognition (Man et al. 2015). The compositions of the sensory part of the inflammasome determine its triggering mechanisms. For example, NLRs have tripartite domain organization which consists of an N-terminal CARD or baculovirus inhibitor of apoptosis protein repeat (BIR) or PYD to mediate homotypic protein-protein interactions, a central nucleotide-binding domain (NBD) that can initiate adenosine triphosphate (ATP)-induced oligomerization, as well as a C-terminal containing series of leucine-rich repeats (LRRs) which function as ligand sensors and autoregulators (Gross et al. 2011). Although the human genome encodes for 23 NLRs, only some of these NLR proteins such as NLRP1, NLRP3, NLRP6, NLRP7, NLRP9, NLRP12, and NLRC4 were found to form inflammasomes and activate caspase-1 (He et al. 2016). Among others, the NOD-, LRR- and pyrin domain-containing protein 3 (NLRP3) inflammasome is extensively studied due to its involvement in a vast number of diseases including metabolic disorders like T2D and obesity, central nervous system disorders like Alzheimer's and Parkinson diseases, and various autoimmune diseases (Fu & Wu 2023).

The activation of NLRP3 inflammasome requires two signals, PAMPs and DAMPs. First, priming of NLRP3 takes place when NF $\kappa$ B pathway is triggered through the activation of TLR4 by PAMPs (Figure 10, Liu & Yu 2021). In this step, NF $\kappa$ B will act as a transcription factor enhancing the expression of proinflammatory cytokines and

other genes involved in the inflammasome function like *NLRP3*, *IL1B* and *CASP1*. Second, translated NLRP3 protein senses cytosolic PAMPs and DAMPs such as crystalline substances, extracellular ATP, organelle damage and ion imbalance. Simultaneous activation by PAMPs and DAMPs trigger the homotypic oligomerization of NLRP3 and recruits ASC and procaspase-1. The resulting supramolecular complex acts as a platform for caspase-1 to catalyse the activation of the cytokines' precursors, pro-IL1 $\beta$  and pro-IL18 into mature pro-inflammatory cytokines (Figure 10, Liu & Yu 2021, Fu & Wu 2023).

In T1D, an association with *NLRP3* gene was revealed in Brazilian patients in which two single-nucleotide polymorphisms were addressed (Pontillo et al. 2010). Moreover, genetically modified animals with NLRP3 deficiency showed protective role against T1D progression through inhibiting the chemokines and chemokine receptors which mediate immune cells migration into the pancreatic islets (Hu et al. 2015). Another study demonstrated that during the development of streptozotocin-induced T1D, NLRP3 inflammasome is activated by mitochondrial DNA which triggers caspase-1-dependent IL1 $\beta$  production and corresponds to pathogenic cellular response (Carlos et al. 2017).

In the gut, the NLRP3 inflammasome has received much attention due to its association with inflammatory diseases such as inflammatory bowel disease. However, increasing evidence suggest its role in maintaining gastrointestinal tract homeostasis and microbiota compositions (Pan et al. 2022). Although many studies have been investigating the role of NLRP3 in governing neurodegeneration or electrophysiological changes in central nervous system diseases, very limited research has focused on its role in enteric neuropathy.

The inhibition of NLRP3-IL1 $\beta$  pathway in the macrophages rescued myenteric neuronal injury that was induced in intestinal ischemia/reperfusion model (Gao et al. 2022). However, an *in vivo* model of colitis showed that NLRP3 inflammasome is dispensable for enteric neuronal death. On the other hand, it is suggested that a different mechanism of neuronal death occurs in the setting of Crohn's disease. These discrepancies in the role of NLRP3 inflammasome in enteric neuropathy could stem from the differences in cytokine contributions and microbial alterations among different diseases (Wagatsuma & Nakase 2020). To date, no study has investigated the role of NLRP3 inflammasome in hyperglycaemia-induced myenteric neuropathy. In T1D, TLR4 expression and immunoreactivity in the myenteric neurons were changed in a gut region-

specific manner (Bódi et al. 2023). Since TLR4 is an inducer for the NLRP3 inflammasome, it is plausible to study the perturbation in neuronal NLRP3 inflammasome and investigate its role in inducing IL1 $\beta$  expression.

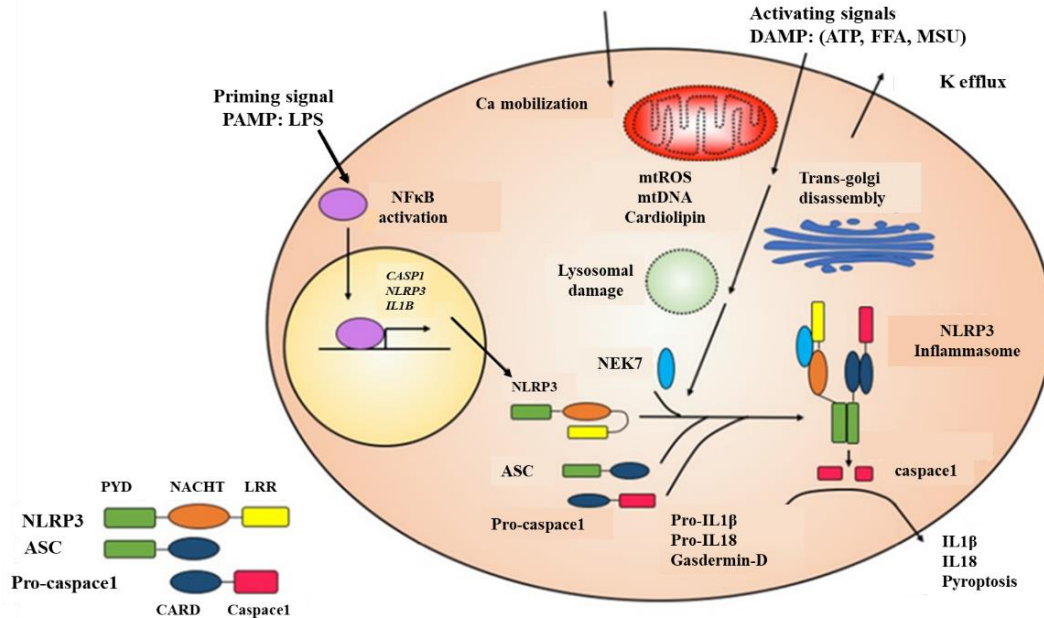


**Figure 10. Triggering of NLRP3 inflammasome assembly and activation.** Activation of the NLRP3 inflammasome complex requires an initial priming step followed by an activating step. Priming step happens when a PAMPs such as LPS is recognised by TLR4 leading to the activation of NF- $\kappa$ B signalling pathway. NF- $\kappa$ B translocate to the nucleus and induces the transcription of *NLRP3*, *CASP1* and *IL1B* genes. During the activation step, DAMPs like ATP, nigericin, FFAs, MSU, or cholesterol crystals trigger a sequence of cellular events. These typically involve potassium efflux, calcium mobilization, mitochondrial damage leading to the release of ROS, DNA, and cardiolipin, trans-Golgi disassembly, and rupture of lysosomes. NLRP3 protein can sense these cellular responses leading to conformational change that facilitates its oligomerization in the presence of NEK7. Oligomerized NLRP3 subsequently recruits ASC, which in turn recruits Caspase-1, leading to the formation of the NLRP3 inflammasome complex. Caspase-1 undergoes auto-cleavage, generating the active enzyme, which then cleaves pro-IL-1 $\beta$  and pro-IL-18 to release mature cytokines. Active caspase-1 also cleaves gasdermin D which forms membrane pores and induces pyroptosis. (PAMP: pathogen-associated molecular patterns, LPS: lipopolysaccharide, NF- $\kappa$ B: nuclear factor kappa-light-chain-enhancer of activated B cells, NLRP3: the NOD-, LRR- and pyrin domain-containing protein 3, DAMP: damage-associated molecular patterns, ATP: adenosine triphosphate, FFAs: free fatty acids, MSU: monosodium urate, mt: mitochondrial, ROS: reactive oxygen species, NEK7: never in mitosis gene A-related kinase 7, NOD: nucleotide-binding oligomerization domain, LRR: Leucine-rich repeats, ASC: adaptor protein apoptosis-associated speck-like protein containing a caspase-activation and recruitment domain, CARD: caspase-activation and recruitment domain, IL1 $\beta$ : Interleukin 1 $\beta$ ) (modified from Liu & Yu 2021).

## 2. AIMS

We hypothesize that T1D-related myenteric neuropathy might be mediated by changes in the expression of the pleiotropic inflammatory cytokine IL1 $\beta$  as a potent player in enteric neuroinflammation. Considering that the distinct subpopulations of enteric neurons have different susceptibility to hyperglycaemic damage, therefore, it raised the question of whether IL1 $\beta$  is also involved in different vulnerability of neuronal populations in diabetes.

To investigate the role of IL1 $\beta$  in diabetes-induced region-specific myenteric neuropathy and to elucidate its possible impact on diabetic damage of different myenteric neuronal populations, we applied fluorescent immunohistochemistry and different molecular methods using acute and chronic STZ-induced T1D rat models to answer the following questions:

### **In the intestine**

- Is there any difference in the proportion of IL1 $\beta$ -immunoreactive (IR) myenteric neurons along the duodenum-ileum-colon axis in healthy controls? What are the effects of acute and chronic hyperglycaemia as well as insulin treatment on the proportion of IL1 $\beta$ -IR myenteric neurons in different gut segments?
- Are there any variations in the proportion of IL1 $\beta$ -IR myenteric nNOS neurons (inhibitory motor and interneurons) along the oro-anal axis of the gut under control, diabetic, and insulin-treated diabetic conditions?
- Does the proportion of IL1 $\beta$ -IR myenteric CGRP neurons (mainly myenteric IPANs) differ among the distinct intestinal segments of control, diabetic, and insulin-treated diabetic rats?
- What are the effects of diabetes and insulin treatment on the IL1 $\beta$  protein levels in the tissue homogenates of intestinal smooth muscle layers and myenteric plexus?
- Are there any differences in the expression pattern of IL1 $\beta$  mRNA in the myenteric ganglia, smooth muscle, and mucosa layers of the intestinal wall along the intestinal tract of control, diabetic, and insulin-treated diabetic rats?
- Is there any correlation between diabetes-related IL1 $\beta$  changes and region-dependent diabetic myenteric neuropathy?

### **In the pancreas**

- Are there any effects of acute and chronic hyperglycaemia as well as insulin replacement on the IL1 $\beta$  protein levels in tissue homogenates of the pancreas?
- How does the pancreatic IL1 $\beta$  mRNA levels change in chronic diabetes and after insulin treatment?

### **In the serum**

- What are the effects of acute and chronic hyperglycaemia on IL1 $\beta$  serum levels?
- Is there any effect of insulin treatment on the IL1 $\beta$  concentration in the serum?

IL1 $\beta$  activation requires the expression and formation of an inflammasome complex, therefore, we were interested in investigating whether the NLRP3 inflammasome protein is involved in the diabetes-related IL1 $\beta$  induction. To understand the possible involvement of NLRP3 protein in diabetes-related myenteric neuropathy, we raised the following questions:

- Is there any difference in the density of NLRP3-labelling gold particles within the myenteric ganglia along the duodenum-ileum-colon axis of control rats?
- How do chronic hyperglycaemia and insulin treatment change the density of NLRP3-labelling gold particles in the myenteric ganglia of the different gut regions?
- Are there any differences in the expression pattern of NLRP3 mRNA among the myenteric ganglia, smooth muscle, and mucosa layers of the intestinal wall along the intestinal tract of control animals?
- How do chronic hyperglycaemia and insulin treatment alter the NLRP3 mRNA expression in the distinct intestinal wall layers and gut segments?
- Is there any correlation between the changes in IL1 $\beta$  and NLRP3 expression in the myenteric ganglia and their environment in the investigated segments of the experimental groups?

### **3. MATERIALS AND METHODS**

#### **3.1. Animal models**

Adult male Wistar rats (Toxi-Coop Zrt., Hungary) weighing 200-250 g, kept on standard laboratory chow and with free access to drinking water, were used throughout the experiments.

For the acute (1-week) diabetic rat model, animals were randomly divided into two groups: STZ-induced diabetics (n=8), and age- and sex-matched controls (n=6). For the chronic (10-weeks) diabetic animal model, rats were divided randomly into three groups: STZ-induced diabetics (n=20), insulin-treated STZ-induced diabetics (n=17), and sex- and age-matched controls (n=20). Hyperglycaemia was induced by a single injection of STZ (Sigma–Aldrich, Hungary) at 60 mg/kg in the intraperitoneal cavity (Izbéki et al. 2008). Animals with non-fasting glucose concentrations higher than 18 mmol/L were considered diabetic. From this time on, the insulin-treated group of hyperglycaemic animals received subcutaneous injection of insulin (Humulin M3, Eli Lilly Nederland, Netherlands) each morning (2 IU) and afternoon (3 IU). Normal saline was administered subcutaneously to diabetic and control groups. Physiological parameters such as weight and blood glucose levels were measured daily for the acute and weekly for the chronic animal experiments. Diabetic animals that recovered spontaneously and whose blood glucose level decreased under 18 mmol/L during the 10-week experiment were excluded. In all procedures involving experimental animals, the principles of the National Institute of Health (Bethesda, USA) guidelines and the EU directive 2010/63/EU for the protection of animals used for scientific purposes were strictly followed, and all the experiments were approved by the National Scientific Ethical Committee on Animal Experimentation (National Competent Authority), with the license number XX./1636/2019.

#### **3.2. Blood sampling and tissue handling**

Depending on the acute and chronic animal experiments, one week or ten weeks after the onset of hyperglycaemia, blood samples were collected from the tail vein of each animal into the vacuum collection tubes (BD Vacutainer® SST™ II Advance). Collected blood samples were centrifuged for 10 min at 3200 rpm (20 °C) and supernatant (serum) was extracted and used for ELISA.

Later, the animals were anesthetized by intraperitoneal injection of chloral hydrate (375 mg/kg) and sacrificed by cervical dislocation. Pancreatic and intestinal segments of diabetic, insulin-treated diabetic, and control rats were dissected and rinsed in 0.05 M

phosphate buffer (PB; pH 7.4). The head of the pancreas was used for experiments, while gut samples were taken from the duodenum (1 cm distal to the pylorus), ileum (1 cm proximal to the ileo-caecal junction), and proximal colon (1 cm distal to the cecum), and processed for fluorescent immunohistochemistry, transmission electron microscopy, ELISA, and RNAscope multiplex fluorescent V2 assay (RNAscope). For fluorescent immunohistochemistry, the intestinal segments were cut along the mesentery, pinched flat, and fixed overnight at 4 °C in 4% paraformaldehyde solution buffered with 0.1 M PB (pH 7.4). Samples were then washed, the layers of mucosa, submucosa, and circular smooth muscle were removed, and whole mounts with the myenteric plexus adhering to the longitudinal smooth muscle were prepared. For post-embedding electron microscopy, pieces (2-3 mm) of the gut segments were fixed in 2% formaldehyde and 2% glutaraldehyde solution and then further fixed in 1% OsO<sub>4</sub> for 1 hour. After rinsing the samples in PBS and dehydrating in increasing ethanol concentrations and acetone, they were embedded in Embed812 (Electron Microscopy Sciences, USA). For the ELISA, small pieces of the pancreas and 3 cm-long segments from the duodenum, ileum, and colon were cut along the mesentery and pinched flat. Layers of mucosa and submucosa were removed leaving tissue containing smooth muscle layers and the myenteric plexus in between which were snap-frozen in liquid nitrogen and stored at -80 °C until use. For RNAscope, pieces (2-3 mm) of gut segments and pancreas were immersed in O.C.T<sup>TM</sup> (Tissue-Tek, Netherlands) medium and fresh-frozen in liquid nitrogen for further cryosectioning (5 µm).

### **3.3. Double-labelling fluorescent immunohistochemistry**

For double-labelling fluorescent immunohistochemistry, whole-mount preparations derived from different gut segments were immunostained with primary antibodies against IL1 $\beta$  and HuC/HuD, nNOS, or CGRP, as well as NLRP3 and HuC/HuD. Briefly, the whole mounts were washed and permeabilized by 0.025% Triton X-100 in tris(hydroxymethyl)aminomethane-buffered saline (TBS) twice for 5 minutes each. After blocking for 30 minutes with 1% bovine serum albumin (BSA) and 10% normal goat serum in TBS, the whole mounts were incubated overnight with the primary antibodies (Table 1) at 4 °C. After washing in 0.025% Triton X-100 in TBS, whole mounts were incubated with secondary antibodies (Table 2) for 1 hour at room temperature followed by washing in TBS and mounting on slides in Fluoromount Aqueous Mounting Medium (Sigma-Aldrich, Hungary). Immunostained whole-mounts were observed and

photographed with a Zeiss Imager Z.2 fluorescent microscope equipped with an Axiocam 506 mono camera (Zeiss, Germany). An average of fifty myenteric ganglia were taken from each gut segment per experimental group, and the proportions of IL1 $\beta$ -IR, IL1 $\beta$ -nNOS-IR, and IL1 $\beta$ -CGRP-IR myenteric neurons were calculated per ganglion.

**Table 1. Primary antibodies used during double-labelling fluorescent immunohistochemistry.**

Antibody	Host species	Type	Dilution	Cat. No.	Manufacturer
anti-HuC/HuD	rabbit	monoclonal	1:200	ab184267	Abcam, UK
anti-HuC/HuD	mouse	monoclonal	1:50	A-21271	Invitrogen, USA
anti-IL1 $\beta$	mouse	monoclonal	1:50	sc-52012	Santa Cruz Biotechnology, USA
anti-nNOS	rabbit	polyclonal	1:200	189901	Cayman Chemical, USA
anti-CGRP	rabbit	polyclonal	1:100	3394223	EMD Millipore Corporation, USA
anti-NLRP3	rabbit	polyclonal	1:100	SAB5700723	Sigma Aldrich, USA

**Table 2. Secondary antibodies used during double-labelling fluorescent immunohistochemistry.**

Antibody	Target species	Type	Dilution	Cat. No.	Manufacturer
Alexa Flour 488	anti-rabbit	polyclonal	1:200	A11008	Thermo Fisher Scientific, USA
Cy <sup>TM</sup> 3	anti-mouse	polyclonal	1:200	RRID: 2338690	Jackson ImmunoResearch Laboratories, USA

### 3.4. Post-embedding immunohistochemistry

Four embedded blocks originated from each intestinal segment and condition were used to prepare ultrathin (70 nm) sections which were mounted on nickel grids and processed for NLRP3 immunogold labelling. Ultrathin sections were treated with 1% periodic acid and 1% sodium periodate, washed with distilled water, TBS, followed by blocking in 1% BSA for 30 minutes. After washing again with distilled water and TBS, samples were incubated overnight with anti-NLRP3 (rabbit polyclonal; Cat. No.

SAB5700723, Sigma-Aldrich, USA; final dilution 1:200) primary antibody at room temperature. Samples were washed in TBS, then permeabilized with a solution containing 1% BSA, 0.005% Tween-20 in (tris(hydroxymethyl)aminomethane (pH=7.6), followed by incubation with anti-rabbit IgG (conjugated to 18 nm gold particles; Cat. No. 111-215-144; Jackson ImmunoResearch, USA; final dilution 1:20) secondary antibody for 3 hours. Negative controls were performed to assess the specificity of the immunoreaction by omitting the primary antibody in the labelling protocol and incubating the sections only in the gold-conjugated secondary antibody. Sections were counterstained with uranyl acetate (Merck, Germany) and lead citrate (Merck, Germany), and were examined and photographed with a JEOL JEM 1400 transmission electron microscope. The subcellular distributions of the gold particles labelling NLRP3 were determined in the myenteric ganglia. Fifty digital photographs of five myenteric ganglia per intestinal segment per condition were conducted at a magnification of 20,000 $\times$  with the AnalySIS 3.2 program (Soft Imaging System GmbH, Germany). ImageJ (National Institute of Health, USA) was used to quantify the number of gold labelling and the intensity of the labelling was expressed as the total number of gold particles per unit area ( $\mu\text{m}^2$ ).

### **3.5. Measurement of tissue and serum interleukin 1 $\beta$ concentrations**

Pancreatic and intestinal tissue samples were crushed into powder in a mortar and homogenized in 500  $\mu\text{L}$  homogenizing buffer (100  $\mu\text{L}$  protease inhibitor cocktail (Sigma-Aldrich, Hungary) in 20 mL 0.05 M PB). Tissue homogenates were centrifuged at 5000 rpm for 20 min at 4  $^{\circ}\text{C}$ . IL1 $\beta$  level in the different tissue samples and sera was determined using quantitative ELISA according to the manufacturer's instructions (GA-E0128RT, GenAsia Biotech Co., China). Optical density was measured at 450 nm (Benchmark Microplate Reader; Bio-Rad, Hungary). Tissue concentrations of IL1 $\beta$  were expressed as ng/mg protein whereas blood IL1 $\beta$  levels were expressed as ng/mL serum.

### **3.6. Bradford protein micromethod for the determination of tissue protein content**

A commercial protein assay kit was used to determine the protein content in tissue samples. Bradford reagent was added to each sample. After mixing and following 10 min incubation, the samples were assayed spectrophotometrically at 595 nm. Protein level was expressed as mg protein/mL.

### **3.7. RNAscope multiplex fluorescent V2 assay**

To detect IL1 $\beta$  mRNA (in case of pancreas and intestinal layers) and NLRP3 mRNA (in case of intestinal layers), the RNAscope multiplex fluorescent V2 assay (Cat. No. 323100, Advanced Cell Diagnostics, USA) was used according to the manufacturer's instructions. Briefly, fresh-frozen cryosections (5  $\mu$ m) were fixed in 4% paraformaldehyde and dehydrated in increasing ethanol concentrations. The cryosections were incubated in hydrogen peroxide, followed by protease IV treatment and then hybridized with rat IL1 $\beta$  probe (Cat. No. 314011-C2, Advanced Cell Diagnostics, USA; final dilution 1:50) or NLRP3 probe (Cat. No. 510041, Advanced Cell Diagnostics, USA) for 2 hours at 40 °C. After a three-step signal amplification, HRP signal development was performed followed by conjugation of a fluorophore (Opal<sup>TM</sup> 520 Reagent Pack, FP1487001KT, Akoya Biosciences, USA; final dilution 1:100, 30 min at 40 °C). Tissues were counterstained with DAPI, mounted with Fluoromount<sup>TM</sup> Aqueous Mounting Medium (Sigma–Aldrich, Hungary), and imaging was attained with a Zeiss Imager Z.2 fluorescent microscope equipped with an AxioCam 506 mono camera (Zeiss, Germany). Positive and negative control probes were run to assess sample RNA quality and optimal permeabilization. An average of fifteen digital photographs were taken from the pancreas or the different intestinal layers (myenteric ganglia, smooth muscle, and mucosa/submucosa) of each gut segment and experimental group, and the number of punctate dots labelling IL1 $\beta$  or NLRP3 mRNA was quantified per unit area (mm<sup>2</sup>).

### **3.8. Statistical analysis**

Data were checked for Gaussian distribution by a D'Agostino-Pearson omnibus normality test. Two-tailed T-test with a Mann-Whitney test was used to analyse data from two comparison groups (acute experiment). Data retrieved from multiple comparison groups were analysed by Kruskal–Wallis test with a Dunn's multiple comparisons test (chronic experiment). All analyses were carried out with GraphPad Prism 6.0 (GraphPad Software, USA). A probability of  $p < 0.05$  was set as the level of significance. All data were expressed as mean  $\pm$  SEM.

## 4. RESULTS

### 4.1. Physiological parameters of experimental animals

#### 4.1.1. Acute diabetic rat model

The weight and blood glucose concentrations of the acute diabetic and control animals were monitored daily for one week and summarized in Table 3. Animals' final weight has increased compared to the initial weight in both diabetic and control groups ( $p < 0.05$ ). Acute diabetic animals were hyperglycaemic during the one-week experimental period with an average daily blood glucose of  $29.1 \pm 1.01$  mmol/L. This was significantly higher than their initial blood glucose level ( $29.1 \pm 1.01$  mmol/L vs  $5.91 \pm 0.19$  mmol/L,  $p < 0.0001$ ) as well as the average daily blood glucose level of controls ( $29.1 \pm 1.01$  mmol/L vs  $6.39 \pm 0.12$  mmol/L,  $p < 0.05$ ).

**Table 3. Weight and glycaemic characteristics of the acute diabetic experimental animals.**

	Weight (g)		Blood glucose level (mmol/L)	
	Initial	Final	Initial	Final (average)
<b>Controls (n = 6)</b>	$219.0 \pm 7.18$	$275.0 \pm 9.2^a$	$6.83 \pm 0.26$	$6.39 \pm 0.12$
<b>Diabetics (n = 8)</b>	$216.5 \pm 4.98$	$256.3 \pm 8.19^a$	$5.91 \pm 0.19$	$29.1 \pm 1.01^{b,c}$

Data are expressed as mean  $\pm$  SEM; <sup>a</sup> $p < 0.05$ , <sup>b</sup> $p < 0.0001$  vs initial; <sup>c</sup> $p < 0.05$  vs final controls.

#### 4.1.2. Chronic diabetic rat model

The weight and blood glucose concentrations of the chronic diabetic, insulin-treated diabetic, and control rats were monitored weekly during the 10-week experiment and summarized in Table 4. Diabetic rats were characterized by long-lasting chronic hyperglycaemia with an average blood glucose concentration of  $27.42 \pm 0.93$  mmol/L, which was more than four times higher than that of the controls ( $5.82 \pm 0.08$  mmol/L). Immediate insulin treatment inhibited extremely high glucose levels, but these were still higher than that of controls ( $13.23 \pm 1.06$  mmol/L,  $p < 0.01$ ). All the experimental rats gained weight during the 10-week experimental period, although the final body weight of diabetic animals was significantly lower compared to the insulin-treated diabetic ( $p < 0.0001$ ) and control ( $p < 0.0001$ ) rats.

**Table 4. Weight and glycaemic characteristics of the chronic diabetic experimental animals.**

	Weight (g)		Blood glucose level (mmol/L)	
	Initial	Final	Initial	Final (average)
<b>Controls (n = 20)</b>	213.0 ± 5.09	457.6 ± 13.88 <sup>c</sup>	5.1 ± 0.28	5.82 ± 0.08
<b>Diabetics (n = 20)</b>	214.7 ± 5.39	322.5 ± 1.32 <sup>a,c</sup>	5.56 ± 0.32	27.42 ± 0.93 <sup>c,e</sup>
<b>Insulin-treated diabetics (n = 17)</b>	217.7 ± 4.81	444.8 ± 14.2 <sup>c,g</sup>	5.31 ± 0.37	13.23 ± 1.06 <sup>b,d,f</sup>

Data are expressed as mean ± SEM; <sup>a</sup>  $p < 0.01$ , <sup>b</sup>  $p < 0.001$ , <sup>c</sup>  $p < 0.0001$  vs initial; <sup>d</sup>  $p < 0.01$ , <sup>e</sup>  $p < 0.0001$  vs final controls; <sup>f</sup>  $p < 0.01$ , <sup>g</sup>  $p < 0.0001$  vs final diabetics.

#### 4.2. Effect of acute and chronic hyperglycaemia on the proportion of interleukin 1 $\beta$ -immunoreactive myenteric neurons

Using double-labelling fluorescent immunohistochemistry, whole-mount preparations of myenteric plexus were labelled with anti-HuC/HuD pan-neuronal marker to visualize all myenteric neurons in ganglia, and anti-IL1 $\beta$  to detect the IL1 $\beta$ -IR myenteric neurons in different gut segments of the acute (Figure 11A, 12A) and chronic (Figure 14A-C) diabetic experimental groups. The level of IL1 $\beta$  immunoreactivity was analysed by two means. First, we calculated the proportion of IL1 $\beta$ -IR myenteric neurons per total myenteric neuronal number (Equation 1). Second, we measured the proportion of IL1 $\beta$ -IR myenteric neurons-containing ganglia (those ganglia that contained at least one IL1 $\beta$ -IR neuron) per total number of investigated ganglia (Equation 2).

##### Equation 1.

$$\text{Proportion of IL1}\beta\text{-IR myenteric neurons (\%)} = \frac{\text{Number of IL1}\beta\text{-IR myenteric neurons per ganglion}}{\text{Total number of myenteric neurons per ganglion}} \times 100$$

##### Equation 2.

$$\text{Proportion of IL1}\beta\text{-IR neurons-containing ganglia (\%)} = \frac{\text{Number of IL1}\beta\text{-IR neurons-containing ganglia}}{\text{Total number of ganglia}} \times 100$$

#### 4.2.1. Acute diabetic rat model

In control rats of the acute diabetic model, the proportion of IL1 $\beta$ -IR myenteric neurons revealed significant differences between the small intestine and colon, where the colon displayed the highest proportion compared to the duodenum and ileum (23.39 ± 2.39% vs 3.42 ± 1.02% and 6.76 ± 1.22%, respectively,  $p < 0.0001$ ; Figure 11B).

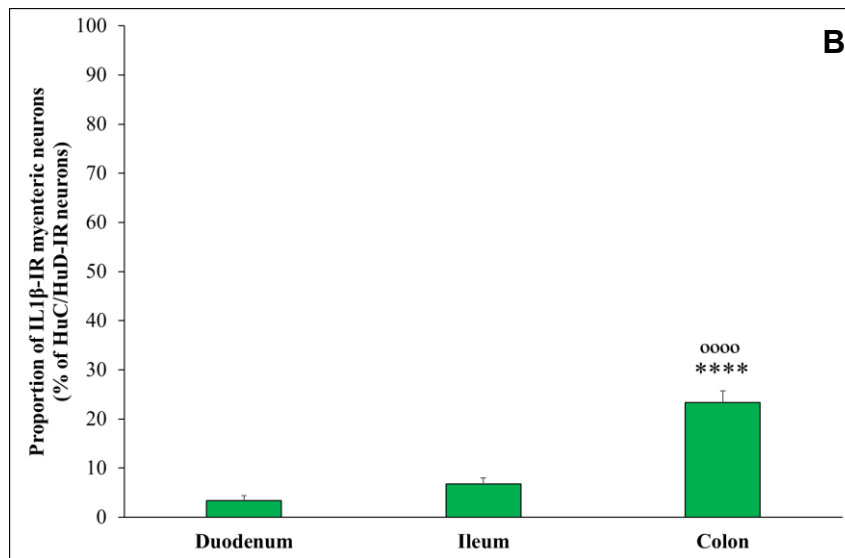
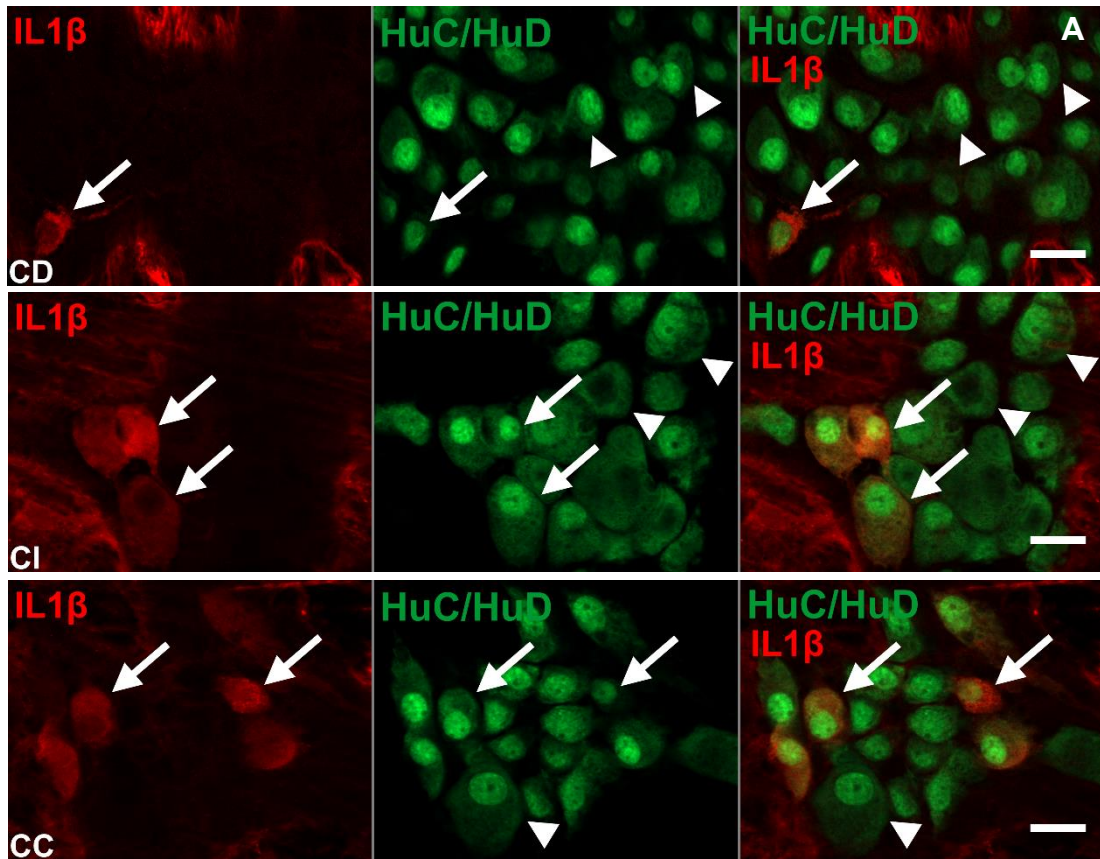


**Figure 11. Representative fluorescent micrographs of whole-mount preparations of myenteric ganglia from the duodenum, ileum, and colon of acute control rats after IL1 $\beta$ -HuC/HuD double-labelling immunohistochemistry (A).** HuC/HuD as a pan-neuronal marker was applied to label myenteric neurons. CD: control duodenum, CI: control ileum, CC: control colon; arrows: IL1 $\beta$ -immunoreactive myenteric neurons, arrowheads: myenteric neurons. Scale bars: 20  $\mu$ m. **Proportion of IL1 $\beta$ -immunoreactive myenteric neurons in the duodenum, ileum, and colon of acute control rats (B).** A significantly higher proportion of IL1 $\beta$ -immunoreactive myenteric neurons was detected in the colon compared to the duodenum and ileum. Data are expressed as mean  $\pm$  SEM. \*\*\*\*  $p < 0.0001$  (relative to control duodenum); oooo  $p < 0.0001$  (between control ileum and colon).

Acute hyperglycaemia resulted in significant changes in the small intestine where a 4-fold increase in the proportion of IL1 $\beta$ -IR myenteric neurons was seen in the duodenum compared to controls ( $13.83 \pm 2.64\%$  vs  $3.44 \pm 1.02\%$ ,  $p < 0.01$ ) and an almost 2-fold increase was observed in the ileum ( $12.01 \pm 2.12\%$  vs  $6.76 \pm 1.22\%$ ,  $p < 0.05$ ; Figure 12). However, no significant changes were observed in the colon of acute diabetics compared to controls.

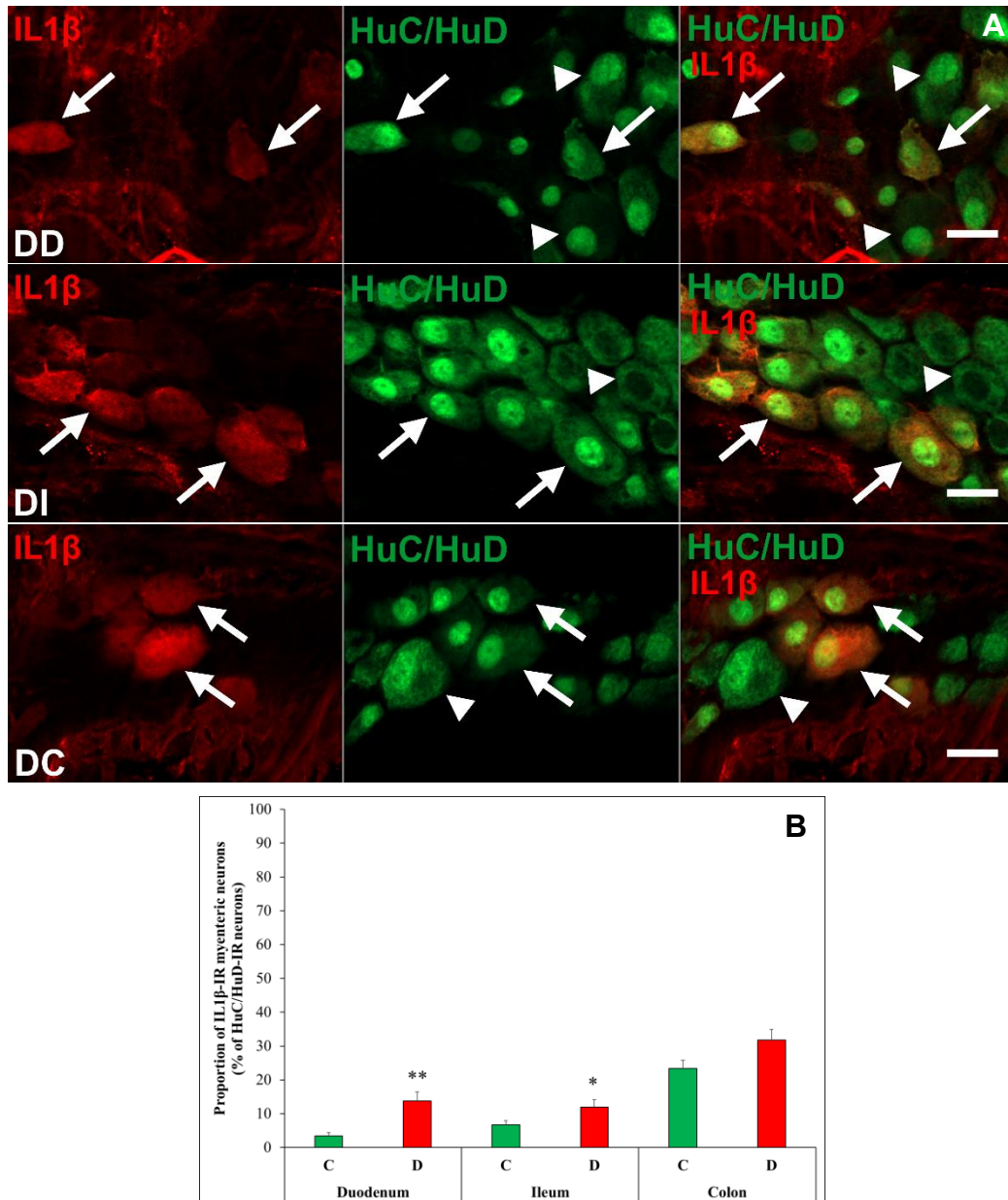


**Figure 12. Representative fluorescent micrographs of whole-mount preparations of myenteric ganglia from the duodenum, ileum, and colon of acute diabetic rats after IL1 $\beta$ -HuC/HuD double-labelling immunohistochemistry (A).** HuC/HuD as a pan-neuronal marker was applied to label myenteric neurons. DD: diabetic duodenum, DI: diabetic ileum, DC: diabetic colon; arrows: IL1 $\beta$ -immunoreactive myenteric neurons, arrowheads: myenteric neurons. Scale bars: 20  $\mu$ m. **Proportion of IL1 $\beta$ -immunoreactive myenteric neurons related to the total myenteric neuronal number in the duodenum, ileum, and colon of acute diabetic rats (B).** In the acute diabetic group, the proportion of IL1 $\beta$ -immunoreactive myenteric neurons was significantly increased in the duodenum and ileum. Data are expressed as mean  $\pm$  SEM. \*  $p < 0.05$ , \*\*  $p < 0.01$  (relative to controls). C: controls, D: diabetics.

Regarding the proportion of IL1 $\beta$ -IR neurons-containing ganglia in control animals, an increasing tendency toward the distal part was also revealed with the highest proportion in the colon (95.74%, Figure 13). In diabetics, this proportion was induced in all the investigated segments compared to controls. In the duodenum, there was an almost 2-fold increase where it changed from 35.36% to 62.22%, and in the ileum, it increased from 51.06% to 73.91%. In the colon of diabetics, all the investigated ganglia contained at least one IL1 $\beta$ -IR neuron (Figure 13).

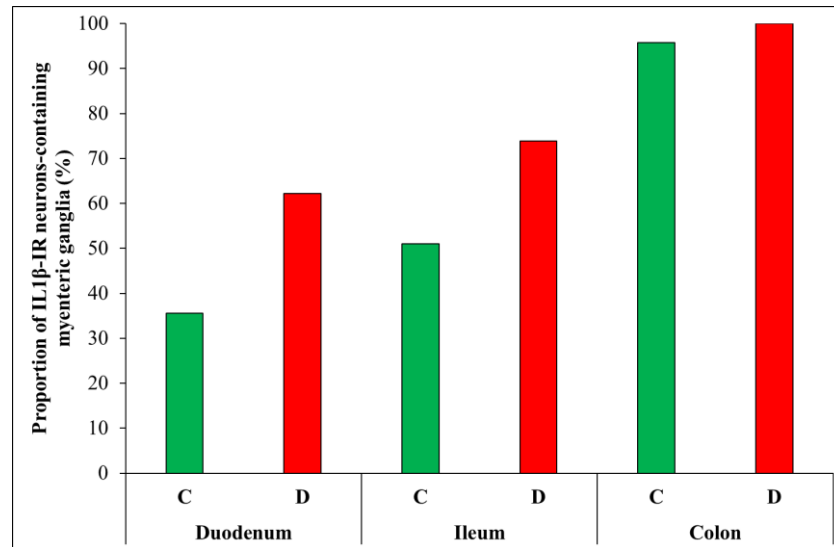


**Figure 13. Proportion of IL1 $\beta$ -immunoreactive myenteric neurons-containing ganglia in the duodenum, ileum, and colon of acute diabetic and control rats.** In controls, the proportion of IL1 $\beta$ -immunoreactive myenteric neurons-containing ganglia showed an increasing tendency from the proximal to distal parts. In the diabetic group, this proportion was increased in the duodenum and ileum compared to controls. C: controls, D: diabetics.

#### 4.2.2. Chronic diabetic rat model

In controls, similar to the acute model, the proportion of IL1 $\beta$ -IR myenteric neurons differed significantly between the small intestine and the colon. In the colon, more than 50% of the myenteric neurons were IR to IL1 $\beta$  ( $50.7 \pm 4.75\%$ ) compared to nearly 20% ( $18.97 \pm 2.05\%$ ) and 13% ( $13.11 \pm 2.93\%$ ) in the duodenum and the ileum, respectively ( $p < 0.0001$ ; Figure 14A, 14D).

In diabetic rats, a significant increase in the proportion of IL1 $\beta$ -IR myenteric neurons was apparent in all the investigated segments compared to those of controls ( $p < 0.01$ ; Figure 15). In the colon, a 20% increase resulted in more than 70% of myenteric neurons displaying immunoreactivity to IL1 $\beta$  ( $71.14 \pm 3.29\%$ ) in this gut segment, whereas this proportion almost doubled in both the duodenum ( $34.04 \pm 4.06\%$ ) and ileum ( $24.62 \pm 3.11\%$ ) compared to controls (Figure 14B, 15). Insulin-treated diabetic rats

showed no significant differences in the proportion of IL1 $\beta$ -IR myenteric neurons compared to controls which indicates that immediate insulin treatment protected the myenteric neurons from diabetic IL1 $\beta$  induction (Figure 14C, 15).

Moreover, similar to the acute diabetic model, chronic hyperglycaemic animals displayed an increase in the proportion of IL1 $\beta$ -IR myenteric neurons-containing ganglia in all gut segments despite the high baseline level that was present in controls (Figure 16). Although insulin treatment protected against the diabetes-induced increase in the neuronal IL1 $\beta$ -immunoreactivity, it did not prevent the increase in the proportion of IL1 $\beta$ -IR neurons-containing ganglia in the colon (Figure 16).

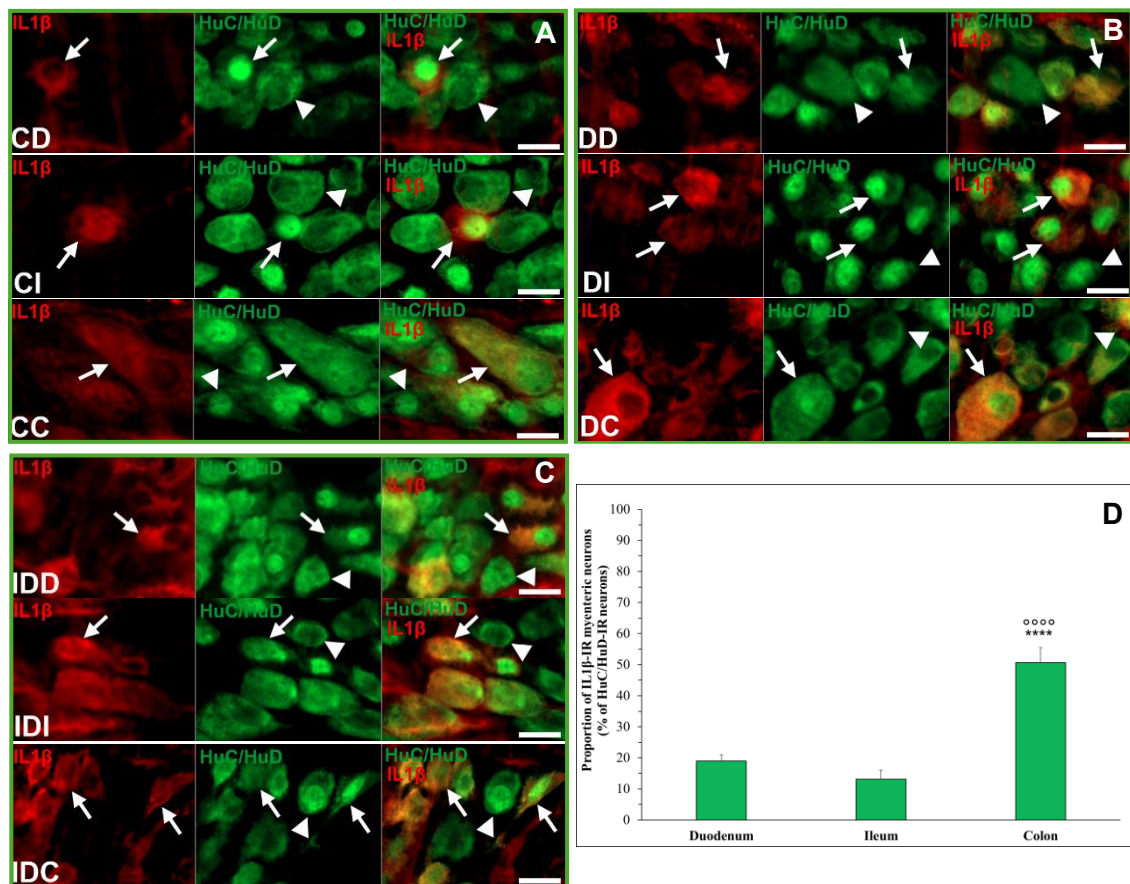


**Figure 14. Representative fluorescent micrographs of whole-mount preparations of myenteric ganglia from the duodenum, ileum, and colon of control (A), diabetic (B), and insulin-treated diabetic (C) rats after IL1 $\beta$ -HuC/HuD double-labelling immunohistochemistry.** HuC/HuD as a pan-neuronal marker was applied to label myenteric neurons. CD: control duodenum, CI: control ileum, CC: control colon, DD: diabetic duodenum, DI: diabetic ileum, DC: diabetic colon, IDD: insulin-treated diabetic duodenum, IDI: insulin-treated diabetic ileum, IDC: insulin-treated diabetic colon; arrows: IL1 $\beta$ -immunoreactive myenteric neurons, arrowheads: myenteric neurons. Scale bars: 20  $\mu$ m. **Proportion of IL1 $\beta$ -immunoreactive myenteric neurons in the duodenum, ileum, and colon of control rats (D).** A significantly higher proportion of IL1 $\beta$ -immunoreactive myenteric neurons was detected in the colon compared to the duodenum and ileum. Data are expressed as mean  $\pm$  SEM. \*\*\*\*  $p < 0.0001$  (relative to control duodenum); oooo  $p < 0.0001$  (between control ileum and colon).

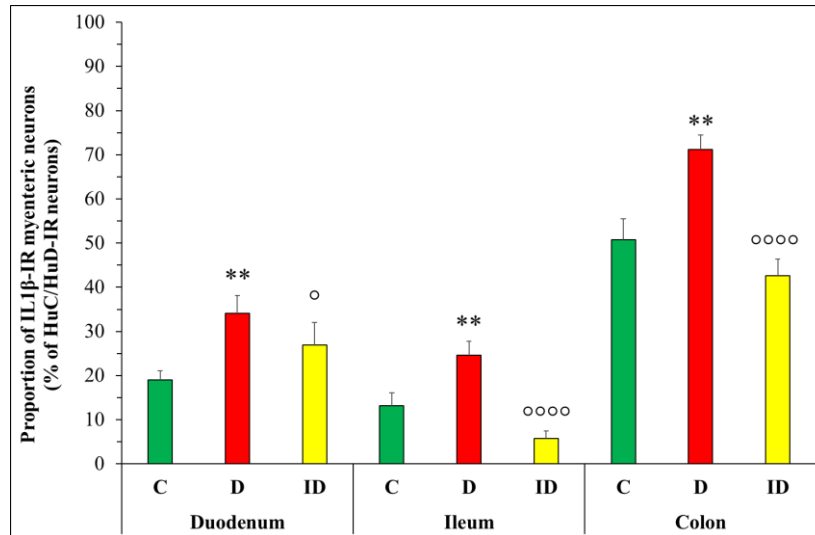


**Figure 15. Proportion of IL1 $\beta$ -immunoreactive myenteric neurons of the duodenum, ileum, and colon of control, diabetic, and insulin-treated diabetic rats.** In the diabetic group, the proportion of IL1 $\beta$ -immunoreactive myenteric neurons was significantly increased in all gut segments. Data are expressed as mean  $\pm$  SEM. \*\*  $p < 0.01$  (relative to controls); °  $p < 0.05$ , °°°°  $p < 0.0001$  (between diabetics and insulin-treated diabetics). C: controls, D: diabetics, ID: insulin-treated diabetics.

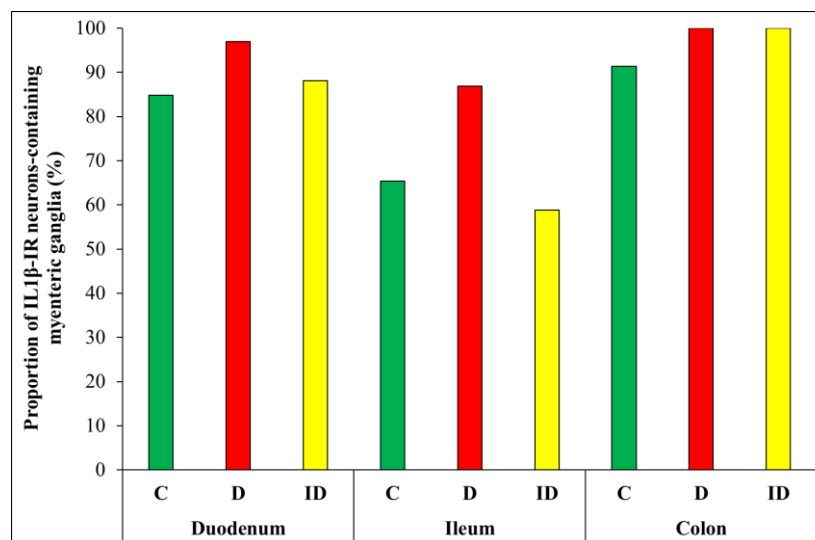


**Figure 16. Proportion of IL1 $\beta$ -immunoreactive myenteric neurons-containing ganglia in the duodenum, ileum, and colon of control, diabetic, and insulin-treated diabetic rats.** In controls, the proportion of IL1 $\beta$ -immunoreactive myenteric neurons-containing ganglia was the lowest in the ileum and the highest in the colon. In the diabetic group, this proportion was increased in all gut segments. Insulin treatment did reverse the diabetes-induced increase in the proportion of IL1 $\beta$ -immunoreactive myenteric neurons-containing ganglia only in the small intestine. C: controls, D: diabetics, ID: insulin-treated diabetics.

#### 4.3. Effect of chronic hyperglycaemia on the proportion of interleukin 1 $\beta$ -immunoreactive nNOS neurons

The localization of IL1 $\beta$  in the nitergic neuronal population was analysed after double-labelling fluorescent immunohistochemistry of IL1 $\beta$  and nNOS on whole-mount preparations of the myenteric plexus (Figure 17).

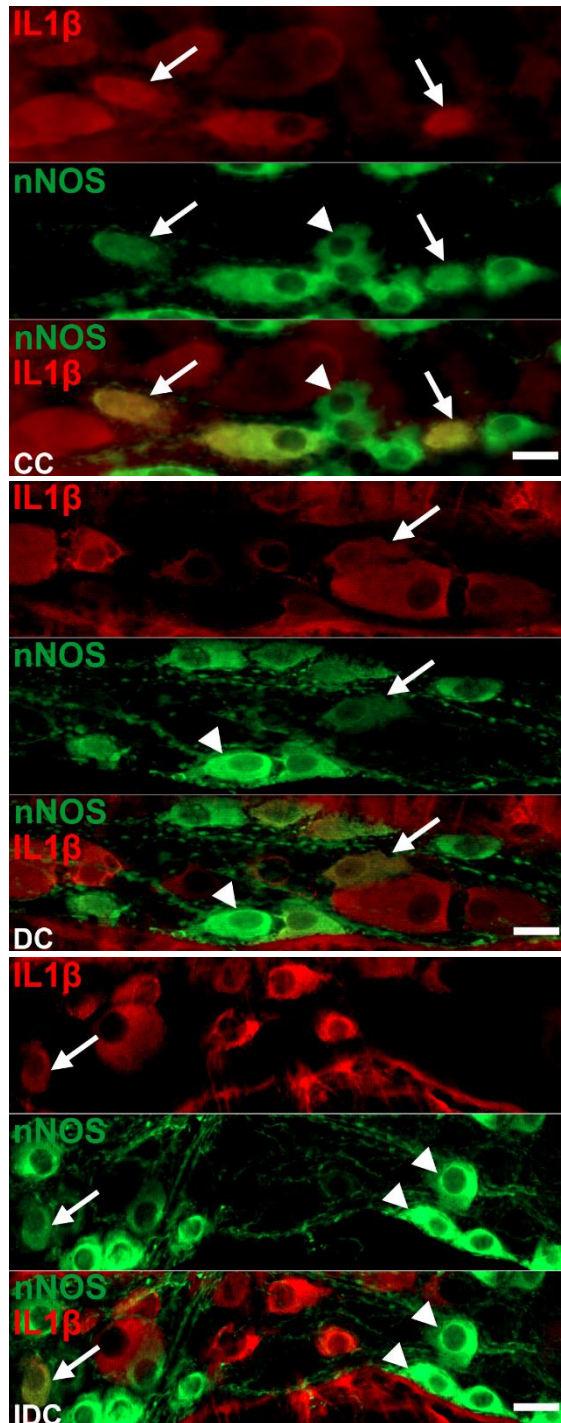


**Figure 17. Representative fluorescent micrographs of whole-mount preparations of myenteric ganglia from the colon of control, diabetic, and insulin-treated diabetic rats after IL1 $\beta$ -nNOS double-labelling immunohistochemistry.** CC: control colon, DC: diabetic colon, IDC: insulin-treated diabetic colon; arrows: IL1 $\beta$ -nNOS-immunoreactive myenteric neurons, arrowheads: nNOS-immunoreactive neurons. Scale bars: 20  $\mu$ m.

In controls, the proportion of IL1 $\beta$ -nNOS-IR neurons per total nNOS-IR myenteric neurons was the lowest in the duodenum ( $12.64 \pm 2.03\%$ ) and significantly higher in the distal segments (ileum:  $36.36 \pm 2.18\%$ ; colon:  $26.21 \pm 2.13\%$ ,  $p < 0.0001$ ; Figure 18).

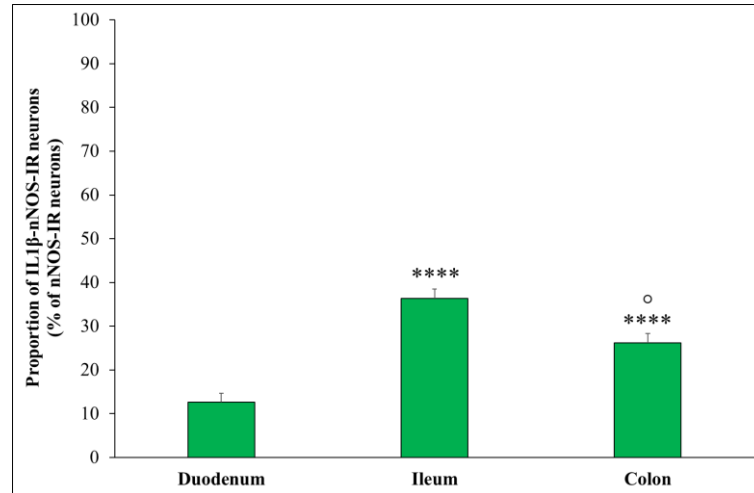


**Figure 18. Proportion of IL1 $\beta$ -nNOS-immunoreactive neurons related to the total number of nNOS-immunoreactive neurons in the myenteric ganglia of the duodenum, ileum, and colon of control rats.** A significantly lower proportion of IL1 $\beta$ -nNOS-immunoreactive myenteric neurons was detected in the duodenum compared to the ileum and colon of controls. Data are expressed as mean  $\pm$  SEM; \*\*\*\*  $p < 0.0001$  (relative to control duodenum); °  $p < 0.05$  (between control ileum and colon).

In the diabetic group, the proportion of IL1 $\beta$ -nNOS-IR neurons of total nNOS-IR myenteric neurons was significantly induced only in the colon relative to controls ( $36.94 \pm 2.76\%$  vs  $26.21 \pm 2.13\%$ ,  $p < 0.01$ ; Figure 19A), with no alterations detected in the other gut segments. Insulin treatment did not prevent the diabetic induction of IL1 $\beta$ -nNOS-IR myenteric neuronal proportion of the colon and reduced that in the ileum (Figure 19A).

To investigate the population of IL1 $\beta$ -IR neurons representing nitrergic subsets, we calculated the proportion of IL1 $\beta$ -nNOS-IR neurons per total IL1 $\beta$ -IR myenteric neurons. In controls, this proportion ranged between 40% to 50% in all gut segments (Figure 19B). In diabetics, there was a significant decrease in the proportion of IL1 $\beta$ -nNOS-IR neurons related to the total IL1 $\beta$ -IR neurons in the small intestine (duodenum:  $26.77 \pm 2.46\%$  vs  $40.1 \pm 3.65\%$ ,  $p < 0.05$ ; ileum:  $31.88 \pm 2.41\%$  vs  $43.48 \pm 2.37\%$ ,  $p < 0.05$ ), whereas diabetes did not affect that in the colonic segment compared to controls. Insulin treatment was beneficial both in the duodenum and ileum (Figure 19B).

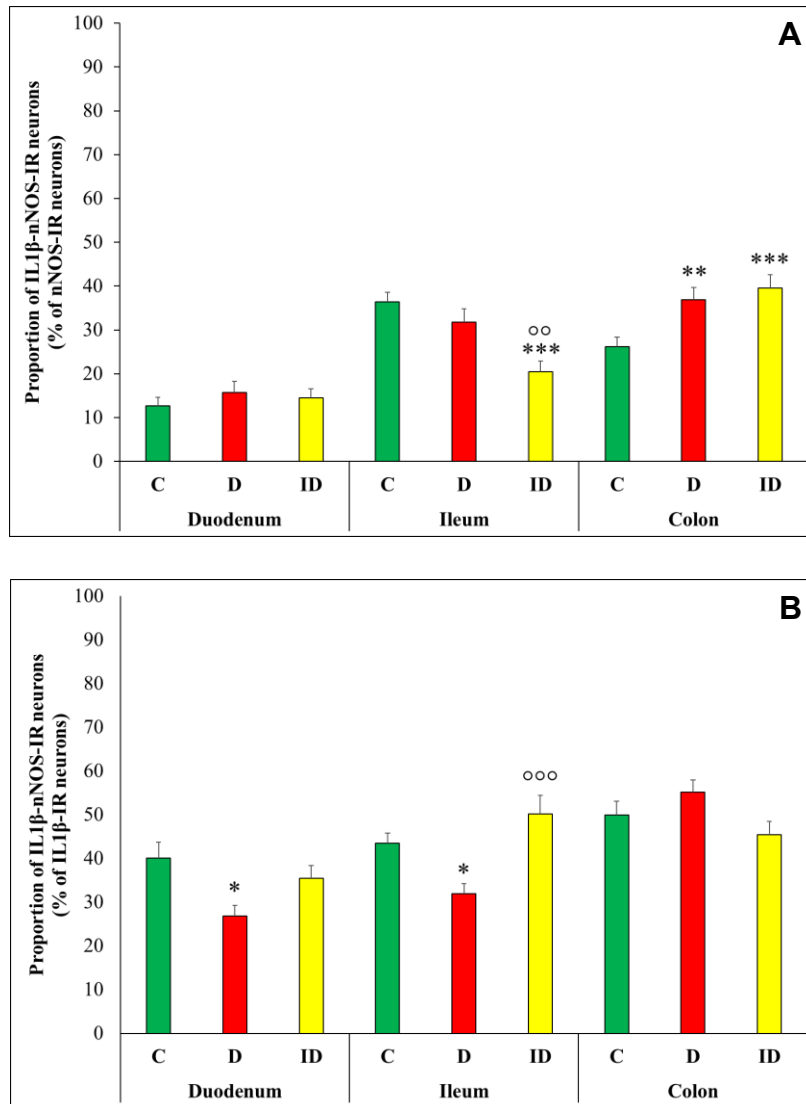


**Figure 19. Proportion of IL1β-nNOS-immunoreactive neurons related to the total number of nNOS-immunoreactive neurons in the myenteric ganglia of the duodenum, ileum, and colon of control, diabetic, and insulin-treated diabetic rats (A).** The proportion of IL1β-nNOS-immunoreactive neurons was significantly increased only in the colon of diabetics compared to controls. **Proportion of IL1β-nNOS-immunoreactive neurons related to the total number of IL1β-immunoreactive neurons in the myenteric ganglia of the duodenum, ileum, and colon of control, diabetic, and insulin-treated diabetic rats (B).** A significant decrease in the proportion of IL1β-nNOS-immunoreactive neurons was detected in the duodenum and the ileum of diabetics compared to controls. Data are expressed as mean ± SEM. \*  $p < 0.05$ , \*\*  $p < 0.01$ , \*\*\*  $p < 0.001$  (relative to controls); °°  $p < 0.01$ , °°°  $p < 0.001$  (between diabetics and insulin-treated diabetics). C: controls, D: diabetics, ID: insulin-treated diabetics.

Lastly, from those ganglia that are IR to IL1 $\beta$ , we calculated the proportion of IL1 $\beta$ -nNOS-IR neurons-containing myenteric ganglia. In controls, this value was higher in the distal parts (ileum: 97.06% and colon: 95.16%) compared to 72.54% in the duodenum. In diabetics, the proportion of IL1 $\beta$ -nNOS-IR neurons-containing myenteric ganglia was reduced in the duodenum and ileum compared to controls (65.63% and 88.24%, respectively), whereas it was somewhat increased in the colon (98.36%; Figure 20). In the insulin-treated diabetics, while the duodenal and ileal gut segments had lower proportions than that of controls (67.86% and 81.67%, respectively), the colonic proportion reached 100% (Figure 20).

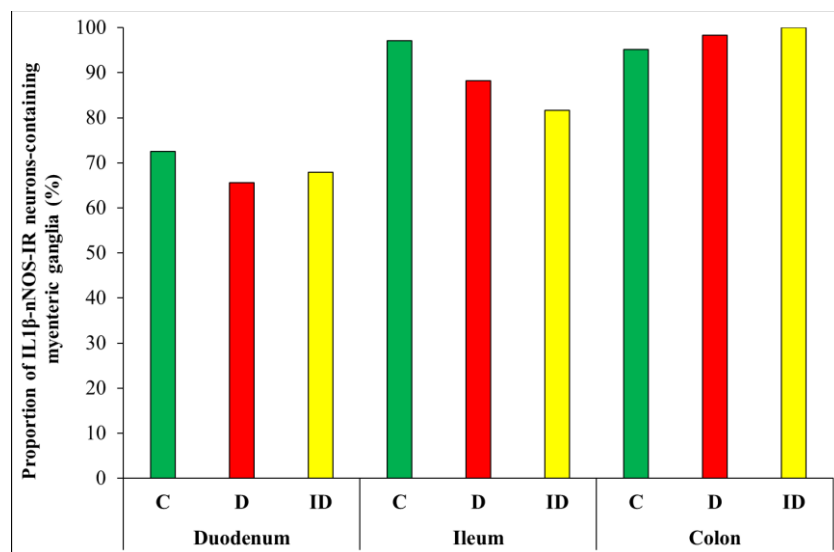


**Figure 20. Proportion of IL1 $\beta$ -nNOS-immunoreactive myenteric neurons-containing ganglia in the duodenum, ileum, and colon of control, diabetic, and insulin-treated diabetic rats.** Data were obtained by calculating the percentage (%) of the number of IL1 $\beta$ -nNOS-immunoreactive myenteric neurons-containing ganglia per the number of IL1 $\beta$ -immunoreactive ganglia. C: controls, D: diabetics, ID: insulin-treated diabetics.

#### 4.4. Effect of chronic hyperglycaemia on the proportion of interleukin 1 $\beta$ -immunoreactive CGRP neurons

Myenteric neurons which are IR for IL1 $\beta$  and CGRP were visualized using double-labelling fluorescent immunohistochemistry on whole-mount preparations (Figure 21).

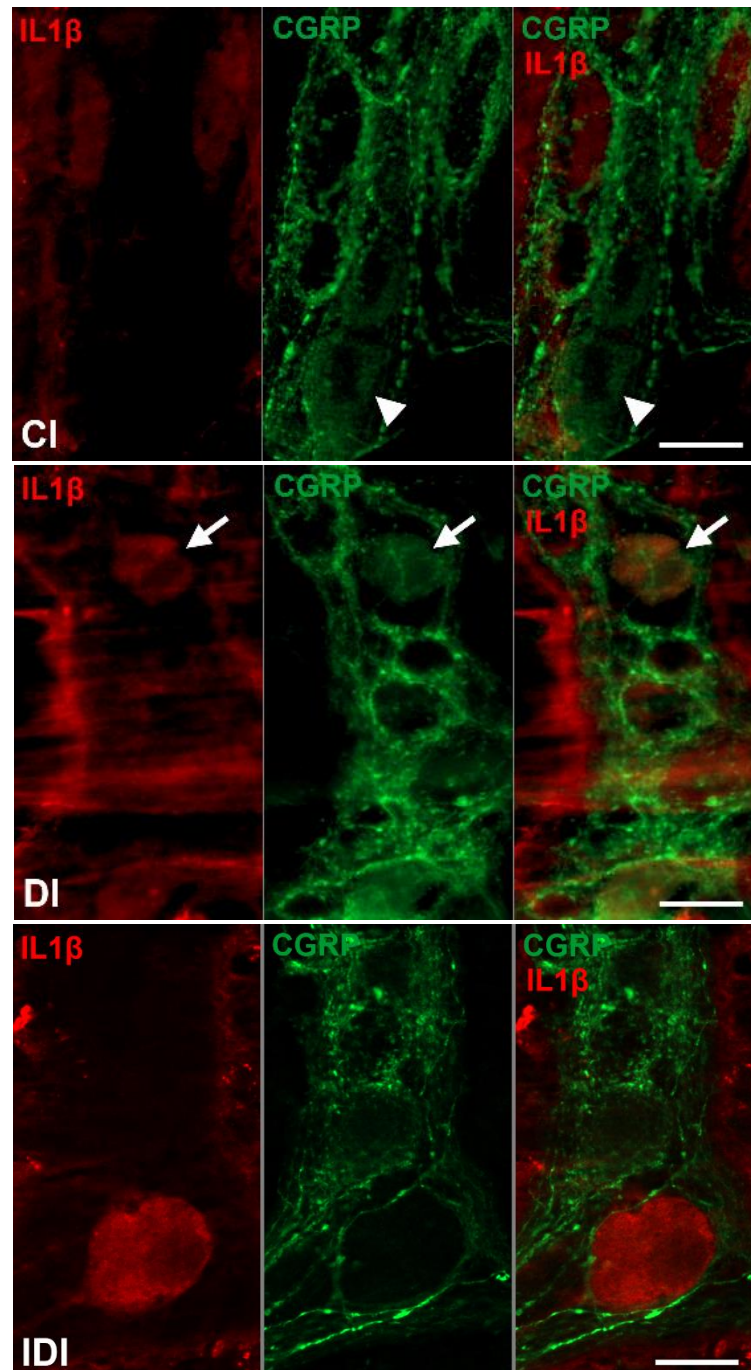


**Figure 21.** Representative fluorescent micrographs of whole-mount preparations of myenteric ganglia from the ileum of control, diabetic, and insulin-treated diabetic rats after IL1 $\beta$ -CGRP double-labelling immunohistochemistry. CI: control ileum, DI: diabetic ileum, IDI: insulin-treated diabetic ileum; arrows: IL1 $\beta$ -CGRP-immunoreactive myenteric neurons, arrowheads: CGRP-immunoreactive neurons. Scale bars: 20  $\mu$ m.

In control animals, the proportion of IL1 $\beta$ -CGRP-IR neurons per total CGRP-IR myenteric neurons ranged between 40-50% in all gut segments (Figure 22A). In diabetics, the ileum was the only gut segment where this proportion was significantly increased compared to controls ( $64.56 \pm 4.17\%$  vs  $42.13 \pm 3.8\%$ ,  $p < 0.01$ ; Figure 22A). Insulin treatment partially prevented the diabetes-induced changes in the ileum and significantly increased IL1 $\beta$ -CGRP-IR neuronal proportion in the colon ( $77.42 \pm 3.84\%$ ) compared to both controls ( $47.76 \pm 4.36\%$ ,  $p < 0.0001$ ) and diabetics ( $56.2 \pm 3.24\%$ ,  $p < 0.001$ ; Figure 22A).

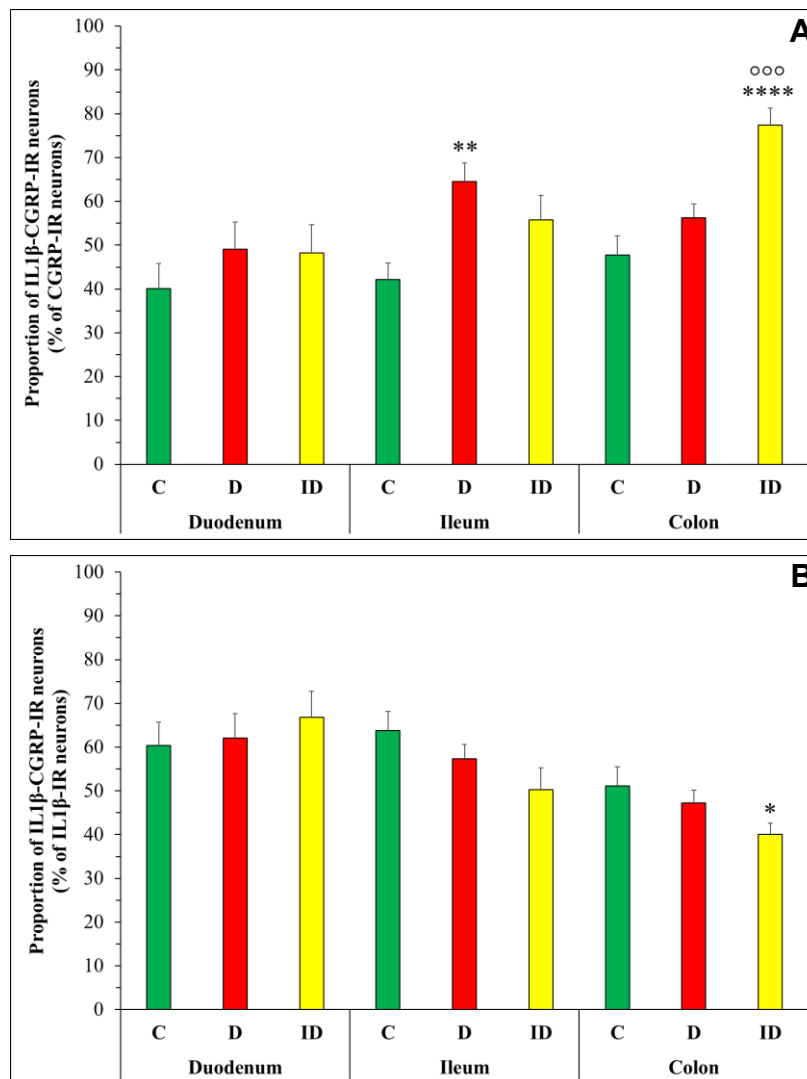


**Figure 22. Proportion of IL1 $\beta$ -CGRP-immunoreactive neurons related to the total number of CGRP-immunoreactive neurons in the myenteric ganglia of the duodenum, ileum, and colon of control, diabetic, and insulin-treated diabetic rats (A). The proportion of IL1 $\beta$ -CGRP-immunoreactive neurons significantly increased only in the ileum of diabetics relative to controls. Proportion of IL1 $\beta$ -CGRP-immunoreactive neurons related to the total number of IL1 $\beta$ -immunoreactive neurons in the myenteric ganglia of the duodenum, ileum, and colon of control, diabetic, and insulin-treated diabetic rats (B). Data are expressed as mean  $\pm$  SEM. \*  $p < 0.05$ , \*\*  $p < 0.01$ , \*\*\*\*  $p < 0.0001$  (relative to controls); <sup>ooo</sup>  $p < 0.001$  (between diabetics and insulin-treated diabetics).**

Considering the other aspects, the proportion of IL1 $\beta$ -CGRP-IR neurons per total IL1 $\beta$ -IR myenteric neurons ranged between 50-60% in controls and was slightly higher in the small intestine compared to the colon (Figure 22B). Diabetes did not alter the proportion of IL1 $\beta$ -CGRP-IR neurons per total IL1 $\beta$ -IR myenteric neurons in the investigated segments. However, this proportion was reduced in the colonic segments of insulin-treated diabetic rats compared to controls ( $40.03 \pm 2.64\%$  vs  $51.16 \pm 4.3\%$ ,  $p < 0.05$ ; Figure 22B).

Lastly, the proportion of IL1 $\beta$ -CGRP-IR neurons-containing ganglia was displayed (Figure 23). In all the investigated segments, more than 85% of IL1 $\beta$ -IR myenteric ganglia contained at least one IL1 $\beta$ -CGRP-IR neuron, with slight variations among the different experimental conditions (Figure 23). Under hyperglycaemia, the proportion of IL1 $\beta$ -CGRP-IR neurons-containing ganglia was slightly decreased in the duodenum of diabetics (86.1%) compared to controls (94.4%), whereas it was slightly increased in the diabetic colon compared to controls (98.36% vs 88.37%, Figure 23).

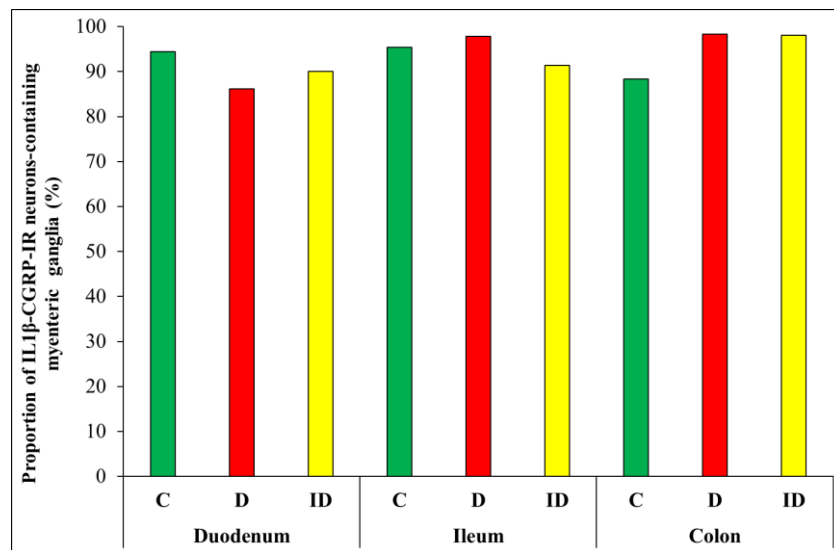


**Figure 23. Proportion of IL1 $\beta$ -CGRP-immunoreactive myenteric neurons-containing ganglia in the duodenum, ileum, and colon of control, diabetic, and insulin-treated diabetic rats.** Data were obtained by calculating the percentage (%) of the number of IL1 $\beta$ -CGRP-immunoreactive myenteric neurons-containing ganglia per the number of IL1 $\beta$ -immunoreactive ganglia. C: controls, D: diabetics, ID: insulin-treated diabetics.

## 4.5. Effect of hyperglycaemia on interleukin 1 $\beta$ protein levels

### 4.5.1. Tissue level of interleukin 1 $\beta$ in colonic muscle/myenteric plexus homogenates

Since the proportion of the IL1 $\beta$ -IR myenteric neurons was the highest in the colonic gut samples under control conditions, this gut segment was used to measure IL1 $\beta$  concentration in tissue homogenates that contained the intestinal smooth muscle and the myenteric plexus. IL1 $\beta$  protein concentration per total protein content was at lower levels in the control samples of the chronic experiment (Figure 24). Diabetes resulted in a 5-fold increase in the IL1 $\beta$  level in the colon compared to controls ( $0.94 \pm 0.26$  ng/mg vs  $0.29 \pm 0.04$  ng/mg,  $p < 0.05$ ) which was abolished in the insulin-treated group ( $0.40 \pm 0.03$  ng/mg; Figure 24).

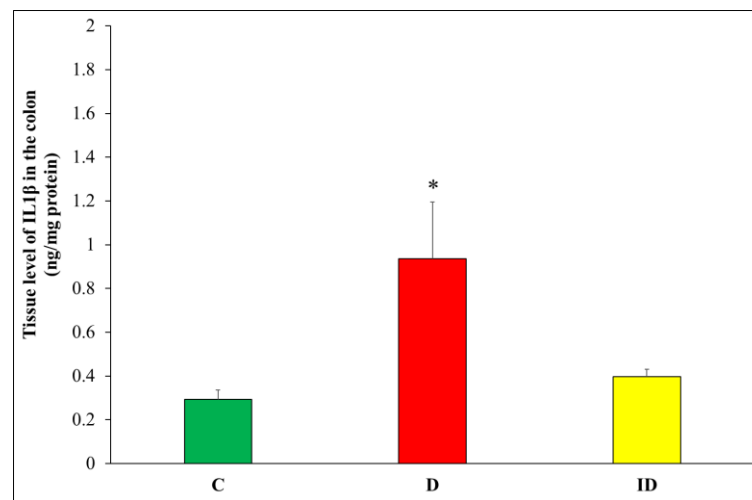


**Figure 24.** Tissue level of IL1 $\beta$  in intestinal smooth muscle layer homogenates including the myenteric plexus from the colon of control, diabetic, and insulin-treated diabetic rats. The IL1 $\beta$  tissue level was significantly increased in diabetics relative to controls, which was prevented by insulin treatment. Data are expressed as mean  $\pm$  SEM. \*  $p < 0.05$  (relative to controls). C: controls, D: diabetics, ID: insulin-treated diabetics.

### 4.5.2. Levels of interleukin 1 $\beta$ in the pancreatic tissue and serum

IL1 $\beta$  levels in the pancreatic tissues and sera were also measured in the acute and chronic diabetic rat models (Figure 25). Pancreatic tissue level of IL1 $\beta$  was significantly increased in the diabetics of acute hyperglycaemic animals compared to controls ( $6.54 \pm 1.84$  ng/mg vs  $1.08 \pm 0.34$  ng/mg,  $p < 0.05$ ), however, in the chronic experimental groups neither the diabetics nor the insulin-treated diabetics showed any significant changes in IL1 $\beta$  levels relative to controls ( $2.43 \pm 0.74$  ng/mg vs  $2.03 \pm 0.66$  ng/mg; Figure 25A).

Serum IL1 $\beta$  levels from the acute and chronic diabetics were slightly increased compared to their control counterparts (acute:  $8.24 \pm 0.57$  ng/ml vs  $6.62 \pm 0.74$  ng/ml; chronic:  $6.36 \pm 0.42$  ng/ml vs  $5.31 \pm 0.34$  ng/ml) with no significant changes (Figure 25B).

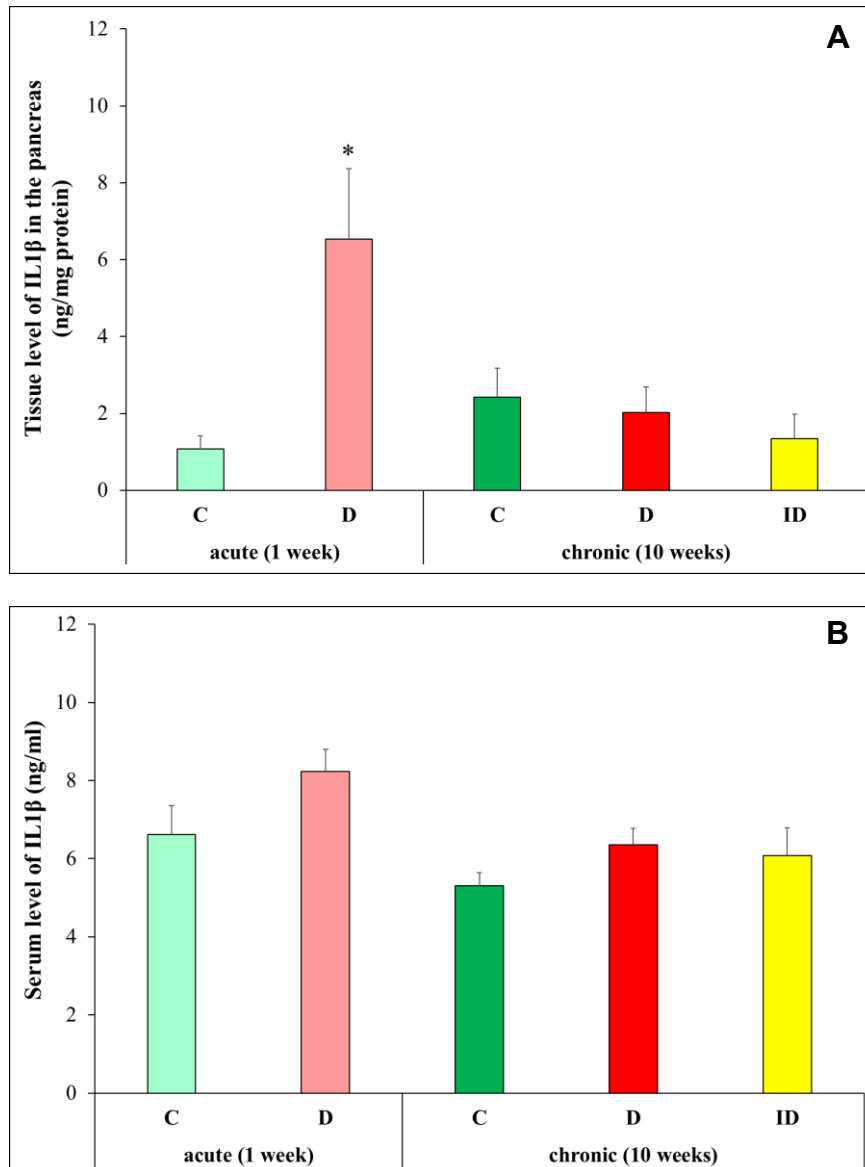


**Figure 25. Pancreatic (A) and serum (B) levels of IL1 $\beta$  of control, diabetic, and insulin-treated diabetic rats of acute and chronic experimental models.** **A:** Pancreatic tissue level of IL1 $\beta$  was significantly increased in the diabetics of acute but not chronic hyperglycaemic model. **B:** No significant changes were observed in the concentration of serum IL1 $\beta$  either among the experimental groups or between acute and chronic experimental animals. Data are expressed as mean  $\pm$  SEM. \*  $p < 0.05$  (relative to controls). C: controls, D: diabetics, ID: insulin-treated diabetics.

#### 4.6. Effect of chronic hyperglycaemia on the expression of interleukin 1 $\beta$ mRNA

IL1 $\beta$  mRNA level detected by RNAscope on cryosections in controls revealed variations in IL1 $\beta$  mRNA dots/mm<sup>2</sup> depending on the investigated gut segment and the intestinal wall layer (Figures 26-28). The number of punctate dots labelling IL1 $\beta$  mRNA was the lowest in the intestinal smooth muscle layer in all gut segments of control rats, while it was highest in the myenteric ganglia of the duodenum and colon (3400  $\pm$  429 dots/mm<sup>2</sup> and 3361  $\pm$  279.5 dots/mm<sup>2</sup>, respectively). In the ileum, the highest value was measured in the mucosa (4558  $\pm$  486.7 dots/mm<sup>2</sup>), which was roughly double that of the duodenum and colon (Table 5).

**Table 5. Quantitative evaluation of IL1 $\beta$  mRNA labelling dots in different intestinal wall layers and gut segments of control rats.**

	<b>Duodenum</b> (dots/mm <sup>2</sup> )	<b>Ileum</b> (dots/mm <sup>2</sup> )	<b>Colon</b> (dots/mm <sup>2</sup> )
<b>Myenteric ganglia</b>	3400 $\pm$ 429	2420 $\pm$ 486.7	3361 $\pm$ 279.5
<b>Smooth muscle</b>	1251 $\pm$ 181.5 <sup>b</sup>	1629 $\pm$ 257.7	1080 $\pm$ 146 <sup>c</sup>
<b>Mucosa</b>	1948 $\pm$ 281.4	4558 $\pm$ 486.7 <sup>a,e,f</sup>	2549 $\pm$ 279.5 <sup>d,g</sup>

Data are expressed as mean  $\pm$  SEM; <sup>a</sup>  $p < 0.05$ , <sup>b</sup>  $p < 0.001$ , <sup>c</sup>  $p < 0.0001$  vs myenteric ganglia in the same gut segment; <sup>d</sup>  $p < 0.01$ , <sup>e</sup>  $p < 0.001$  vs smooth muscle in the same gut segment; <sup>f</sup>  $p < 0.001$  vs duodenum in the same intestinal layer; <sup>g</sup>  $p < 0.01$  vs ileum in the same intestinal layer.

In the myenteric ganglia of diabetic rats, the number of IL1 $\beta$  mRNA labelling dots was significantly increased in all gut segments ( $p < 0.05$ ); the greatest increase was observed in the duodenum where the dot density was almost tripled (Figure 27A). In the same gut region of insulin-treated diabetic rats, the number of dots remained at control level (Figure 27A). The number of IL1 $\beta$  mRNA labelling dots in the intestinal smooth muscle of diabetics increased by a lesser extent as well, and this change was significant in the duodenum and colon ( $p < 0.05$ ; Figure 27B).

In the mucosa of diabetics, IL1 $\beta$  mRNA expression varied differently in different gut segments (Figure 28). A robust, more than five times increase in dot number was observed in the duodenum ( $p < 0.0001$ ), and almost double in the ileum ( $p < 0.05$ ), however, no change was detected in the colonic mucosa (Figure 28B). Insulin treatment completely prevented the diabetic alterations in the ileum and partially in the duodenum (Figure 28B).

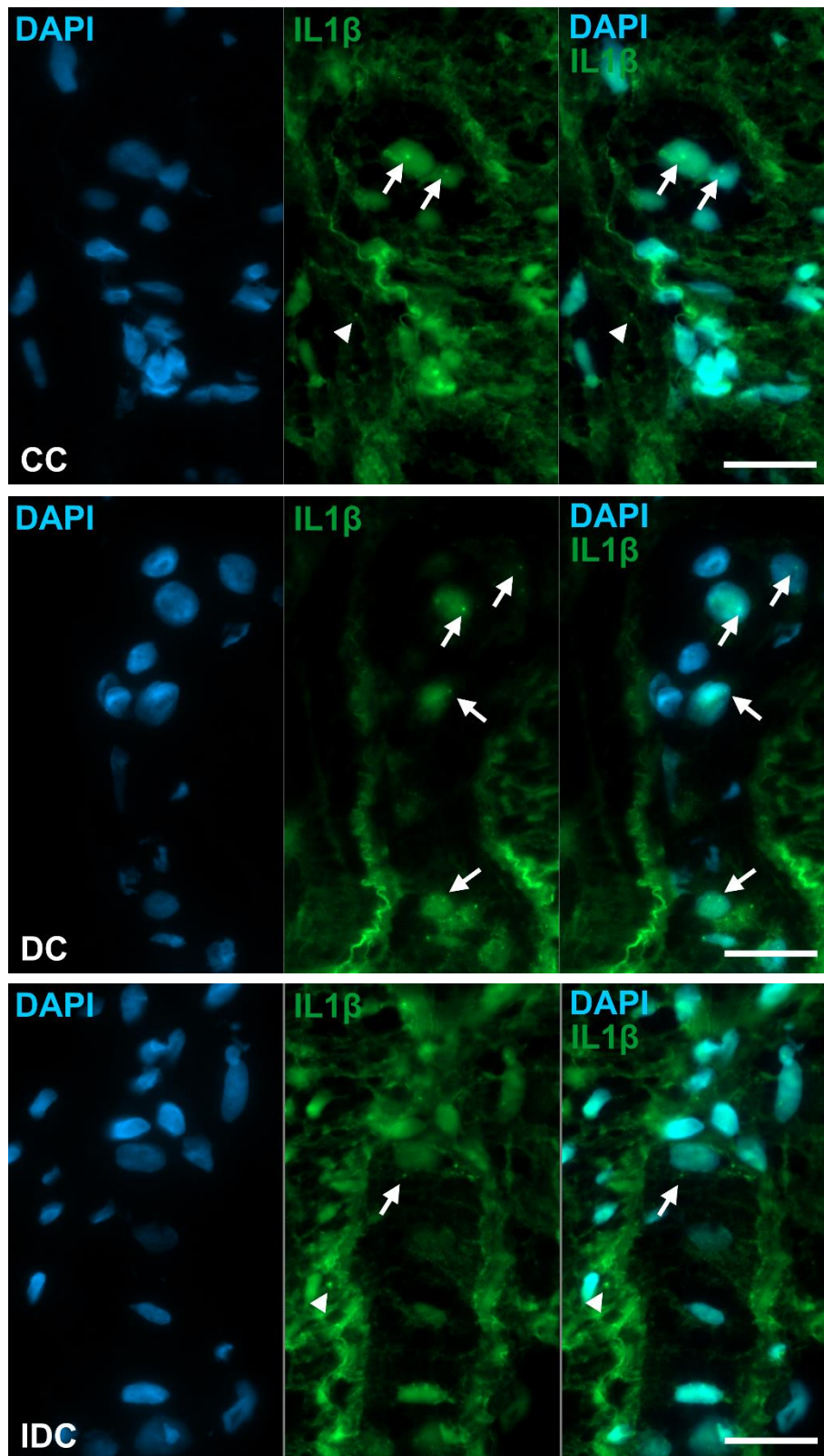


**Figure 26. Representative micrographs of cryosections of myenteric ganglia from the colon of control, diabetic, and insulin-treated diabetic rats after IL1 $\beta$  RNAscope. IL1 $\beta$  mRNA appear as green punctate dots in the myenteric ganglia (arrows) and smooth muscle (arrowheads), nuclei were counterstained with DAPI (blue). CC: control colon, DC: diabetic colon, IDC: insulin-treated diabetic colon. Scale bars: 20  $\mu$ m.**

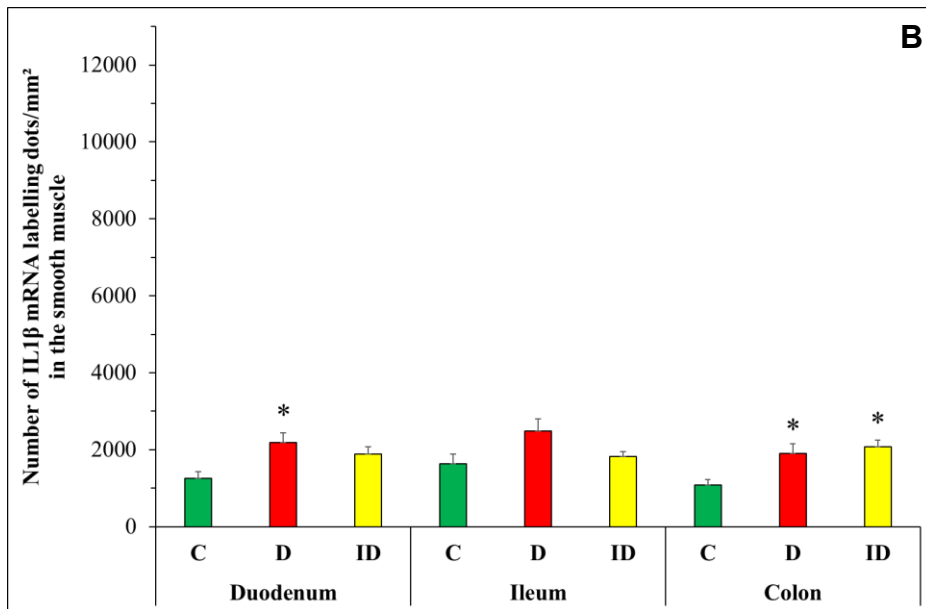
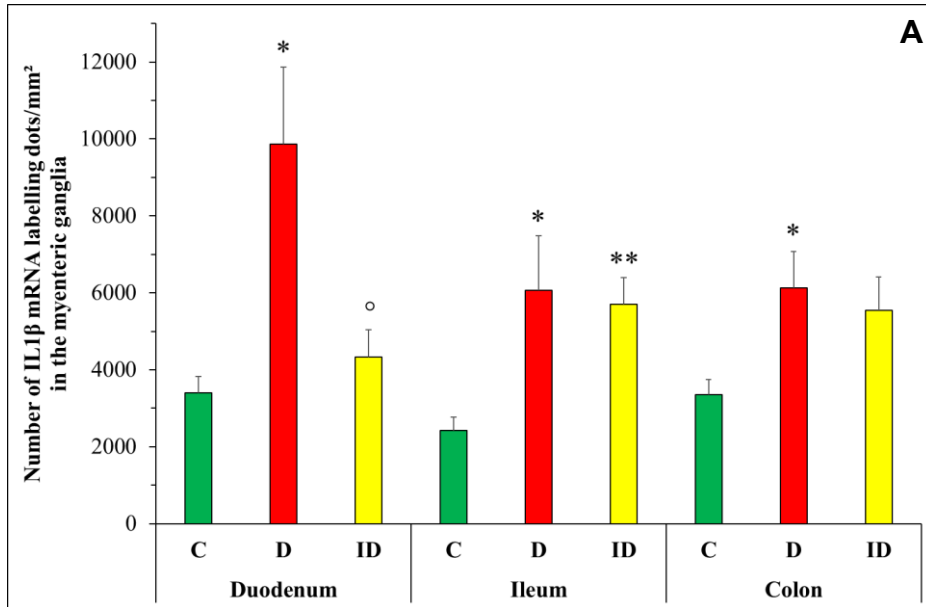


**Figure 27. Expression of IL1 $\beta$  mRNA in the myenteric ganglia (A) and smooth muscle (B) of the duodenum, ileum, and colon of control, diabetic, and insulin-treated diabetic rats. A:** The number of IL1 $\beta$  mRNA dots was significantly increased in the myenteric ganglia of all gut segments of diabetics relative to controls. Insulin treatment was most beneficial in the duodenum. **B:** IL1 $\beta$  mRNA level of smooth muscle was significantly increased in the duodenum and colon of diabetics relative to controls. Data are expressed as mean  $\pm$  SEM. \*  $p < 0.05$ , \*\*  $p < 0.01$  (relative to controls); °  $p < 0.05$  (between diabetics and insulin-treated diabetics). C: controls, D: diabetics, ID: insulin-treated diabetics.

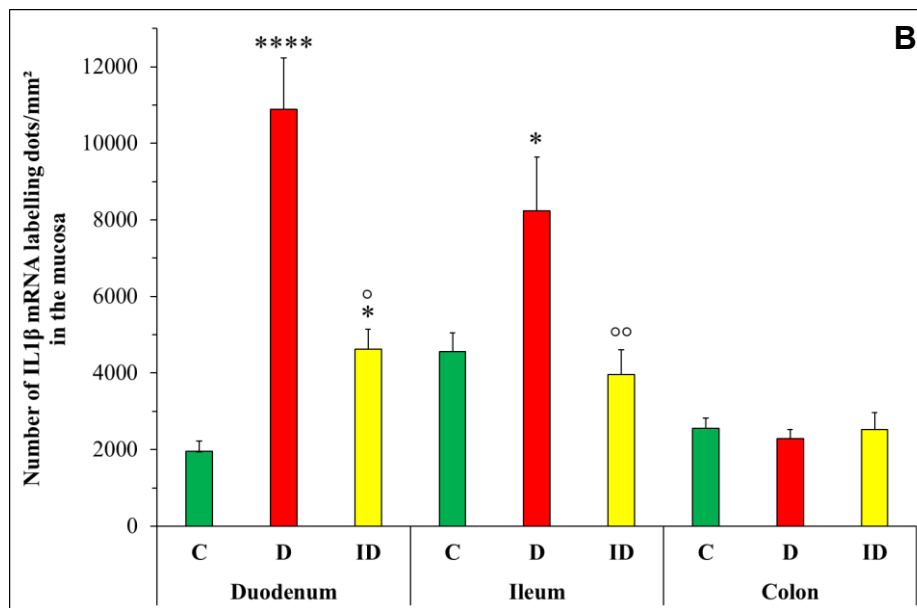
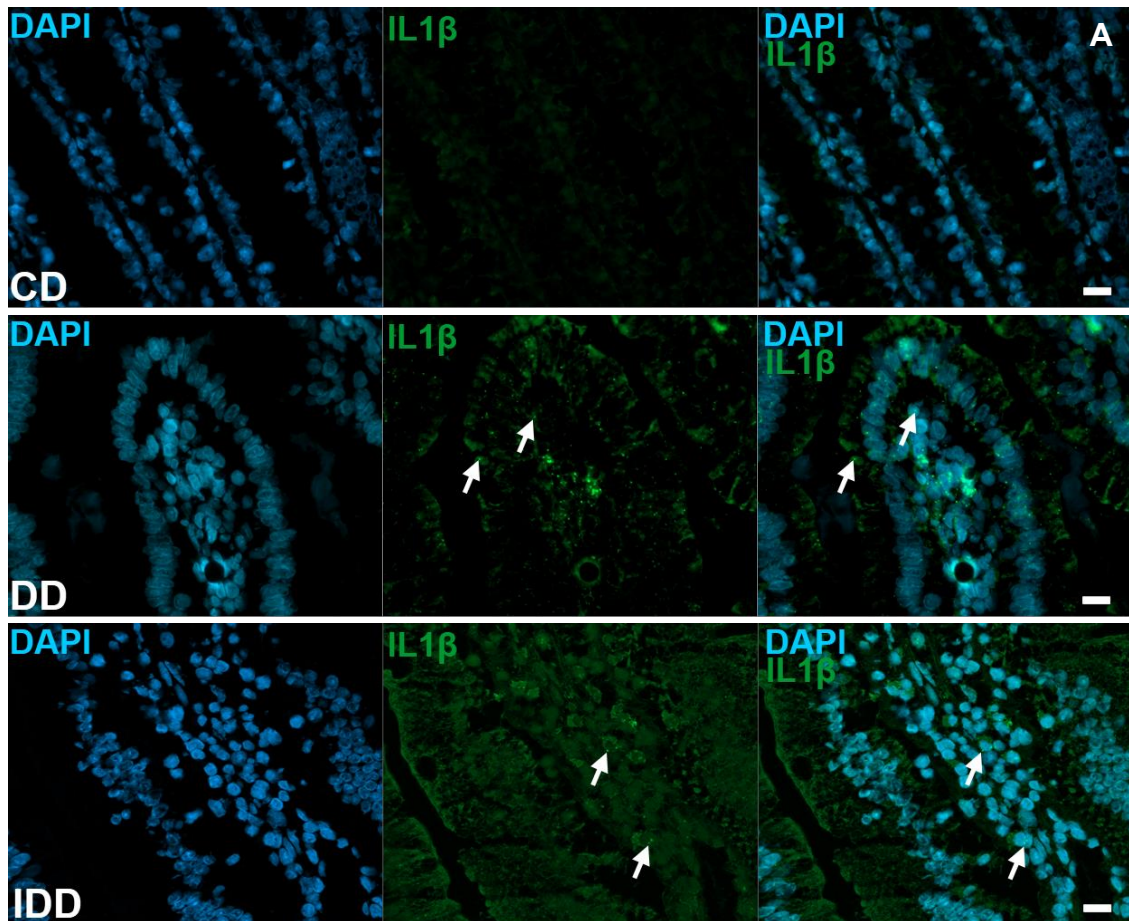


**Figure 28. Representative micrographs of cryosections of mucosa from the duodenum of control, diabetic, and insulin-treated diabetic rats after IL1 $\beta$  RNAscope (A).** IL1 $\beta$  mRNA appear as green punctate dots (arrows), nuclei were counterstained with DAPI (blue). CD: control duodenum, DD: diabetic duodenum, IDD: insulin-treated diabetic duodenum. Scale bars: 20  $\mu$ m. **Expression of IL1 $\beta$  mRNA in the intestinal mucosa of the duodenum, ileum, and colon of control, diabetic, and insulin-treated diabetic rats (B).** IL1 $\beta$  mRNA level in the mucosa was significantly increased in the small intestine of diabetics relative to controls. Insulin treatment completely prevented the diabetic alterations in the ileum and partially in the duodenum. Data are expressed as mean  $\pm$  SEM. \*  $p < 0.05$ , \*\*\*\*  $p < 0.0001$  (relative to controls); °  $p < 0.05$ , °°  $p < 0.01$  (between diabetics and insulin-treated diabetics). C: controls, D: diabetics, ID: insulin-treated diabetics.

Cryosections from the pancreas of different experimental groups were also utilized to quantify IL1 $\beta$  mRNA expression using IL1 $\beta$  RNAscope technique (Figure 29). Diabetes robustly increased the expression of pancreatic IL1 $\beta$  mRNA compared to controls ( $23061 \pm 708.5$  dots/mm $^2$  vs  $3236 \pm 267.6$  dots/mm $^2$ ,  $p < 0.0001$ ; Figure 30). The insulin-treated group showed a significant decrease in pancreatic IL1 $\beta$  mRNA compared to untreated diabetics ( $7918 \pm 593.7$  dots/mm $^2$ ,  $p < 0.0001$ ), however, this value was still significantly higher than that of controls ( $p < 0.001$ ; Figure 30).

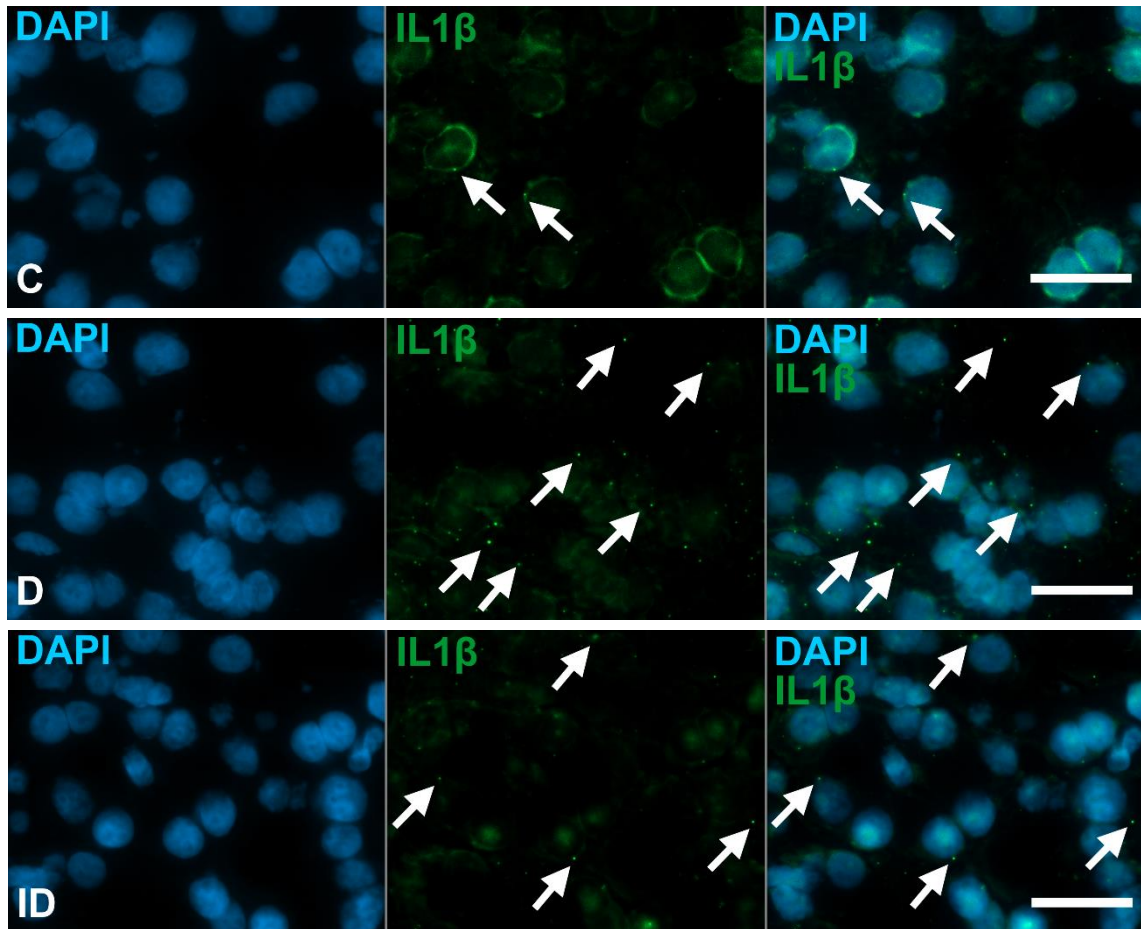


**Figure 29.** Representative micrographs of cryosections of the pancreas from control, diabetic, and insulin-treated diabetic rats after IL1 $\beta$  RNAscope. IL1 $\beta$  mRNA appear as green punctuate dots (arrows), nuclei were counterstained with DAPI (blue). C: controls, D: diabetics, ID: insulin-treated diabetics. Scale bars: 20  $\mu$ m.

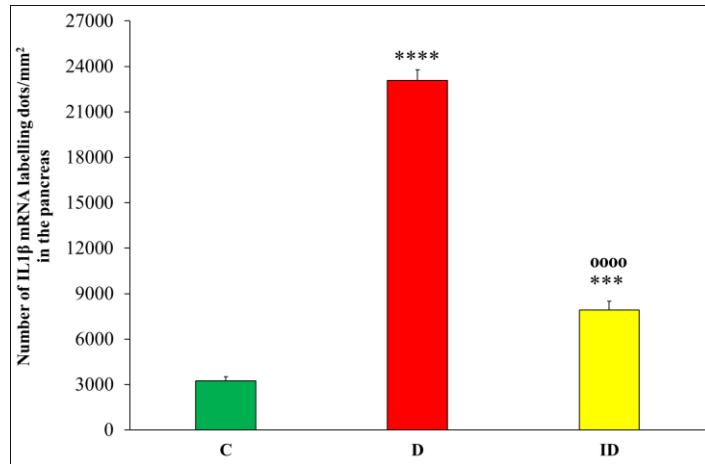


**Figure 30. Expression of IL1 $\beta$  mRNA in the pancreas of control, diabetic, and insulin-treated diabetic rats after IL1 $\beta$  RNAscope.** Diabetes robustly increased the number of IL1 $\beta$  mRNA dots, and insulin treatment partially protected against the diabetes-induced increase in IL1 $\beta$  mRNA level. Data are expressed as mean  $\pm$  SEM. \*\*\*  $p < 0.001$ , \*\*\*\*  $p < 0.0001$  (relative to controls); 0000  $p < 0.0001$  (between diabetics and insulin-treated diabetics). C: controls, D: diabetics, ID: insulin-treated diabetics.

#### 4.7. NLRP3 immunoreactivity and localization in the myenteric neurons

The presence of NLRP3 immunoreactivity was detected in the myenteric neurons of the duodenum, ileum, and colon of experimental animals after NLRP3-HuC/HuD double-labelling fluorescent immunohistochemistry. Neuronal varicosities were largely IR to NLRP3 (Figure 31).

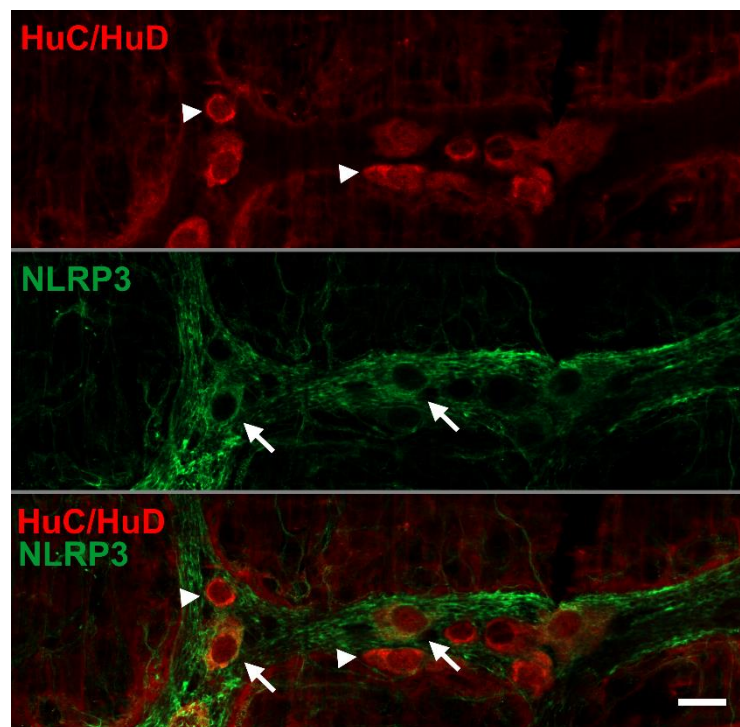


**Figure 31. Representative fluorescent micrograph of a whole-mount preparation of myenteric ganglia from the ileum of a control rat after NLRP3-HuC/HuD double-labelling immunohistochemistry.** HuC/HuD as a pan-neuronal marker was applied to label myenteric neurons. Arrows: NLRP3-immunoreactive myenteric neurons, arrowheads: myenteric neurons. Scale bar: 20  $\mu$ m.

#### 4.8. Quantitative evaluation of NLRP3 density within the myenteric ganglia

Immunogold electron microscopy was used to quantify NLRP3 protein expression and investigate its subcellular localization in the myenteric ganglia of the different gut segments of control, diabetic, and insulin-treated diabetic rats (Figure 32, 33A). NLRP3 gold labels appeared in the cytosol of the perikarya, inside or in close vicinity to mitochondria, as well as in the neuropil region (Figure 32).

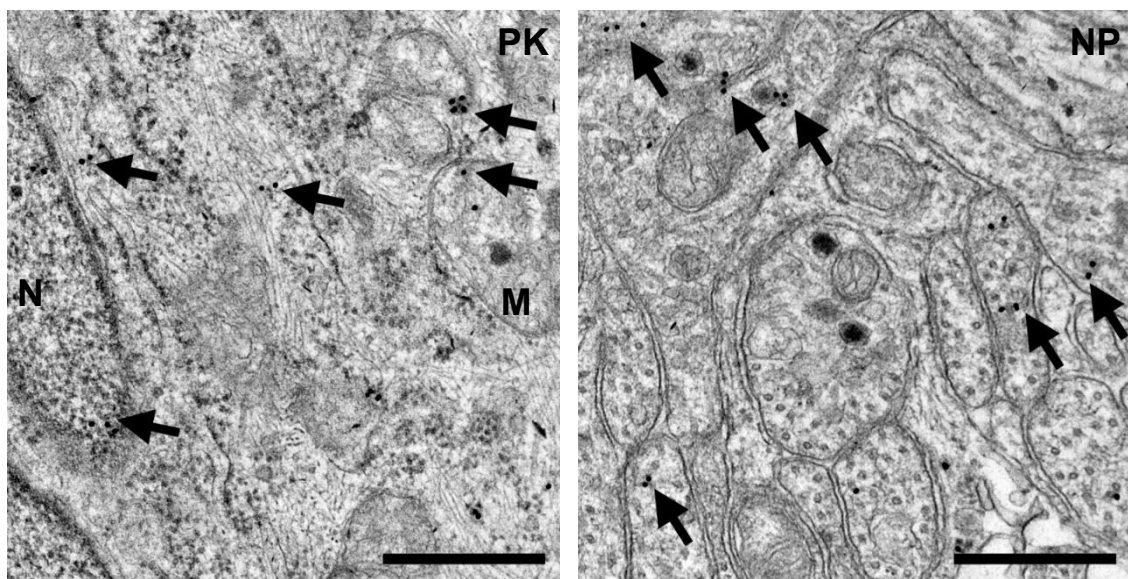


**Figure 32. Representative electron micrographs of myenteric neuronal perikaryon and neuropil from the colon of a control rat after NLRP3 post-embedding immunohistochemistry.** NLRP3 gold labels appear in and near the mitochondria, inside the nucleus, as well as in the neuropil region. PK: perikaryon, NP: neuropil, N: nucleus, M: mitochondrion; arrows: 18 nm gold particles labelling NLRP3. Scale bars: 500 nm.

Quantitative evaluation of NLRP3-labelling gold particles in the myenteric ganglia showed similar distribution among the gut segments of controls. In diabetics, there was a gut segment-specific decrease in NLRP3 gold labels compared to controls (Figure 33). In the duodenum of diabetics, NLRP3 gold labels became almost half of that in the controls ( $1.45 \pm 0.12$  labels/ $\mu\text{m}^2$  vs  $2.81 \pm 0.21$  labels/ $\mu\text{m}^2$ ,  $p < 0.0001$ ), whereas in the colon there was a 1.5-fold decrease in myenteric NLRP3 expression ( $2.28 \pm 0.16$  labels/ $\mu\text{m}^2$  vs  $3.46 \pm 0.24$  labels/ $\mu\text{m}^2$ ,  $p < 0.01$ ; Figure 33B). Insulin treatment caused a robust increase in NLRP3 density in the myenteric ganglia of the duodenum and colon compared to controls and diabetics (duodenum:  $4.28 \pm 0.22$  labels/ $\mu\text{m}^2$ ,  $p < 0.0001$ ; colon:  $5.82 \pm 0.36$  labels/ $\mu\text{m}^2$ ,  $p < 0.0001$ ; Figure 33B).

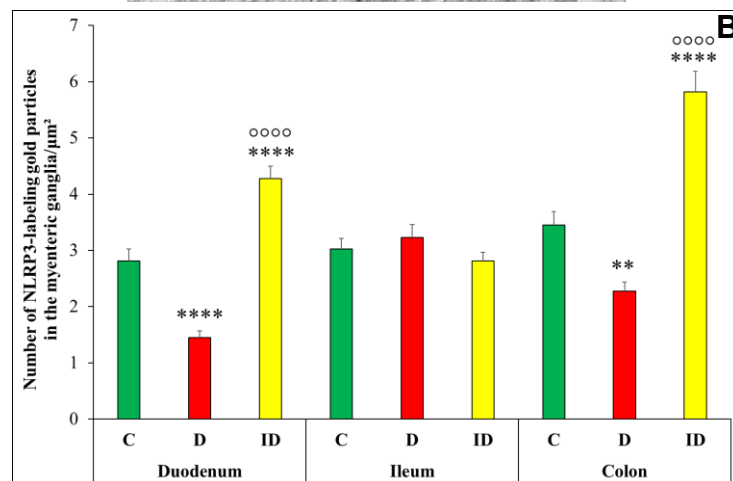
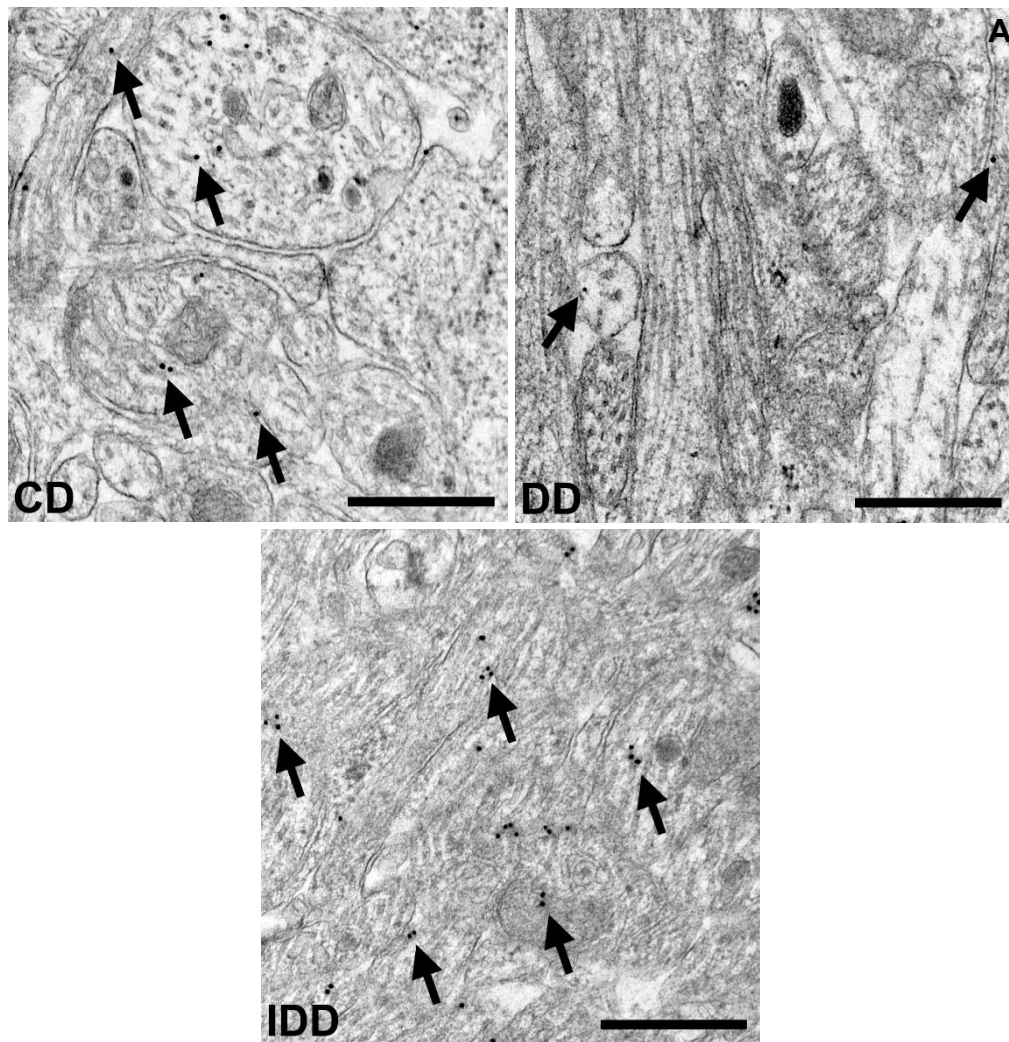


**Figure 33. Representative electron micrographs of myenteric ganglia from the duodenum of control, diabetic, and insulin-treated diabetic rats after NLRP3 post-embedding immunohistochemistry (A).** The number of NLRP3 labelling gold particles was decreased in diabetic rats relative to controls. CD: control duodenum, DD: diabetic duodenum, IDD: insulin-treated diabetic duodenum; arrows: 18 nm gold particles labelling NLRP3. Scale bars: 500 nm. **Quantitative evaluation of gold particles labelling NLRP3 in the myenteric ganglia from different gut segments of control, diabetic, and insulin-treated diabetic rats (B).** NLRP3 density was decreased in the myenteric ganglia of the duodenum and colon in diabetics relative to controls. In insulin-treated diabetics, a robust increase occurred in the same gut segments. Data are expressed as mean  $\pm$  SEM. \*\*  $p < 0.01$ , \*\*\*\*  $p < 0.0001$  (relative to controls); ○○○○  $p < 0.0001$  (between diabetics and insulin-treated diabetics). C: controls, D: diabetics, ID: insulin-treated diabetics.

#### 4.9. Effect of chronic hyperglycaemia on the expression of NLRP3 mRNA

Fluorescent images from gut cryosections hybridized with NLRP3 probe revealed that NLRP3 mRNA is present in different layers of the intestinal wall of controls (Figures 34-36). The number of NLRP3 mRNA labelling dots was the lowest in the intestinal smooth muscle layer in all gut segments with relatively similar distribution among the gut segments (Table 6). In the myenteric ganglia, no significant differences were observed in the number of NLRP3 mRNA dots along the duodenum-ileum-colon axis of controls (Table 6). In the mucosal layer, the number of punctate dots labelling NLRP3 mRNA was the highest in the duodenum and the lowest in the colon (duodenum:  $3572 \pm 145.9$  dots/mm<sup>2</sup> vs ileum:  $2873 \pm 189.2$  dots/mm<sup>2</sup>,  $p < 0.01$ ; vs colon:  $1648 \pm 206.1$  dots/mm<sup>2</sup>,  $p < 0.0001$ ; Table 6).

**Table 6. Quantitative evaluation of NLRP3 mRNA labelling dots in different intestinal layers and gut segments of control rats.**

	<b>Duodenum</b> (dots/mm <sup>2</sup> )	<b>Ileum</b> (dots/mm <sup>2</sup> )	<b>Colon</b> (dots/mm <sup>2</sup> )
<b>Myenteric ganglia</b>	$3437.0 \pm 473.6$	$2394.0 \pm 320.2$	$2909.0 \pm 768.4$
<b>Smooth muscle</b>	$803.7 \pm 73.65^c$	$877.8 \pm 93.75^b$	$927.2 \pm 143.4^a$
<b>Mucosa</b>	$3572.0 \pm 145.9^d$	$2873.0 \pm 189.2^{d,e}$	$1648.0 \pm 206.1^{f,g}$

Data are expressed as mean  $\pm$  SEM; <sup>a</sup> $p < 0.05$ , <sup>b</sup> $p < 0.01$ , <sup>c</sup> $p < 0.0001$  vs myenteric ganglia in the same gut segment; <sup>d</sup> $p < 0.0001$  vs smooth muscle in the same gut segment; <sup>e</sup> $p < 0.01$ , <sup>f</sup> $p < 0.0001$  vs duodenum in the same intestinal layer; <sup>g</sup> $p < 0.01$  vs ileum in the same intestinal layer.

In diabetic rats, significant decrease in the number of NLRP3 mRNA dots was observed in the myenteric ganglia of the duodenum ( $1810 \pm 221.5$  vs  $3437 \pm 473.6$  dots/mm<sup>2</sup>,  $p < 0.05$ ) and in all the intestinal wall layers of the ileum compared to controls (Figure 35, 36B). In the ileal myenteric ganglia and smooth muscle, more than 1.5-fold decrease was observed in the number of NLRP3 mRNA dots relative to controls (myenteric ganglia:  $1449 \pm 427.2$  dots/mm<sup>2</sup> vs  $2394 \pm 320.2$  dots/mm<sup>2</sup>,  $p < 0.05$ ; smooth muscle:  $569.5 \pm 68.65$  dots/mm<sup>2</sup> vs  $877.8 \pm 93.75$  dots/mm<sup>2</sup>,  $p < 0.05$ ; Figure 35). In the ileal mucosa, NLRP3 mRNA level underwent a 1.2-fold decrease in diabetics compared to controls ( $2375 \pm 266.5$  dots/mm<sup>2</sup> vs  $2873 \pm 189.2$  dots/mm<sup>2</sup>,  $p < 0.05$ ; Figure 36B). Insulin treatment did not protect against the hyperglycaemia-induced decrease in the number of NLRP3 mRNA dots observed in the ileal intestinal wall layers (Figure 35, 36B), whereas it decreased that in the intestinal wall layers of the duodenum (Figure 35,

36B). Interestingly, the only observed increase in NLRP3 mRNA expression was detected in the colonic mucosa of this experimental group compared to controls and diabetics ( $p < 0.0001$ ; Figure 36B).

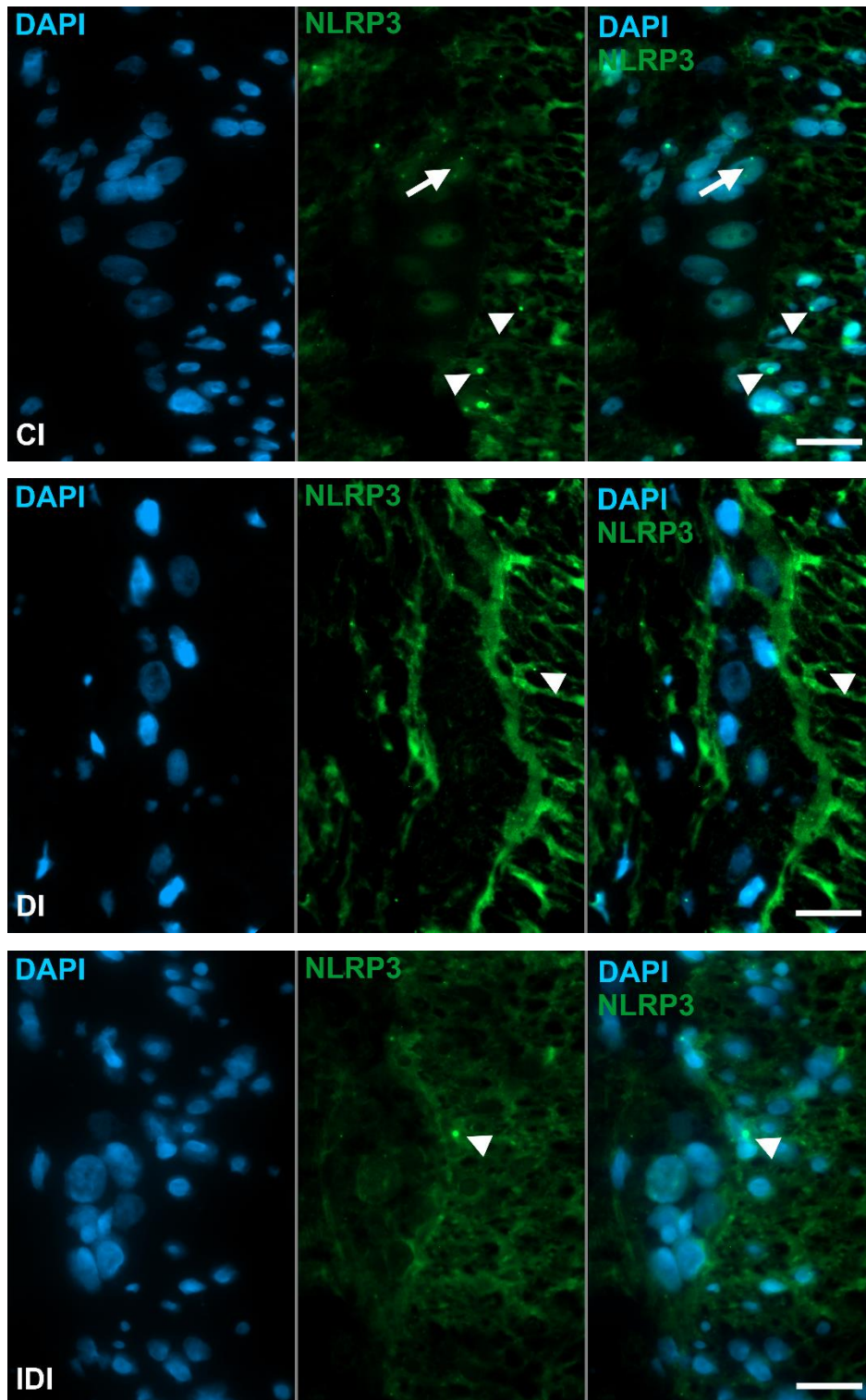


**Figure 34.** Representative micrographs of cryosections of myenteric ganglia and smooth muscle layers from the ileum of control, diabetic, and insulin-treated diabetic rats after NLRP3 RNAscope. NLRP3 mRNA appear as green punctate dots in the myenteric ganglia (arrows) and smooth muscle (arrowheads), nuclei were counterstained with DAPI (blue). CI: control ileum, DI: diabetic ileum, IDI: insulin-treated diabetic ileum. Scale bars: 20  $\mu\text{m}$ .

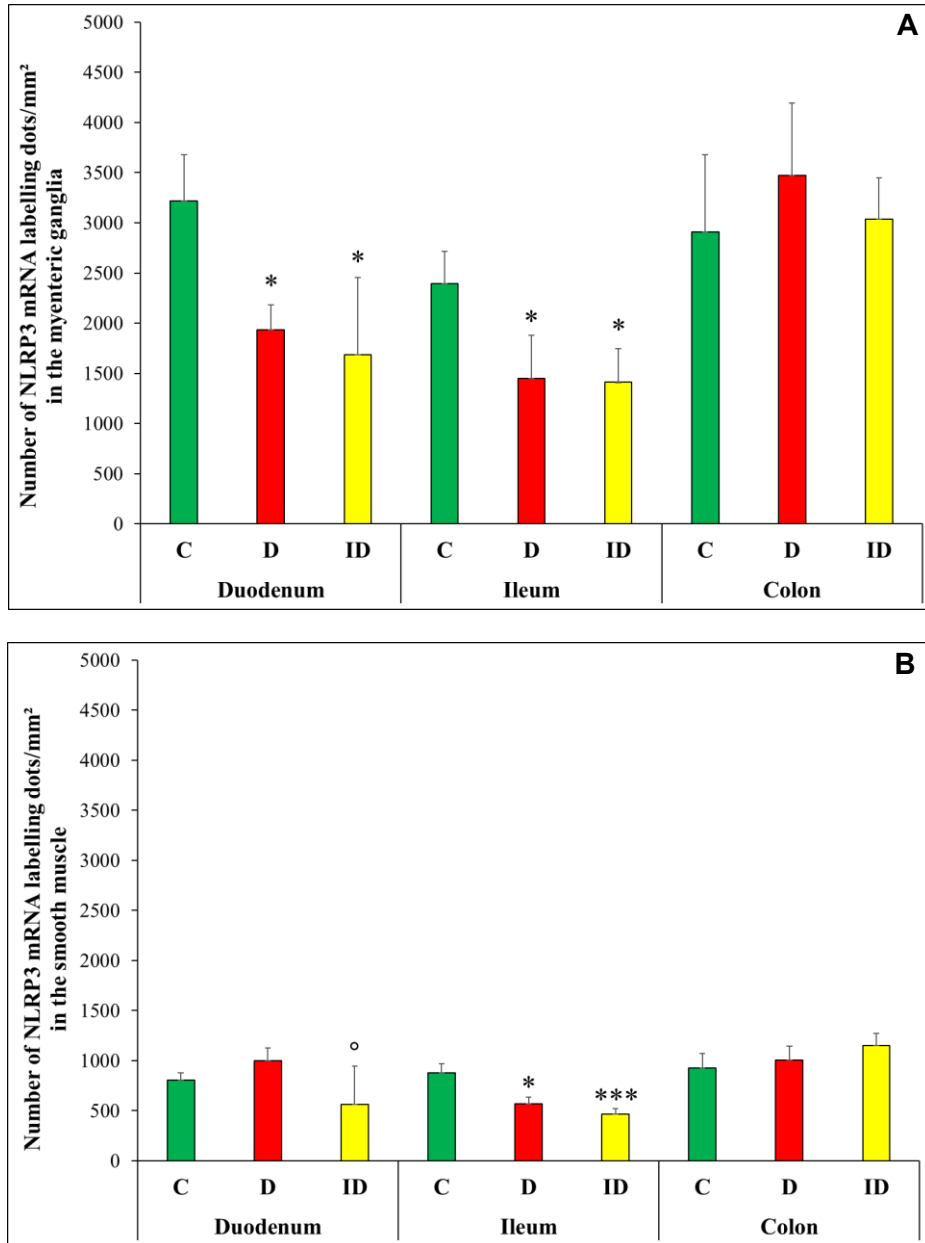


**Figure 35.** Expression of NLRP3 mRNA in the myenteric ganglia (A) and smooth muscle (B) of the duodenum, ileum, and colon of control, diabetic, and insulin-treated diabetic rats. The number of NLRP3 mRNA dots was significantly decreased in the myenteric ganglia of the small intestine and in the ileal smooth muscle layers of diabetics relative to controls, which was not prevented by insulin treatment. Data are expressed as mean  $\pm$  SEM. \*  $p < 0.05$ , \*\*\*  $p < 0.001$  (relative to controls); °  $p < 0.05$  (between diabetics and insulin-treated diabetics). C: controls, D: diabetics, ID: insulin-treated diabetics.

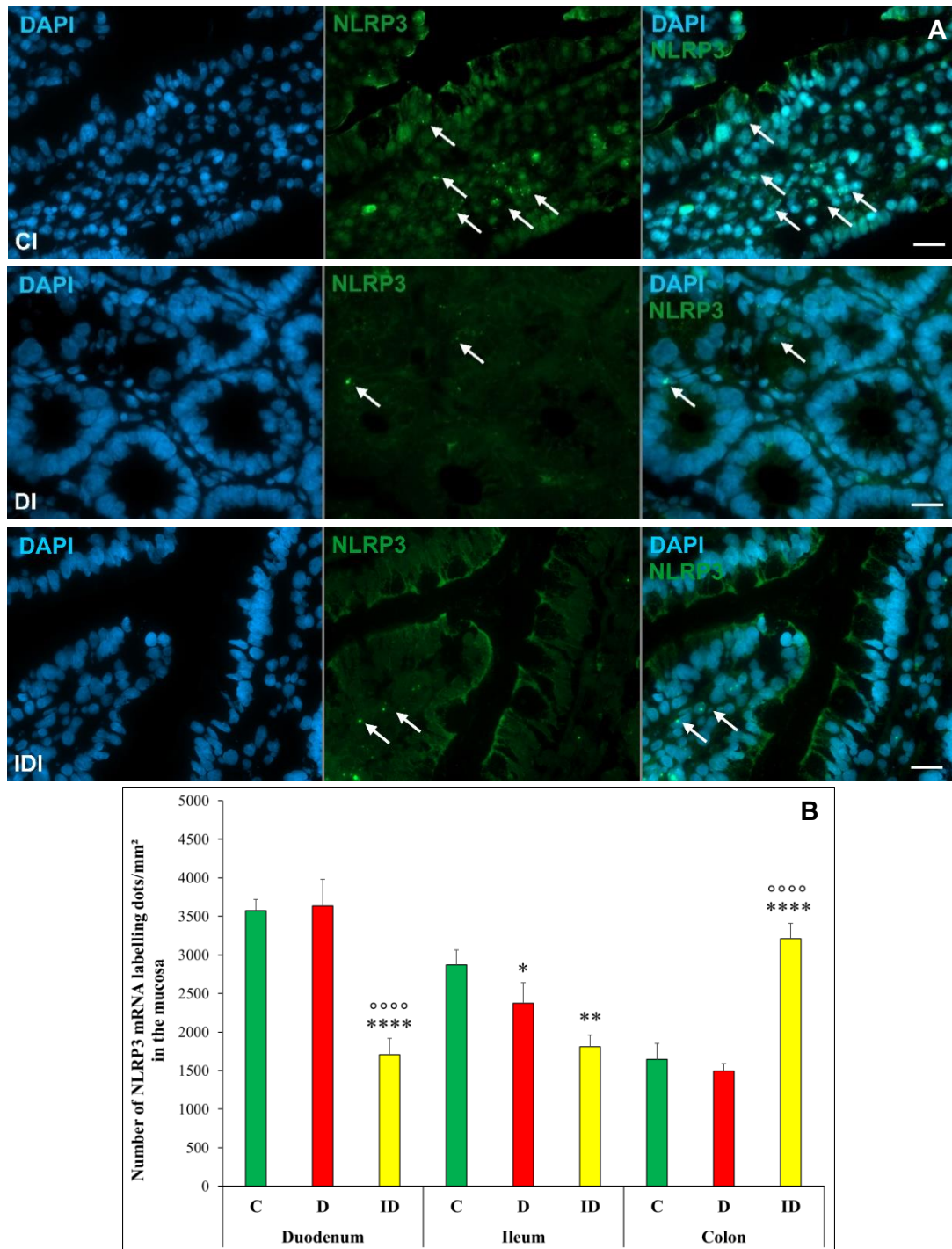


**Figure 36. Representative micrographs of cryosections from the ileum of control, diabetic, and insulin-treated diabetic rats after NLRP3 RNAscope (A).** NLRP3 mRNA appear as green punctate dots (arrows), nuclei were counterstained with DAPI (blue). CI: control ileum, DC: diabetic ileum, IDI: insulin-treated diabetic ileum. Scale bars: 20  $\mu$ m. **Expression of NLRP3 mRNA in the intestinal mucosa of the duodenum, ileum, and colon of control, diabetic, and insulin-treated diabetic rats (B).** The number of NLRP3 mRNA dots was significantly decreased in the ileal mucosa of diabetics relative to controls. Insulin treatment did not prevent the diabetes-induced decrease in NLRP3 mRNA dots in the ileum and decreased that in the duodenum relative to controls and diabetics. The only observed increase in NLRP3 mRNA levels was in the colonic mucosa of the insulin-treated diabetics. Data are expressed as mean  $\pm$  SEM. \*  $p < 0.05$ , \*\*  $p < 0.01$ , \*\*\*\*  $p < 0.0001$  (relative to controls), ○○○○  $p < 0.0001$  (between diabetics and insulin-treated diabetics). C: controls, D: diabetics, ID: insulin-treated diabetics.

## 5. DISCUSSION

Our earlier findings revealed intestinal region-specific alterations in the nitrergic myenteric neurons of STZ-induced diabetic rat model (Izbéki et al. 2008). To understand the aetiology behind the regional loss of nitrergic neurons, we have previously investigated the region-dependent changes in oxidative stress markers (Jancsó et al. 2015), endogenous antioxidants (Chandrakumar et al. 2017), as well as inflammatory cytokines including TNF $\alpha$  and its receptors in the same diabetic model (Bódi et al. 2021, Barta et al. 2023). These alterations in pro-oxidant/antioxidant balance and activated cytokines often trigger proinflammatory pathways which ultimately lead to the activation of the pleiotropic cytokine IL1 $\beta$  (Fukata et al. 2009).

While IL1 $\beta$  is mainly produced by macrophages, various cell types including epithelial and endothelial cells, smooth muscle cells, neurons, and glial cells, have been reported to express it as well (Kaneko et al. 2019, Ren & Torres 2009, Copray et al. 2001, Guo et al. 2007) and several factors can influence its release (Lopez-Castejon et al. 2011). Consequently, the activity and role of IL1 $\beta$  extend beyond inflammation and are implicated in the regulation of many physiological processes including glucose metabolism, homeostasis of the intestinal barrier, and neuronal stimulation (Dror et al. 2017, Lima 2023).

Since IL1 $\beta$  is strongly connected to metabolism and gut health (Dror et al. 2017, Lima 2023), we hypothesized that diabetes-related myenteric neuropathy might be mediated by changes in the expression of this cytokine as a potent player in enteric neuroinflammation. Moreover, considering that the distinct subpopulations of enteric neurons have different susceptibility to hyperglycaemic damage (Liu et al. 1999, Izbéki et al. 2008, Chandrakumar et al. 2017, Mezei et al. 2021), it raised the question of whether IL1 $\beta$  is also involved in different vulnerability of neuronal populations in T1D. To investigate the role of IL1 $\beta$  in diabetes-induced region-specific myenteric neuropathy and to elucidate its possible impact on diabetic damage of different myenteric neuronal populations, we applied fluorescent immunohistochemistry, immunogold electron microscopy, protein measurement, as well as RNAscope using acute and chronic STZ-induced T1D rat models.

It was imperative to initially investigate the distribution of IL1 $\beta$  along the gastrointestinal tract under healthy conditions. In control animals, a marked difference was observed in the proportion of IL1 $\beta$ -IR myenteric neurons between the small and large

intestines in which the colon displayed higher levels of IL1 $\beta$ -IR myenteric neurons. Colonic region of the gastrointestinal tract is rich in anaerobic microbiota which maintain a high pro-oxidant state even under normal conditions (Brown & Esterházy 2021, Sanders et al. 2004). Similarly, some key members of the host-defence and innate immunity, such as TNF $\alpha$  and TLR4, also displayed higher basal distribution in the colon than in the small intestine (Bódi et al. 2021, 2023, Price et al. 2018). Collectively, these factors may explain the higher baseline level of IL1 $\beta$  immunoreactivity in the colonic myenteric neurons. Moreover, localization and immunoreactivity of IL1 $\beta$  within specific neuronal subpopulations revealed variations in their IL1 $\beta$  proportions even in the different gut segments. A higher proportion of IL1 $\beta$ -nNOS-IR neurons was observed in distal segments, similar to the proportion of total IL1 $\beta$ -IR myenteric neurons. Since IL1 $\beta$  was shown to stimulate nNOS-IR neurons (Tjwa et al. 2003), it is interesting to understand whether IL1 $\beta$  immunoreactivity was homogenous within all the nitrenergic neuronal subsets themselves like those expressing the haem oxygenase1 (Chandrakumar et al. 2017). In contrast to nNOS neurons, IL1 $\beta$ -CGRP-IR myenteric neurons displayed an equal distribution within the investigated gut segments with relatively high proportions ranging between 40 and 50% of the total number of CGRP-IR neurons. These results highlight the presence of neuronal population-specific expression of IL1 $\beta$  in the myenteric ganglia of the distinct gut segments reflecting the physiological importance of IL1 $\beta$  even in healthy conditions.

On the mRNA level, the transcription of IL1 $\beta$  displayed distinct spatial patterns within the different intestinal wall layers along the intestinal tract of controls. In both duodenum and colon, IL1 $\beta$  mRNA was highly concentrated within the myenteric ganglia. Enteric neurons within the myenteric ganglia are enriched with specialized immune cells; glial cells (Rühl et al. 2004). These cells act as immunomodulators using different inflammatory cytokines including IL1 $\beta$  to mediate their function (Rühl et al. 2004). Additionally, IL1 $\beta$  mRNA signals were also evident in nuclei that were morphologically characteristic of neurons. A study has shown that specific enteric neurons produced and released the cytokine IL6 to inhibit the differentiation of T regulatory cells *in vitro* (Yan et al. 2021). Thus, myenteric neurons possibly express IL1 $\beta$  mRNA and may utilize this cytokine for neuroplastic as well as neuro-immune modulatory functions. Moreover, while duodenal myenteric IL1 $\beta$  mRNA level was as explicit as in the colon, it is plausible to assume the presence of mechanisms counteracting its activation in the small intestine

while inducing it in the colon. Indeed, some regulatory processes exist that antagonise IL1 $\beta$  activity including the presence of IL1Ra as well as binding of IL1 $\beta$  to its cell membrane decoy receptor; IL1R2 (Dinarello 2009) or preventing its activation into a mature IL1 $\beta$  by inflammasomes (Latz 2010). In contrast to the duodenum and colon, ileal IL1 $\beta$  mRNA was not only the most prominent in the mucosal layer, but it was also the highest compared to other gut segments in this intestinal wall layer. It is not surprising that IL1 $\beta$  was highly expressed in the ileal but not the colonic mucosa. Previous research demonstrated higher expression of pro-inflammatory cytokines including IL1 $\beta$  from the ileal dendritic cells compared to the colon where colonic mucosa contained more regulatory dendritic cells (Mann et al. 2016) which may be an adaptation against the greater bacterial load in the colon (Zoetendal et al. 2004, Tomas et al. 2012).

In hyperglycaemic states, a time-dependent and region-specific induction of IL1 $\beta$  was observed in the myenteric neurons of the investigated gut segments. A general induction in the proportion of IL1 $\beta$ -IR myenteric neurons was observed in all gut segments with higher extent in the small intestine of chronic diabetic rats. Although IL1 $\beta$  induction was already seen in the myenteric neurons of the duodenum and ileum of the acute diabetic rats, colonic myenteric neurons only developed that after chronic hyperglycaemia. This may reflect that a prolonged state of hyperglycaemia and the associated increase in inflammatory cytokines is required to upregulate IL1 $\beta$  in the myenteric ganglia of this gut segment. Moreover, since the distal parts of the intestine are more susceptible to pro-oxidative environment due to the presence of anaerobic microbial content (Tomas et al. 2012), colonic myenteric neurons might have developed mechanisms to combat such states rendering them more tolerant to the short-term increase in oxidative stress associated with acute hyperglycaemia (Maleki et al. 1997). A previous study revealed a high baseline level of haem oxygenase2-IR myenteric neurons in the colon compared to the small intestine (Chandrakumar et al. 2017) which may hinder the robust increase in hyperglycaemia-associated upregulation in pro-inflammatory cytokines such as IL1 $\beta$ . However, these protective mechanisms seem to get exhausted under chronic hyperglycaemia. Indeed, a former study showed that peripheral nitrergic neurons underwent a two-phase time-dependent nitrergic neuropathy in a STZ-induced diabetic rat model (Cellek et al. 2003). Thus, it would be intriguing to understand the association of IL1 $\beta$  induction in short- and long-term hyperglycaemia-induced neuronal damage.

Our observation was also confirmed in the colonic tissue homogenates of intestinal smooth muscle layers including the myenteric plexus. Thus, these results reflect that the entire enteric nervous system reacts to the long-lasting hyperglycaemic state suggesting a role for IL1 $\beta$  in enteric neuroinflammation. High glucose concentration can activate IL1 $\beta$  precursors in different cells (Honma et al. 2020, Maedler et al. 2002), which then stimulates NF $\kappa$ B activation (Flodströma et al. 1996), a key element of many pro-inflammatory signalling pathways. Pro-inflammatory cytokines can also facilitate neurite growth via the upregulation of neurotrophic factors in annulus cells (Gruber et al. 2012, Gruber et al. 2017), cortical neural precursors (Park et al. 2018) and myenteric neurons (Gougeon et al. 2015). Therefore, the increase in inflammatory cytokines could serve as a compensatory mechanism to replace the loss of myenteric neurons or the disruption in neuronal connectivity (neuronal plasticity) during chronic hyperglycaemia.

Moreover, a strict regionality in IL1 $\beta$  immunoreactivity was unveiled in different myenteric subpopulations, e.g. nNOS and CGRP neurons of chronic hyperglycaemic rats. Hyperglycaemia-induced increase in the proportions of IL1 $\beta$ -IR myenteric neurons was non-homogeneous within the different neuronal populations along the gastrointestinal tract. Indeed, while the proportion of IL1 $\beta$ -IR nitrergic neurons (per total nitrergic neurons) increased only in the colonic segment of diabetics relative to controls, it did not change elsewhere. Moreover, since the proportion of IL1 $\beta$ -IR nitrergic neurons (per total IL1 $\beta$ -IR neurons) did not change in the colonic segment among the different experimental groups, it is plausible that the induction in IL1 $\beta$ -IR myenteric neurons in this gut region was highly due to the increase in IL1 $\beta$ -containing nNOS neurons. Former studies (Chandrakumar et al. 2017, Izbéki et al. 2008) have shown that the nitrergic myenteric system undergoes a regional disruption under diabetic conditions. While the density of these inhibitory motor and interneurons decreased in all the investigated segments, there was no concurrent neuronal loss in the duodenal ganglia. In light of this, it is noteworthy that, despite the nitrergic loss in the colon of diabetics, there was still an increase in the proportion of IL1 $\beta$ -containing nNOS neurons. Other studies have shown that IL1 $\beta$  is involved in the stimulation of NF $\kappa$ B-mediated inducible NOS expression (Cho et al. 2012, Kim et al. 2004). Furthermore, it has also been shown that IL1 $\beta$  specifically activates different neuronal and glial cell populations in the myenteric and submucous plexuses of the guinea pig ileum and colon (Tjwa et al. 2003). In this study, the majority of activated myenteric neurons were nNOS-IR, while most activated submucous neurons

expressed vasoactive intestinal polypeptide in both gut segments (Tjwa et al. 2003). Whether the induced neuronal IL1 $\beta$  plays a protective or disruptive role in nitroergic neuropathy still requires further investigations.

The proportion of IL1 $\beta$ -containing CGRP neurons was specifically elevated only in the ileal ganglia whereas it remained unchanged in the duodenal and colonic ganglia of diabetics. Since myenteric CGRP neurons are mostly IPANs and are consequently essential sensors and transducers of luminal stimuli (Mitsui 2009), the alterations in microbial composition in diabetes may serve as a possible explanation for our results. Indeed, we previously detected a substantial microbial rearrangement and robust *Klebsiella* invasion in the ileum (Wirth et al. 2014), together with a significant increase in endogenous haem oxygenase defence system (Chandrakumar et al. 2017). While several studies have demonstrated that CGRP-like immunoreactivity was decreased in both enteric plexuses of the diabetic rat ileum and colon (Chandrasekharan et al. 2007, Shotton et al. 2004, Spitzgeus et al. 2004), others have detected an increase in the number of CGRP-containing neurons in the pig small intestine (Bulc et al. 2020). These discrepancies in results may be due to the species-specific differences in experiments. Furthermore, IL1 $\beta$  was shown to directly induce the release of CGRP from sensory neurons of the dorsal root ganglia in a concentration-dependent manner (Hou et al. 2003). Since CGRP can modulate immune cell function, the role of neuropeptide-cytokine interactions underscores the significance of conducting additional investigations in diabetic enteric neuropathy (Chandrasekharan et al. 2007).

At the transcriptional level, IL1 $\beta$  mRNA induction was evident in the myenteric ganglia of all investigated gut segments of diabetic rats, and IL1 $\beta$  mRNA level was also increased in intestinal smooth muscle except the ileum. The number of IL1 $\beta$  mRNA-labelling dots in the smooth muscle of the gut wall indicates that it contributes to diabetes-induced cytokines production, however, this involvement is comparatively lower than that observed in the myenteric ganglia. Previously, an enhanced IL1 $\beta$  mRNA expression was shown in the colonic muscle of rats with colitis (Khan & Al-Awadi 1997). Furthermore, IL1 $\beta$  was proved to induce IL6 mRNA and protein expression in cultured muscle cells of the rat jejunum (Khan et al. 1995). In our experiment, the mucosal IL1 $\beta$  mRNA level was robustly induced in the small intestine, especially in the duodenum of diabetics. Diabetic alterations of the mucosa-associated gut microbiota (Wirth et al. 2021) may induce mucosal IL1 $\beta$  production (Benedetti et al. 2020) and contribute to the

increased intestinal permeability (Al-Sadi et al. 2007, Kaminsky et al. 2021). Moreover, increased expression of sodium-glucose transporter1 in the small intestinal enterocytes under chronic hyperglycaemia (Debnam et al. 1995) could induce the absorption of glucose (Koepsell 2020) through which an overexpression in mucosal IL1 $\beta$  may be mediated (Honma et al. 2020).

T1D is represented mainly as a dysfunction in pancreatic  $\beta$ -cells of the Langerhans islets (Gillespie 2006). Whereas IL1 $\beta$  mRNA was robustly increased in chronic hyperglycaemic state, only acute hyperglycaemia was associated with the increase in IL1 $\beta$  protein levels. Treatment with STZ induces apoptotic cell death of  $\beta$ -cells which is mediated by the acute expression of inflammatory cytokines including IL1 $\beta$  and the recruitment of macrophages and dendritic cells (Pirot et al. 2008). Moreover, IL1 $\beta$  has been shown to be crucial for insulin signalling in pancreatic  $\beta$ -cells as these cells express IL1R1, whereas neighbouring intra-islets endocrine cells and exocrine cells express IL1 $\beta$  (Burke et al. 2018). In chronic hyperglycaemia, very few  $\beta$ -cells are present and the destructive effect of STZ is diminished which may limit signals that lead to the activation of IL1 $\beta$ . A study has demonstrated a downregulation in IL1 $\beta$  and inflammasome proteins in the pancreas, blood mononuclear cells, and granulocytes under severe T1D conditions (Liu et al. 2017). Although we did not observe a downregulation in IL1 $\beta$  in either the pancreas or the serum of chronic hyperglycaemic rats, the unchanged serum IL1 $\beta$  level suggests that this rat model is more likely to represent a hyperglycaemic model. This rules out any possible induction in inflammation that may have originated from the pancreas or systemic circulation (Pereira et al. 2020). Since these results reveal an intestinal localization of IL1 $\beta$  induction, more studies are required to investigate the cell-type specific expression patterns of pro-IL1 $\beta$ , IL1 $\beta$ , IL1Ra, IL1R1, and inflammasome markers within the pancreas under chronic hyperglycaemia.

Moreover, a compartmentalized view regarding the different gut segments is more likely to explain the region-specific and layer-dependent diabetes-related induction in IL1 $\beta$ . For instance, IL1 $\beta$  immunoreactivity in CGRP neurons was only induced in the myenteric ganglia of the ileum. This coincided with the induction of IL1 $\beta$  mRNA in the mucosa but not the smooth muscle layer surrounding the myenteric ganglia. Therefore, it is assumable that IL1 $\beta$  induction in this gut segment originated from the luminal and mucosal parts and later was mediated through CGRP neurons toward the myenteric ganglia.

As we have seen, chronic hyperglycaemia caused a segment-specific and intestinal layer-dependent IL1 $\beta$  induction on both the mRNA and protein levels. For IL1 $\beta$  activation, an inflammasome complex is required to be assembled to enzymatically mediate the activation of pro-IL1 $\beta$  into an active IL1 $\beta$  (Lopez-Castejon & Brough 2011). Many studies have demonstrated the role of NLRP3 inflammasome-forming protein in the homeostasis of both gut and glucose metabolism (Hirota et al. 2011, Dror et al. 2017) and its involvement in disorders affecting these compartments additional to its role in neurodegenerative diseases (Shen et al. 2020, Pellegrini et al. 2021). Therefore, we aimed to understand NLRP3 role in diabetes-induced region-specific myenteric neuropathy and its implications in IL1 $\beta$  activation in our experiments.

In controls, the number of NLRP3-labelling gold particles was evenly distributed within the myenteric ganglia along the duodenum-ileum-colon axis. Interestingly, chronic hyperglycaemia caused a gut segment-specific decrease in NLRP3 gold labels within the myenteric ganglia. This downregulation in myenteric ganglionic NLRP3 took place in the duodenum and colon but not the ileum. Inflammasome-forming proteins including NLRP3 have been shown to be inhibited by some neurotransmitters including nitric oxide (Hernandez-Cuellar et al. 2014), adrenergic (Chen et al. 2019, Mathies et al. 2020), as well as cholinergic activation (Ke et al. 2017). A study demonstrated the inhibition of NLRP3 activation by nicotinic agonists and phosphocholine-modified macromolecules through purinergic receptors (Hecker et al. 2015). Further investigations revealed an increase in myenteric neuronal immunoreactivity of choline acetyltransferase (Lincoln et al. 1984) and vesicular acetylcholine transporter (Bulc et al. 2020) in STZ-induced rat and porcine diabetic models, respectively.

Molecular analysis of NLRP3 transcripts of control rats showed regional differences in the mucosal layer with higher NLRP3 transcription in the small intestine compared to the colon, consistent with our previous observation regarding IL1 $\beta$  mRNA levels. Hyperglycaemia decreased NLRP3 mRNA levels in the myenteric ganglia of the small intestine. In the ileum, the decrease of NLRP3 mRNA was also observed in the micro- and macro-environment of the myenteric ganglia represented by the reduction in all ileal intestinal layers. These results reflect that hyperglycaemia-related NLRP3 downregulation was regulated on the protein or the mRNA levels differently depending on the investigated segment. For instance, in the duodenum, both NLRP3 protein density and mRNA levels within the myenteric ganglia were significantly decreased in diabetic

animals compared to the control rats. However, colonic NLRP3 downregulation in the myenteric ganglia occurred only on the protein level. These differences in the regulation of NLRP3 within the myenteric ganglia as a response to hyperglycaemia represent a gut region-specific modification of NLRP3 on the transcriptional, posttranslational, and activation levels. In an animal model of obesity-induced diabetes, the expression of NLRP1, NLRP3, and NLRP6 were decreased in the small intestine compared to their control counterparts (Frühbeck et al. 2024) which coincided with the increase in inflammatory markers. Moreover, a study demonstrated the inhibition of NLRP3 inflammasome by inducing haem oxygenase1 (Luo et al. 2014), that have also been robustly induced in the myenteric neurons of the diabetic ileum (Chandrakumar et al. 2017). Limiting the propagation of inflammation is a regulatory and compensatory mechanism that tissues undergo to prevent further destruction in biological barriers and tissues (Afonina et al. 2017). However, this can further downregulate key pattern recognition receptors such as NLRP3 that are crucial in the host-defence and innate immunity within the intestinal wall layers. Indeed, a downregulated NLRP1 and NLRP3 in the circulatory system was associated with poor prognosis in T1D patients (Liu et al. 2017). Therefore, the downregulation in NLRP3 inflammasome besides others, may play a role in the disrupted intestinal barrier seen in diabetes. Other inflammasome-forming proteins and IL1 $\beta$  activators should be investigated such as NLRC4, cathepsin D and caspase-8 (Gurung & Kanneganti 2015, Van Opdenbosch et al. 2017, Chauhan et al. 2018), which may play role in hyperglycaemia-induced IL1 $\beta$  activation in the myenteric ganglia and their environment. However, activation and regulation of different inflammasome-forming proteins and enzymes is a complex process (Kang et al. 2013, Van Opdenbosch et al. 2017), and studying the expression of NLRP3 in different time points along the progression of the disease may help further our understanding about the role of this inflammasome protein in hyperglycaemia.

The clinical significance of our results highlights the importance of IL1 $\beta$  antagonism to treat the regional neuropathy in T1D. However, IL1 $\beta$  levels should be tackled with therapeutics delivered specifically into the intestinal tissue or cell type. For instant, mechanisms utilizing luminal pH differences in intestinal segments can be adopted to modify current IL1 $\beta$  antagonists. Additionally, bioactive nanovesicles derived from grapefruit were taken up by intestinal macrophages and thus can be loaded with anti-inflammatory drugs to alleviate intestinal inflammation (Wang et al. 2014). However,

cells are able to naturally antagonise IL1 $\beta$  function through the upregulation of IL1R2 or IL1Ra, and concomitant expression of these should be analysed prior to IL1 $\beta$  inhibition. Furthermore, enterosynes refers to molecules originating from the gut which have the capacity to modulate duodenal contraction by targeting the ENS. These molecules can be chemically diverse and related to hormones, bioactive peptides/lipids, nutrients, microbiota, and immune factors (Knauf et al. 2020). The utilization of such molecules to target intestinal contractility in T1D should not be overlooked.

On the other hand, while many studies pushed toward the possibility of NLRP3 antagonism during metabolic diseases including T1D (Jiang et al. 2018), more evidence is revealed highlighting its downregulation rather than upregulation under hyperglycaemia (Frühbeck et al. 2024). However, experimental pharmacological studies are needed to investigate whether the restoration of IL1 $\beta$  levels in the myenteric neurons and their environment could reverse the downregulation in NLRP3 in hyperglycaemic animal models. Finally, since NLRP3 inflammasome was downregulated in this animal model, more studies are needed to unravel the possible mechanisms by which IL1 $\beta$  is activated in the gut under hyperglycaemia.

In conclusion, IL1 $\beta$  is a crucial cytokine expressed by cells in the intestinal tract and display a spatial and segment-specific expressional patterns in healthy rats. Hyperglycaemia causes intestinal region-specific and layer-dependent induction in this cytokine. Specific myenteric neurons react to hyperglycaemia and become a higher source for IL1 $\beta$  production. This highlights the role of IL1 $\beta$  in myenteric subpopulation-specific neuropathy that can give rise to diabetic dysmotility. Moreover, since NLRP3 is regionally downregulated in chronic hyperglycaemia, it is assumable that hyperglycaemia-related IL1 $\beta$  induction is not mediated through the NLRP3 inflammasome protein rendering it dispensable for IL1 $\beta$  activation in the gut in T1D.

## 6. THESIS MAIN FINDINGS

1. We revealed an intestinal segment-specific IL1 $\beta$  immunoreactivity within the total and different subpopulations of the myenteric neurons in control rats. In diabetic rats, chronic hyperglycaemia induced both IL1 $\beta$  mRNA levels and protein immunoreactivity in the myenteric ganglia of all gut segments with specific induction of IL1 $\beta$  immunoreactivity in nNOS and CGRP neuronal subsets of the distal gut segments. Immediate insulin treatment exerted cell-type specific protection against the hyperglycaemia-induced IL1 $\beta$  expression.
2. We found a similar distribution of NLRP3-labelling gold particles in the myenteric ganglia of the investigated gut segments in control rats. In diabetic rats, chronic hyperglycaemia regionally decreased the density of NLRP3 gold labels in the myenteric ganglia of the duodenum and colon. NLRP3 mRNA levels were also particularly decreased in the myenteric ganglia of the small intestine. The region-dependent downregulation of NLRP3 on the protein and mRNA level was not protected by insulin treatment.

Based on these findings, the induction of IL1 $\beta$  suggests its key role in the region-dependent and neuronal population-specific diabetic myenteric neuropathy. Moreover, although NLRP3 inflammasome protein seems to be dispensable for the hyperglycaemia-induced IL1 $\beta$  activation, the downregulation of NLRP3 as a crucial regulator of intestinal barrier, may regionally affect the neuronal environment in T1D.

## 7. ACKNOWLEDGMENT

*“Whoever is not thankful to people, then he is not thankful to God”*

First, I am deeply thankful to my supervisor *Dr. Nikolett Bódi* for her constant teaching, guidance, and support throughout my PhD journey. Without this great supervision, I would not have achieved what I have today. So, a big thank you from the heart for everything in and outside the lab.

I would also like to express my deep appreciation to *Dr. Mária Bagyánszki* for offering me the opportunity to conduct my PhD research in her laboratory, and for her immense kindness, great humbleness, and constant support.

Special thanks to our lab members: *Dr. Zita Szalai* for her help throughout our experiments especially during the ELISA measurements, and to my great colleagues *Abigél Egyed-Kolumbán*, *Bence Barta*, and *Benita Onhausz* for their help, flexibility, and learning in the lab, for the laughs we shared, the friendship, and their precious support and help throughout this journey inside and outside the lab.

Thanks to our former lab members: *Szilvia Kiss* for our times, talks, trips, and jokes, to *Dr. János Balázs* for his help during the animal experiments, to *Dr. Diána Mezei* for teaching me at the beginning of my time in the lab, and to *Katalin Arany* for her technical assistance in the lab.

I would also like to thank the head of the department of Physiology, Anatomy and Neuroscience *Dr. Csaba Varga* for providing different departmental facilities, and to the secretary of our department *Margit Veketyné Váradi* for her administrative help. I am very thankful to the animal house caretakers, many thanks to *Dr. Evelin Fehér* for providing the animals and for her help throughout the animal experiments. I am also thankful to *Nóra Gödör*, *Bettina Lehóczki*, *Illyés Dóra* and *Luca Hús* for their efforts to maintain a suitable environment in the animal house during our annual animal experiments. Thanks to the members of the department and to those with whom I shared a talk, a laugh, a coffee, a joke, or even a smile.

Thanks to the head of the Doctoral School of Biology *Dr. Csaba Vágvolgyi*, to the current coordinator *Dr. Erika Molnár*, and to the former coordinator *Dr. Attila Pécsváradi* for their help throughout my doctoral studies.

Thanks to our collaborators *Dr. Titanilla Szilágyi-Szögi* and *Erika Németh* from the Department of Pathology, Albert Szent-Györgyi Health Centre, for the help with the electron microscope.

Thanks to the members of the Faculty of Science and Informatics especially *Anita Horpácsi* for her immense and fast administrative assistance.

I am also thankful to the Stipendium Hungaricum scholarship of the Tempus Public Foundation and the support from the Hungarian NKFIH fund project, No. FK131789 (OTKA).

Heartfelt thanks to my lovely family: My mother *Ameena* without whom I would not have been able to achieve anything, therefore this work is dedicated to you. To the soul of my beloved father *Mohammad* who left life early. To my sweet sisters *Bayan* and *Ala'a* and my lovely brothers *Ezz-Aldeen* and *Noor-Aldeen*, thanks for all the forms of support you contributed and thanks for always being there for me. Thanks also to my kind cousin *Rahaf* for our conversations and calls throughout my time abroad. Finally, I am deeply thankful to the uncountable friends with whom my time abroad has been smooth, especially *Elham* and *Uddin* who supported me and made me feel home even before the 4-year journey.

## 8. REFERENCES

**Afonina** IS, Zhong Z, Karin M, Beyaert R. Limiting inflammation—the negative regulation of NF- $\kappa$ B and the NLRP3 inflammasome. *Nature immunology*. 2017 Aug 1;18(8):861-9.

**Alexandraki** KI, Piperi C, Ziakas PD, Apostolopoulos NV, Makrilakis K, Syriou V, Diamanti-Kandarakis E, Kaltsas G, Kalofoutis A. Cytokine secretion in long-standing diabetes mellitus type 1 and 2: associations with low-grade systemic inflammation. *Journal of clinical immunology*. 2008 Jul;28:314-21.

**Al-Sadi** RM, Ma TY. IL-1 $\beta$  causes an increase in intestinal epithelial tight junction permeability. *The Journal of Immunology*. 2007 Apr 1;178(7):4641-9.

**Arranz** L, del Mar Arriero M, Villatoro A. Interleukin-1 $\beta$  as emerging therapeutic target in hematological malignancies and potentially in their complications. *Blood reviews*. 2017 Sep 1;31(5):306-17.

**Atkinson** MA, Bluestone JA, Eisenbarth GS, Hebrok M, Herold KC, Accili D, Pietropaolo M, Arvan PR, Von Herrath M, Markel DS, Rhodes CJ. How does type 1 diabetes develop? The notion of homicide or  $\beta$ -cell suicide revisited. *Diabetes*. 2011 May 1;60(5):1370-9.

**Avetisyan** M, Schill EM, Heuckeroth RO. Building a second brain in the bowel. *The Journal of clinical investigation*. 2015 Mar 2;125(3):899-907.

**Bagyánszki** M, Bódi N. Key elements determining the intestinal region-specific environment of enteric neurons in type 1 diabetes. *World Journal of Gastroenterology*. 2023 May 5;29(18):2704.

**Barta** BP, Onhausz B, Doghmi AA, Szalai Z, Balázs J, Bagyánszki M, Bódi N. Gut region-specific TNFR expression: TNFR2 is more affected than TNFR1 in duodenal myenteric ganglia of diabetic rats. *World Journal of Diabetes*. 2023 Jan 1;14(1):48.

**Benedetti** F, Curreli S, Zella D. Mycoplasmas–host interaction: mechanisms of inflammation and association with cellular transformation. *Microorganisms*. 2020 Sep 4;8(9):1351.

**Bo** Y, Fuyuan C, Guangfu Y, Daosong H, Chuanyou L, Liqiang R. Distribution of cholinergic neurons in the myenteric plexus of guinea-pig intestinal tract. *Zhongguo Shen Jing ke xue za zhi= Chinese Journal of Neuroscience*. 1999 Jan 1;15(2):148-50.

**Bódi** N, Szalai Z, Bagyánszki M. Nitrergic enteric neurons in health and disease—focus on animal models. *International Journal of Molecular Sciences*. 2019 Apr 24;20(8):2003.

**Bódi** N, Bagyánszki M. Diabetic enteric neuropathy: Imbalance between oxidative and antioxidative mechanisms. In *Diabetes 2020* Jan 1 (pp. 25-33). Academic Press.

**Bódi** N, Chandrakumar L, Al Doghmi A, Mezei D, Szalai Z, Barta BP, Balázs J, Bagyánszki M. Intestinal region-specific and layer-dependent induction of TNF $\alpha$  in rats with streptozotocin-induced diabetes and after insulin replacement. *Cells*. 2021 Sep 13;10(9):2410.

**Bódi** N, Egyed-Kolumbán A, Onhausz B, Barta BP, Doghmi AA, Balázs J, Szalai Z, Bagyánszki M. Intestinal region-dependent alterations of toll-like receptor 4 expression in myenteric neurons of Type 1 diabetic rats. *Biomedicines*. 2023 Jan 4;11(1):129.

**Boraschi** D, Italiani P, Weil S, Martin MU. The family of the interleukin-1 receptors. *Immunological reviews*. 2018 Jan;281(1):197-232.

**Brehmer** A, Stach W. Morphological classification of NADPHd-positive and-negative myenteric neurons in the porcine small intestine. *Cell and tissue research*. 1996 Dec;287:127-34.

**Brehmer** A, Stach W, Krammer HJ, Neuhuber W. Distribution, morphology and projections of nitrergic and non-nitrergic submucosal neurons in the pig small intestine. *Histochemistry and cell biology*. 1997 Dec;109(1):87-94.

**Brehmer** A, Schrödl F, Neuhuber W. Morphological classifications of enteric neurons—100 years after Dogiel. *Anatomy and embryology*. 1999 Jun;200:125-35.

**Brehmer** A. Classification of human enteric neurons. *Histochemistry and cell biology*. 2021 Aug;156(2):95-108.

**Brokhman** I, Xu J, Coles BL, Razavi R, Engert S, Lickert H, Babona-Pilipos R, Morshead CM, Sibley E, Chen C, van der Kooy D. Dual embryonic origin of the mammalian enteric nervous system. *Developmental biology*. 2019 Jan 15;445(2):256-70.

**Brookes SJ.** Classes of enteric nerve cells in the guinea-pig small intestine. *The Anatomical Record: An Official Publication of the American Association of Anatomists.* 2001 Jan 1;262(1):58-70.

**Brown H, Esterházy D.** Intestinal immune compartmentalization: implications of tissue specific determinants in health and disease. *Mucosal immunology.* 2021 Nov 1;14(6):1259-70.

**Bulc M, Całka J, Palus K.** Effect of streptozotocin-induced diabetes on the pathophysiology of enteric neurons in the small intestine based on the porcine diabetes model. *International Journal of Molecular Sciences.* 2020 Mar 17;21(6):2047.

**Burke SJ, Batdorf HM, Burk DH, Martin TM, Mendoza T, Stadler K, Alami W, Karlstad MD, Robson MJ, Blakely RD, Mynatt RL.** Pancreatic deletion of the interleukin-1 receptor disrupts whole body glucose homeostasis and promotes islet  $\beta$ -cell de-differentiation. *Molecular metabolism.* 2018 Aug 1;14:95-107.

**Butkowski EG, Jelinek HF.** Hyperglycaemia, oxidative stress and inflammatory markers. *Redox Report.* 2017 Nov 2;22(6):257-64.

**Camilleri M.** Diabetic gastroparesis. *New England Journal of Medicine.* 2007 Feb 22;356(8):820-9.

**Carabotti M, Scirocco A, Maselli MA, Severi C.** The gut-brain axis: interactions between enteric microbiota, central and enteric nervous systems. *Annals of gastroenterology: quarterly publication of the Hellenic Society of Gastroenterology.* 2015 Apr;28(2):203.

**Carlos D, Costa FR, Pereira CA, Rocha FA, Yaochite JN, Oliveira GG, Carneiro FS, Tostes RC, Ramos SG, Zamboni DS, Camara NO.** Mitochondrial DNA activates the NLRP3 inflammasome and predisposes to type 1 diabetes in murine model. *Frontiers in Immunology.* 2017 Feb 27;8:187998.

**Cellek S.** Point of NO return for nitrergic nerves in diabetes: a new insight into diabetic complications. *Current pharmaceutical design.* 2004 Nov 1;10(29):3683-95.

**Chandrakumar L, Bagyánszki M, Szalai Z, Mezei D, Bódi N.** Diabetes-related induction of the heme oxygenase system and enhanced colocalization of heme oxygenase 1 and 2 with neuronal nitric oxide synthase in myenteric neurons of different intestinal segments. *Oxidative Medicine and Cellular Longevity.* 2017 Sep 10;2017.

**Chandrasekharan B**, Srinivasan S. Diabetes and the enteric nervous system. *Neurogastroenterology & Motility*. 2007 Dec;19(12):951-60.

**Chauhan D**, Bartok E, Gaidt MM, Bock FJ, Herrmann J, Seeger JM, Broz P, Beckmann R, Kashkar H, Tait SW, Müller R. BAX/BAK-induced apoptosis results in caspase-8-dependent IL-1 $\beta$  maturation in macrophages. *Cell reports*. 2018 Nov 27;25(9):2354-68.

**Chen R**, Zeng L, Zhu S, Liu J, Zeh HJ, Kroemer G, Wang H, Billiar TR, Jiang J, Tang D, Kang R. cAMP metabolism controls caspase-11 inflammasome activation and pyroptosis in sepsis. *Science advances*. 2019 May 22;5(5):eaav5562.

**Cho JM**, Chang SY, Kim DB, Needs PW, Jo YH, Kim MJ. Effects of physiological quercetin metabolites on interleukin-1 $\beta$ -induced inducible NOS expression. *The Journal of Nutritional Biochemistry*. 2012 Nov 1;23(11):1394-402.

**Choi KM**, Zhu J, Stoltz GJ, Vernino S, Camilleri M, Szurszewski JH, Gibbons SJ, Farrugia G. Determination of gastric emptying in nonobese diabetic mice. *American Journal of Physiology-Gastrointestinal and Liver Physiology*. 2007 Nov;293(5):G1039-45.

**Christen U**, Wolfe T, Möhrle U, Hughes AC, Rodrigo E, Green EA, Flavell RA, von Herrath MG. A dual role for TNF- $\alpha$  in type 1 diabetes: islet-specific expression abrogates the ongoing autoimmune process when induced late but not early during pathogenesis. *The Journal of Immunology*. 2001 Jun 15;166(12):7023-32.

**Coprav JC**, Mantingh I, Brouwer N, Biber K, Küst BM, Liem RS, Huitinga I, Tilders FJ, Van Dam AM, Boddeke HW. Expression of interleukin-1 beta in rat dorsal root ganglia. *Journal of neuroimmunology*. 2001 Aug 30;118(2):203-11.

**Costa M**, Brookes SJ, Steele PA, Gibbins I, Burcher E, Kandiah CJ. Neurochemical classification of myenteric neurons in the guinea-pig ileum. *Neuroscience*. 1996 Dec 1;75(3):949-67.

**Czeschik JC**, Hagenacker T, Schäfers M, Büsselberg D. TNF- $\alpha$  differentially modulates ion channels of nociceptive neurons. *Neuroscience letters*. 2008 Apr 4;434(3):293-8.

De Giorgio R, Barbara G, Pinto D, Cogliandro R, Elia G, Tomassetti P, Gizzi G, **Stanghellini V**, Corinaldesi R. The innervation of the digestive tract: its morphofunctional

and neurochemical aspects. *Minerva Gastroenterologica e Dietologica*. 1996 Jun 1;42(2):83-91.

**Debnam ES**, Smith MW, Sharp PA, Srai SK, Turvey A, Keable SJ. The effects of streptozotocin diabetes on sodium-glucose transporter (SGLT1) expression and function in rat jejunal and ileal villus-attached enterocytes. *Pflügers Archiv*. 1995 Jun;430:151-9.

**Dinarelo CA**. Historical insights into cytokines. *European journal of immunology*. 2007 Nov;37(S1):S34-45.

**Dogiel AS**. Zur Frage über die Ganglien der Darmgeflechte bei den Säugethieren. *Anat. Anz.* 1895;10:517-28.

**Dogiel AS**. Zwei arten sympathischer nervenzellen. *Anat. Anz*. 1896;11(67):687.

**Dogiel AS**. Über den Bau der Ganglien in den Geflechten des Darmes und der Gallenblase des Menschen und der Säugethieren. *Arch. Anat. Physiol.(Leipzig)*. 1899;53:130-58.

Dror E, Dalmas E, Meier DT, Wueest S, Thévenet J, Thienel C, Timper K, Nordmann TM, Traub S, Schulze F, Item F. Postprandial macrophage-derived IL-1 $\beta$  stimulates insulin, and both synergistically promote glucose disposal and inflammation. *Nature immunology*. 2017 Mar;18(3):283-92.

**El-Tahan RR**, Ghoneim AM, El-Mashad N. TNF- $\alpha$  gene polymorphisms and expression. *Springerplus*. 2016 Dec;5:1-7.

**Fitzgerald KA**, Luke AJ. The role of the interleukin-1/Toll-like receptor superfamily in inflammation and host defence. *Microbes and infection*. 2000 Jul 1;2(8):933-43.

**Flodströma M**, Welsh N, Eizirik DL. Cytokines activate the nuclear factor  $\kappa$ B (NF- $\kappa$ B) and induce nitric oxide production in human pancreatic islets. *FEBS letters*. 1996 Apr 29;385(1-2):4-6.

**Fowler MJ**. Microvascular and macrovascular complications of diabetes. *Clinical diabetes*. 2008 Apr 1;26(2):77-82.

**Frühbeck G**, Gómez-Ambrosi J, Ramírez B, Becerril S, Rodríguez A, Mentxaka A, Valentí V, Moncada R, Reina G, Baixauli J, Casado M. Decreased expression of the NLRP6 inflammasome is associated with increased intestinal permeability and

inflammation in obesity with type 2 diabetes. *Cellular and Molecular Life Sciences*. 2024 Dec;81(1):77.

**Fu J, Wu H.** Structural mechanisms of NLRP3 inflammasome assembly and activation. *Annual review of immunology*. 2023 Apr 26;41:301-16.

**Fukata M, Vamadevan AS, Abreu MT.** Toll-like receptors (TLRs) and Nod-like receptors (NLRs) in inflammatory disorders. In *Seminars in immunology* 2009 Aug 1 (Vol. 21, No. 4, pp. 242-253). Academic Press.

**Furness JB, Costa M.** Types of nerves in the enteric nervous system. *Commentaries in the Neurosciences*. 1980 Jan 1:235-52.

**Furness JB.** Types of neurons in the enteric nervous system. *Journal of the autonomic nervous system*. 2000 Jul 3;81(1-3):87-96.

**Furness JB, Jones C, Nurgali K, Clerc N.** Intrinsic primary afferent neurons and nerve circuits within the intestine. *Progress in neurobiology*. 2004 Feb 1;72(2):143-64.

**Furness JB.** The organisation of the autonomic nervous system: peripheral connections. *Autonomic Neuroscience: Basic and Clinical*. 2006 Dec 30;130(1):1-5.

**Furness JB.** The enteric nervous system and neurogastroenterology. *Nature reviews Gastroenterology & hepatology*. 2012 May;9(5):286-94.

**Furness JB, Callaghan BP, Rivera LR, Cho HJ.** The enteric nervous system and gastrointestinal innervation: integrated local and central control. *Microbial endocrinology: The microbiota-gut-brain axis in health and disease*. 2014:39-71.

**Gabella G.** On the plasticity of form and structure of enteric ganglia. *Journal of the autonomic nervous system*. 1990 Jul 1;30:S59-66.

**Gao Y, Zhang H, Wang Y, Han T, Jin J, Li J, Tang Y, Liu C.** L-Cysteine Alleviates Myenteric Neuron Injury Induced by Intestinal Ischemia/Reperfusion via Inhibiting the Macrophage NLRP3-IL-1 $\beta$  Pathway. *Frontiers in Pharmacology*. 2022 Jun 8;13:899169.

**Gillespie KM.** Type 1 diabetes: pathogenesis and prevention. *Cmaj*. 2006 Jul 18;175(2):165-70.

**Gougeon PY, Lourens S, Han TY, Nair DG, Ropeleski MJ, Blennerhassett MG.** The pro-inflammatory cytokines IL-1 $\beta$  and TNF $\alpha$  are neurotrophic for enteric neurons. *Journal of Neuroscience*. 2013 Feb 20;33(8):3339-51.

**Grider JR.** CGRP as a transmitter in the sensory pathway mediating peristaltic reflex. *American Journal of Physiology-Gastrointestinal and Liver Physiology.* 1994 Jun 1;266(6):G1139-45.

**Gross O, Thomas CJ, Guarda G, Tschopp J.** The inflammasome: an integrated view. *Immunological reviews.* 2011 Sep;243(1):136-51.

**Gruber HE, Hoelscher GL, Bethea S, Hanley Jr EN.** Interleukin 1-beta upregulates brain-derived neurotrophic factor, neurotrophin 3 and neuropilin 2 gene expression and NGF production in annulus cells. *Biotechnic & Histochemistry.* 2012 Nov 1;87(8):506-11.

**Gruber HE, Jones B, Marrero E, Hanley Jr EN.** Proinflammatory cytokines IL-1 $\beta$  and TNF- $\alpha$  influence human annulus cell signaling cues for neurite growth: In vitro Coculture studies. *Spine.* 2017 Oct 15;42(20):1529-37.

**Gui WS, Wei X, Mai CL, Murugan M, Wu LJ, Xin WJ, Zhou LJ, Liu XG.** Interleukin-1 $\beta$  overproduction is a common cause for neuropathic pain, memory deficit, and depression following peripheral nerve injury in rodents. *Molecular pain.* 2016 May 3;12:1744806916646784.

**Guo W, Wang H, Watanabe M, Shimizu K, Zou S, LaGraize SC, Wei F, Dubner R, Ren K.** Glial-cytokine-neuronal interactions underlying the mechanisms of persistent pain. *Journal of Neuroscience.* 2007 May 30;27(22):6006-18.

**Gurung P, Kanneganti TD.** Novel roles for caspase-8 in IL-1 $\beta$  and inflammasome regulation. *The American journal of pathology.* 2015 Jan 1;185(1):17-25.

**Hansen MB.** The enteric nervous system I: organisation and classification. *Pharmacology & toxicology.* 2003 Mar;92(3):105-13.

**Harreiter J, Roden M.** Diabetes mellitus—Definition, classification, diagnosis, screening and prevention (Update 2019). *Wiener Klinische Wochenschrift.* 2019 May;131:6-15.

**He Y, Hara H, Núñez G.** Mechanism and regulation of NLRP3 inflammasome activation. *Trends in biochemical sciences.* 2016 Dec 1;41(12):1012-21.

**Hecker A, Küllmar M, Wilker S, Richter K, Zakrzewicz A, Atanasova S, Mathes V, Timm T, Lerner S, Klein J, Kaufmann A.** Phosphocholine-modified macromolecules and

canonical nicotinic agonists inhibit ATP-induced IL-1 $\beta$  release. *The Journal of Immunology*. 2015 Sep 1;195(5):2325-34.

**Hernandez-Cuellar** E, Tsuchiya K, Hara H, Fang R, Sakai S, Kawamura I, Akira S, Mitsuyama M. Cutting edge: nitric oxide inhibits the NLRP3 inflammasome. *The Journal of Immunology*. 2012 Dec 1;189(11):5113-7.

**Hibberd** TJ, Yew WP, Dodds KN, Xie Z, Travis L, Brookes SJ, Costa M, Hu H, Spencer NJ. Quantification of CGRP-immunoreactive myenteric neurons in mouse colon. *Journal of Comparative Neurology*. 2022 Dec;530(18):3209-25.

**Hirota** SA, Ng J, Lueng A, Khajah M, Parhar K, Li Y, Lam V, Potentier MS, Ng K, Bawa M, McCafferty DM. NLRP3 inflammasome plays a key role in the regulation of intestinal homeostasis. *Inflammatory bowel diseases*. 2011 Jun 1;17(6):1359-72.

**Honma** K, Machida C, Mochizuki K, Goda T. Glucose and TNF enhance expression of TNF and IL1B, and histone H3 acetylation and K4/K36 methylation, in juvenile macrophage cells. *Gene*. 2020 Dec 1;763:100034.

**Horton** WB, Barrett EJ. Microvascular dysfunction in diabetes mellitus and cardiometabolic disease. *Endocrine reviews*. 2021 Feb 1;42(1):29-55.

**Hou** L, Li W, Wang X. Mechanism of interleukin-1 $\beta$ -induced calcitonin gene-related peptide production from dorsal root ganglion neurons of neonatal rats. *Journal of neuroscience research*. 2003 Jul 15;73(2):188-97.

**Hu** C, Ding H, Li Y, Pearson JA, Zhang X, Flavell RA, Wong FS, Wen L. NLRP3 deficiency protects from type 1 diabetes through the regulation of chemotaxis into the pancreatic islets. *Proceedings of the National Academy of Sciences*. 2015 Sep 8;112(36):11318-23.

**Hyland** NP, Cryan JF. Microbe-host interactions: Influence of the gut microbiota on the enteric nervous system. *Developmental biology*. 2016 Sep 15;417(2):182-7.

**Izbéki** F, Wittman T, Rosztóczy A, Linke N, Bódi N, Fekete É, Bagyánszki M. Immediate insulin treatment prevents gut motility alterations and loss of nitrergic neurons in the ileum and colon of rats with streptozotocin-induced diabetes. *Diabetes Research and Clinical Practice*. 2008 May 1;80(2):192-8.

**Jancsó Z**, Bódi N, Borsos B, Fekete É, Hermes E. Gut region-specific accumulation of reactive oxygen species leads to regionally distinct activation of antioxidant and apoptotic marker molecules in rats with STZ-induced diabetes. *The International Journal of Biochemistry & Cell Biology*. 2015 May 1;62:125-31.

**Jiang D**, Chen S, Sun R, Zhang X, Wang D. The NLRP3 inflammasome: role in metabolic disorders and regulation by metabolic pathways. *Cancer letters*. 2018 Apr 10;419:8-19.

**Kaminsky LW**, Al-Sadi R, Ma TY. IL-1 $\beta$  and the intestinal epithelial tight junction barrier. *Frontiers in immunology*. 2021 Oct 25;12:767456.

**Kaneko N**, Kurata M, Yamamoto T, Morikawa S, Masumoto J. The role of interleukin-1 in general pathology. *Inflammation and regeneration*. 2019 Dec;39:1-6.

**Kang TB**, Yang SH, Toth B, Kovalenko A, Wallach D. Caspase-8 blocks kinase RIPK3-mediated activation of the NLRP3 inflammasome. *Immunity*. 2013 Jan 24;38(1):27-40.

**Katakami N**. Mechanism of development of atherosclerosis and cardiovascular disease in diabetes mellitus. *Journal of atherosclerosis and thrombosis*. 2018 Jan 1;25(1):27-39.

**Ke P**, Shao BZ, Xu ZQ, Chen XW, Wei W, Liu C. Activating  $\alpha 7$  nicotinic acetylcholine receptor inhibits NLRP 3 inflammasome through regulation of  $\beta$ -arrestin-1. *CNS Neuroscience & Therapeutics*. 2017 Nov;23(11):875-84.

**Khaloo P**, Qahremani R, Rabizadeh S, Omid M, Rajab A, Heidari F, Farahmand G, Bitaraf M, Mirmiranpour H, Esteghamati A, Nakhjavani M. Nitric oxide and TNF- $\alpha$  are correlates of diabetic retinopathy independent of hs-CRP and HbA1c. *Endocrine*. 2020 Sep;69:536-41.

**Khan I**, Al-Awadi FM. Colonic muscle enhances the production of interleukin-1 beta messenger RNA in experimental colitis. *Gut*. 1997 Mar 1;40(3):307-12.

**Khan I**, Blennerhassett MG, Kataeva GV, Collins SM. Interleukin 1 $\beta$  induces the expression of interleukin 6 in rat intestinal smooth muscle cells. *Gastroenterology*. 1995 Jun 1;108(6):1720-8.

**Kim MJ, Ryu GR, Kang JH, Sim SS, Rhie DJ, Yoon SH, Hahn SJ, Jeong IK, Hong KJ, Kim MS, Jo YH.** Inhibitory effects of epicatechin on interleukin-1 $\beta$ -induced inducible nitric oxide synthase expression in RINm5F cells and rat pancreatic islets by down-regulation of NF- $\kappa$ B activation. *Biochemical pharmacology*. 2004 Nov 1;68(9):1775-85.

**Kinekawa F, Kubo F, Matsuda K, Fujita Y, Tomita T, Uchida Y, Nishioka M.** Relationship between esophageal dysfunction and neuropathy in diabetic patients. *Official journal of the American College of Gastroenterology| ACG*. 2001 Jul 1;96(7):2026-32.

**Knauf C, Abot A, Wemelle E, Cani PD.** Targeting the enteric nervous system to treat metabolic disorders? "Enterosynes" as therapeutic gut factors. *Neuroendocrinology*. 2020 Jan 8;110(1-2):139-46.

**Koepsell H.** Glucose transporters in the small intestine in health and disease. *Pflügers Archiv-European Journal of Physiology*. 2020 Sep;472(9):1207-48.

**Kulkarni S, Saha M, Slosberg J, Singh A, Nagaraj S, Becker L, Zhang C, Bukowski A, Wang Z, Liu G, Leser JM.** Age-associated changes in lineage composition of the enteric nervous system regulate gut health and disease. *Elife*. 2023 Dec 18;12:RP88051.

**Langley JN.** *The autonomic nervous system*. W. Heffer & Sons Limited; 1921.

**Latz E.** The inflammasomes: mechanisms of activation and function. *Current opinion in immunology*. 2010 Feb 1;22(1):28-33.

**Lima TS.** Beyond an inflammatory mediator: Interleukin-1 in neurophysiology. *Experimental Physiology*. 2023 Jul;108(7):917-24.

**Lincoln J, Bokor JT, Crowe R, Griffith SG, Haven AJ, Burnstock G.** Myenteric plexus in streptozotocin-treated rats: neurochemical and histochemical evidence for diabetic neuropathy in the gut. *Gastroenterology*. 1984 Apr 1;86(4):654-61.

**Liu B, Yu J.** Anti-NLRP3 inflammasome natural compounds: an update. *Biomedicines*. 2021 Feb 1;9(2):136.

**Liu H, Xu R, Kong Q, Liu J, Yu Z, Zhao C.** Downregulated NLRP3 and NLRP1 inflammasomes signaling pathways in the development and progression of type 1 diabetes mellitus. *Biomedicine & Pharmacotherapy*. 2017 Oct 1;94:619-26.

**Liu** MT, Seino S, Kirchgessner AL. Identification and characterization of glucoresponsive neurons in the enteric nervous system. *Journal of Neuroscience*. 1999 Dec 1;19(23):10305-17.

**Lopez-Castejon** G, Brough D. Understanding the mechanism of IL-1 $\beta$  secretion. *Cytokine & growth factor reviews*. 2011 Aug 1;22(4):189-95.

**Luo** P, Liu D, Li C, He WX, Zhang CL, Chang MJ. Enteric glial cell activation protects enteric neurons from damage due to diabetes in part via the promotion of neurotrophic factor release. *Neurogastroenterology & Motility*. 2018 Oct;30(10):e13368.

**Luo** YP, Jiang L, Kang K, Fei DS, Meng XL, Nan CC, Pan SH, Zhao MR, Zhao MY. Hemin inhibits NLRP3 inflammasome activation in sepsis-induced acute lung injury, involving heme oxygenase-1. *International immunopharmacology*. 2014 May 1;20(1):24-32.

**MacEwan** DJ. TNF ligands and receptors—a matter of life and death. *British journal of pharmacology*. 2002 Feb;135(4):855.

**MacEwan** DJ. TNF receptor subtype signalling: differences and cellular consequences. *Cellular signalling*. 2002 Jun 1;14(6):477-92.

**Madrigal** JL, Hurtado O, Moro MA, Lizasoain I, Lorenzo P, Castrillo A, Boscá L, Leza JC. The increase in TNF- $\alpha$  levels is implicated in NF- $\kappa$ B activation and inducible nitric oxide synthase expression in brain cortex after immobilization stress. *Neuropsychopharmacology*. 2002 Feb 1;26(2):155-63.

**Maedler** K, Sergeev P, Ris F, Oberholzer J, Joller-Jemelka HI, Spinas GA, Kaiser N, Halban PA, Donath MY. Glucose-induced  $\beta$  cell production of IL-1 $\beta$  contributes to glucotoxicity in human pancreatic islets. *The Journal of clinical investigation*. 2002 Sep 15;110(6):851-60.

**Maleki** D, Camilleri M, Zinsmeister AR, Rizza RA. Effect of acute hyperglycemia on colorectal motor and sensory function in humans. *American Journal of Physiology-Gastrointestinal and Liver Physiology*. 1997 Oct 1;273(4):G859-64.

**Malik** A, Morya RK, Bhadada SK, Rana S. Type 1 diabetes mellitus: Complex interplay of oxidative stress, cytokines, gastrointestinal motility and small intestinal bacterial overgrowth. *European journal of clinical investigation*. 2018 Nov;48(11):e13021.

**Man SM, Kanneganti TD.** Regulation of inflammasome activation. *Immunological reviews*. 2015 May;265(1):6-21.

**Mandrup-Poulsen T, Pickersgill L, Donath MY.** Blockade of interleukin 1 in type 1 diabetes mellitus. *Nature Reviews Endocrinology*. 2010 Mar;6(3):158-66.

**Mann ER, Bernardo D, English NR, Landy J, Al-Hassi HO, Peake ST, Man R, Elliott TR, Spranger H, Lee GH, Parian A.** Compartment-specific immunity in the human gut: properties and functions of dendritic cells in the colon versus the ileum. *Gut*. 2016 Feb 1;65(2):256-70.

**Maritim AC, Sanders A, Watkins Iii JB.** Diabetes, oxidative stress, and antioxidants: a review. *Journal of biochemical and molecular toxicology*. 2003;17(1):24-38.

**Martinon F, Burns K, Tschopp J.** The inflammasome: a molecular platform triggering activation of inflammatory caspases and processing of proIL- $\beta$ . *Molecular cell*. 2002 Aug 1;10(2):417-26.

**McDaniel ML, Kwon G, Hill JR, Marshall CA, Corbett JA.** Cytokines and nitric oxide in islet inflammation and diabetes. *Proceedings of the Society for Experimental Biology and Medicine*. 1996 Jan;211(1):24-32.

**McEntee CP, Finlay CM, Lavelle EC.** Divergent roles for the IL-1 family in gastrointestinal homeostasis and inflammation. *Frontiers in immunology*. 2019 Jun 7;10:453720.

**McVey Neufeld KA, Perez-Burgos A, Mao YK, Bienenstock J, Kunze WA.** The gut microbiome restores intrinsic and extrinsic nerve function in germ-free mice accompanied by changes in calbindin. *Neurogastroenterology & Motility*. 2015 May;27(5):627-36.

**Means TK, Pavlovich RP, Roca D, Vermeulen MW, Fenton MJ.** Activation of TNF- $\alpha$  transcription utilizes distinct MAP kinase pathways in different macrophage populations. *Journal of leukocyte biology*. 2000 Jun;67(6):885-93.

**Mezei D, Bódi N, Szalai Z, Márton Z, Balázs J, Bagyánszki M.** Immediate Insulin Treatment Prevents Diabetes-Induced Gut Region-Specific Increase in the Number of Myenteric Serotonergic Neurons. *Applied Sciences*. 2021 Jun 26;11(13):5949.

**Michel K**, Kuch B, Dengler S, Demir IE, Zeller F, Schemann M. How big is the little brain in the gut? Neuronal numbers in the enteric nervous system of mice, Guinea pig, and human. *Neurogastroenterology & Motility*. 2022 Dec;34(12):e14440.

**Migliorini P**, Italiani P, Pratesi F, Puxeddu I, Boraschi D. The IL-1 family cytokines and receptors in autoimmune diseases. *Autoimmunity reviews*. 2020 Sep 1;19(9):102617.

**Miller SM**, Narasimhan RA, Schmalz PF, Soffer EE, Walsh RM, Krishnamurthi V, Pasricha PJ, Szurszewski JH, Farrugia G. Distribution of interstitial cells of Cajal and nitrergic neurons in normal and diabetic human appendix. *Neurogastroenterology & Motility*. 2008 Apr;20(4):349-57.

**Mitsui R**. Characterisation of calcitonin gene-related peptide-immunoreactive neurons in the myenteric plexus of rat colon. *Cell and tissue research*. 2009 Jul;337:37-43.

**Mitsui R**. Immunohistochemical characteristics of submucosal Dogiel type II neurons in rat colon. *Cell and tissue research*. 2010 May;340:257-65.

**Neeb L**, Hellen P, Boehnke C, Hoffmann J, Schuh-Hofer S, Dirnagl U, Reuter U. IL-1 $\beta$  stimulates COX-2 dependent PGE2 synthesis and CGRP release in rat trigeminal ganglia cells. *PloS one*. 2011 Mar 4;6(3):e17360.

**Nishida T**, Tsuji S, Tsujii M, Arimitsu S, Sato T, Haruna Y, Miyamoto T, Kanda T, Kawano S, Hori M. Gastroesophageal reflux disease related to diabetes: analysis of 241 cases with type 2 diabetes mellitus. *Journal of gastroenterology and hepatology*. 2004 Mar;19(3):258-65.

**Nolan CJ**. Controversies in gestational diabetes. *Best practice & research clinical obstetrics & gynaecology*. 2011 Feb 1;25(1):37-49.

**Pan H**, Jian Y, Wang F, Yu S, Guo J, Kan J, Guo W. NLRP3 and gut microbiota homeostasis: progress in research. *Cells*. 2022 Nov 24;11(23):3758.

**Park SY**, Kang MJ, Han JS. Interleukin-1 beta promotes neuronal differentiation through the Wnt5a/RhoA/JNK pathway in cortical neural precursor cells. *Molecular brain*. 2018 Dec;11:1-2.

**Pellegrini C**, Fornai M, Benvenuti L, Colucci R, Caputi V, Palazon-Riquelme P, Giron MC, Nericcio A, Garelli F, D'Antongiovanni V, Segnani C. NLRP3 at the crossroads between immune/inflammatory responses and enteric neuroplastic remodelling in a

mouse model of diet-induced obesity. *British Journal of Pharmacology*. 2021 Oct;178(19):3924-42.

**Peltier A**, Goutman SA, Callaghan BC. Painful diabetic neuropathy. *Bmj*. 2014 May 6;348.

**Peraldi P**, Spiegelman B. TNF- $\alpha$  and insulin resistance: summary and future prospects. *Molecular and cellular biochemistry*. 1998 May;182:169-75.

**Pereira CA**, Carlos D, Ferreira NS, Silva JF, Zanotto CZ, Zamboni DS, Garcia VD, Ventura DF, Silva JS, Tostes RC. Mitochondrial DNA promotes NLRP3 inflammasome activation and contributes to endothelial dysfunction and inflammation in type 1 diabetes. *Frontiers in Physiology*. 2020 Jan 17;10:1557.

**Pirot P**, Cardozo AK, Eizirik DL. Mediators and mechanisms of pancreatic beta-cell death in type 1 diabetes. *Arquivos Brasileiros de Endocrinologia & Metabologia*. 2008;52:156-65.

**Pontillo A**, Brandao L, Guimaraes R, Segat L, Araujo J, Crovella S. Two SNPs in NLRP3 gene are involved in the predisposition to type-1 diabetes and celiac disease in a pediatric population from northeast Brazil. *Autoimmunity*. 2010 Dec 1;43(8):583-9.

**Price AE**, Shamardani K, Lugo KA, Deguine J, Roberts AW, Lee BL, Barton GM. A map of toll-like receptor expression in the intestinal epithelium reveals distinct spatial, cell type-specific, and temporal patterns. *Immunity*. 2018 Sep 18;49(3):560-75.

**Qiao YC**, Chen YL, Pan YH, Tian F, Xu Y, Zhang XX, Zhao HL. The change of serum tumor necrosis factor alpha in patients with type 1 diabetes mellitus: A systematic review and meta-analysis. *PloS one*. 2017 Apr 20;12(4):e0176157.

**Rawat M**, Nighot M, Al-Sadi R, Gupta Y, Viszwapriya D, Yochum G, Koltun W, Ma TY. IL1B increases intestinal tight junction permeability by up-regulation of MIR200C-3p, which degrades occludin mRNA. *Gastroenterology*. 2020 Oct 1;159(4):1375-89.

**Ren K**, Dubner R. Neuron–glia crosstalk gets serious: role in pain hypersensitivity. *Current Opinion in Anesthesiology*. 2008 Oct 1;21(5):570-9.

**Ren K**, Torres R. Role of interleukin-1 $\beta$  during pain and inflammation. *Brain research reviews*. 2009 Apr 1;60(1):57-64.

**Rühl** A, Nasser Y, Sharkey KA. Enteric glia. *Neurogastroenterology & Motility*. 2004 Apr;16:44-9.

**Russell** FA, King R, Smillie SJ, Kodji X, Brain SD. Calcitonin gene-related peptide: physiology and pathophysiology. *Physiological reviews*. 2014 Oct;94(4):1099-142.

**Sansom** M, Roelofs JM, Akkermans LM, Henegouwen GV, Smout AJ. Proximal gastric motor activity in response to a liquid meal in type I diabetes mellitus with autonomic neuropathy. *Digestive diseases and sciences*. 1998 Mar;43:491-6.

**Sanders** LM, Henderson CE, Hong MY, Barhoumi R, Burghardt RC, Carroll RJ, Turner ND, Chapkin RS, Lupton JR. Pro-oxidant environment of the colon compared to the small intestine may contribute to greater cancer susceptibility. *Cancer letters*. 2004 May 28;208(2):155-61.

**Sandireddy** R, Yerra VG, Areti A, Komirishetty P, Kumar A. Neuroinflammation and oxidative stress in diabetic neuropathy: futuristic strategies based on these targets. *International journal of endocrinology*. 2014 Oct;2014.

**Sayegh** AI, Ritter RC. Morphology and distribution of nitric oxide synthase-, neurokinin-1 receptor-, calretinin-, calbindin-, and neurofilament-M-immunoreactive neurons in the myenteric and submucosal plexuses of the rat small intestine. *The Anatomical Record Part A: Discoveries in Molecular, Cellular, and Evolutionary Biology: An Official Publication of the American Association of Anatomists*. 2003 Mar;271(1):209-16.

**Schäfers** M, Sorkin L. Effect of cytokines on neuronal excitability. *Neuroscience letters*. 2008 Jun 6;437(3):188-93.

**Shen** H, Guan Q, Zhang X, Yuan C, Tan Z, Zhai L, Hao Y, Gu Y, Han C. New mechanism of neuroinflammation in Alzheimer's disease: the activation of NLRP3 inflammasome mediated by gut microbiota. *Progress in Neuro-Psychopharmacology and Biological Psychiatry*. 2020 Jun 8;100:109884.

**Shotton** HR, Broadbent S, Lincoln J. Prevention and partial reversal of diabetes-induced changes in enteric nerves of the rat ileum by combined treatment with  $\alpha$ -lipoic acid and evening primrose oil. *Autonomic Neuroscience*. 2004 Mar 31;111(1):57-65.

**Spencer** NJ, Smith TK. Mechanosensory S-neurons rather than AH-neurons appear to generate a rhythmic motor pattern in guinea-pig distal colon. *The Journal of physiology*. 2004 Jul;558(2):577-96.

**Spitngeus** A, Suhr O, EI-Salhy M. Diabetic state affects the innervation of gut in an animal model of human type 1 diabetes. *Histol Histopathol*. 2000;15:739-44.

**Stemkowski** PL, Bukhanova-Schulz N, Baldwin T, de Chaves EP, Smith PA. Are sensory neurons exquisitely sensitive to interleukin 1 $\beta$ ?. *Journal of Neuroimmunology*. 2021 May 15;354:577529.

**Takahashi** T. Pathophysiological significance of neuronal nitric oxide synthase in the gastrointestinal tract. *Journal of gastroenterology*. 2003 May;38:421-30.

**Taylor** SL, Renshaw BR, Garka KE, Smith DE, Sims JE. Genomic organization of the interleukin-1 locus. *Genomics*. 2002 May 1;79(5):726-33.

**Thaiss** CA, Levy M, Grosheva I, Zheng D, Soffer E, Blacher E, Braverman S, Tengeler AC, Barak O, Elazar M, Ben-Zeev R. Hyperglycemia drives intestinal barrier dysfunction and risk for enteric infection. *Science*. 2018 Mar 23;359(6382):1376-83.

**Timmermans** JP, Barbiers M, Scheuermann DW, Bogers JJ, Adriaensen D, Fekete E, Mayer B, Van Marck EA, De Groodt-Lasseel MH. Nitric oxide synthase immunoreactivity in the enteric nervous system of the developing human digestive tract. *Cell and tissue research*. 1994 Feb;275:235-45.

**Tjwa** ET, Bradley JM, Keenan CM, Kroese AB, Sharkey KA. Interleukin-1 $\beta$  activates specific populations of enteric neurons and enteric glia in the guinea pig ileum and colon. *American Journal of Physiology-Gastrointestinal and Liver Physiology*. 2003 Dec;285(6):G1268-76.

**Tomas** J, Langella P, Cherbuy C. The intestinal microbiota in the rat model: major breakthroughs from new technologies. *Animal health research reviews*. 2012 Jun;13(1):54-63.

**Van Opdenbosch** N, Van Gorp H, Verdonckt M, Saavedra PH, de Vasconcelos NM, Goncalves A, Walle LV, Demon D, Matusiak M, Van Hauwermeiren F, D'Hont J. Caspase-1 engagement and TLR-induced c-FLIP expression suppress ASC/caspase-8-dependent apoptosis by inflammasome sensors NLRP1b and NLRC4. *Cell reports*. 2017 Dec 19;21(12):3427-44.

**Vijayaraj** SL, Feltham R, Rashidi M, Frank D, Liu Z, Simpson DS, Ebert G, Vince A, Herold MJ, Kueh A, Pearson JS. The ubiquitylation of IL-1 $\beta$  limits its cleavage by caspase-1 and targets it for proteasomal degradation. *Nature Communications*. 2021 May 11;12(1):2713.

**Wagatsuma** K, Nakase H. Contradictory effects of NLRP3 inflammasome regulatory mechanisms in colitis. *International Journal of Molecular Sciences*. 2020 Oct 30;21(21):8145.

**Wang** B, Zhuang X, Deng ZB, Jiang H, Mu J, Wang Q, Xiang X, Guo H, Zhang L, Dryden G, Yan J. Targeted drug delivery to intestinal macrophages by bioactive nanovesicles released from grapefruit. *Molecular Therapy*. 2014 Mar 1;22(3):522-34.

**Weber** A, Wasiliew P, Kracht M. Interleukin-1 (IL-1) pathway. *Science signaling*. 2010 Jan 19;3(105):cm1-.

**Wirth** R, Bódi N, Maróti G, Bagyánszki M, Talapka P, Fekete É, Bagi Z, Kovács KL. Regionally distinct alterations in the composition of the gut microbiota in rats with streptozotocin-induced diabetes. *PLoS One*. 2014 Dec 3;9(12):e110440.

**Wirth** R, Bódi N, Szalai Z, Chandrakumar L, Maróti G, Mezei D. Perturbation of the mucosa-associated anaerobic gut microbiota in streptozotocin-induced diabetic rats. *Acta Biologica Szegediensis*. 2021;65(1):75-84.

**Wood** JD. Application of classification schemes to the enteric nervous system. *Journal of the autonomic nervous system*. 1994 Jun 1;48(1):17-29.

**Wu** W, Feng B, Liu J, Li Y, Liao Y, Wang S, Tao S, Hu S, He W, Shu Q, Liu Z. The CGRP/macrophage axis signal facilitates inflammation recovery in the intestine. *Clinical Immunology*. 2022 Dec 1;245:109154.

**Yan** Y, Ramanan D, Rozenberg M, McGovern K, Rastelli D, Vijaykumar B, Yaghi O, Voisin T, Mosaheb M, Chiu I, Itzkovitz S. Interleukin-6 produced by enteric neurons regulates the number and phenotype of microbe-responsive regulatory T cells in the gut. *Immunity*. 2021 Mar 9;54(3):499-513.

**Yarandi** SS, Srinivasan S. Diabetic gastrointestinal motility disorders and the role of enteric nervous system: current status and future directions. *Neurogastroenterology & Motility*. 2014 May;26(5):611-24.

**Ye L, Huang Y, Zhao L, Li Y, Sun L, Zhou Y, Qian G, Zheng JC.** IL-1 $\beta$  and TNF- $\alpha$  induce neurotoxicity through glutamate production: a potential role for neuronal glutaminase. *Journal of neurochemistry*. 2013 Jun;125(6):897-908.

**Zoetendal EG, Collier CT, Koike S, Mackie RI, Gaskins HR.** Molecular ecological analysis of the gastrointestinal microbiota: a review. *The Journal of nutrition*. 2004 Feb 1;134(2):465-72.

## 9. SUMMARY

The gastrointestinal tract is innervated with an intrinsic neuronal network called the enteric nervous system. This neuronal network encompasses two main ganglionated plexuses: myenteric and submucous plexus in which sensory, motor, and interneurons regulate many gastrointestinal functions including peristalsis, secretion, absorption, and immune modulation. Metabolic diseases like type 1 diabetes (T1D) are associated with myenteric neuropathy resulting in gastrointestinal complications such as motility dysfunction, bloating or hyperalgesia. Our earlier findings revealed gut region-specific nitroergic neuropathy in the myenteric ganglia of a streptozotocin (STZ)-induced T1D rat model. This may be attributed to the upregulated pro-oxidative and pro-inflammatory mechanisms during long-lasting hyperglycaemia. Many of these pro-inflammatory cascades ultimately lead to the activation of the interleukin 1 $\beta$  (IL1 $\beta$ ) cytokine. IL1 $\beta$  is expressed as a pro-IL1 $\beta$  and activated by caspase-1 enzyme inside an inflammasome complex. In the gut, activated IL1 $\beta$  represents a pleiotropic cytokine that is crucial for gut homeostasis and may exert divergent effects on distinct neuronal populations within the myenteric plexus. However, excessive IL1 $\beta$  expression due to hyperglycaemia could disrupt gut homeostasis and possibly contribute to diabetes-related regional damage of neuronal nitric oxide synthase (nNOS) neurons. Additionally, IL1 $\beta$  is implicated in the signalling pathway of calcitonin gene-related peptide (CGRP), suggesting its potential effects on the subset of CGRP-expressing myenteric neurons most of which represent intrinsic primary afferent neurons. Therefore, it is plausible that IL1 $\beta$  may have potential effects on the different populations of myenteric neurons under different metabolic, neuroinflammatory, and spatial circumstances. Among others, the NOD-, LRR- and pyrin domain-containing protein 3 (NLRP3) inflammasome is extensively studied due to its involvement in autoimmune and inflammatory diseases including T1D. Furthermore, this inflammasome-forming protein was suggested to contribute to maintaining gastrointestinal tract homeostasis and microbial compositions. However, fewer studies have focused on the role of NLRP3 in myenteric neurons with discrepancies in its involvement in enteric neuropathy depending on the investigated disease. In T1D, Toll-like receptor 4 expression and immunoreactivity were changed in a gut region-specific manner in the myenteric neurons. Since it is an inducer for NLRP3 inflammasome, it is reasonable to examine the perturbation of neuronal NLRP3 inflammasome protein and investigate its possible association with diabetic IL1 $\beta$  expression.

Therefore, our main goal was to explore the effect of hyperglycaemia and insulin treatment on IL1 $\beta$  and NLRP3 expression in different myenteric neuronal populations and intestinal layers in a type 1 diabetic rat model. One week (acute) or ten weeks (chronic) after the induction of hyperglycaemia, pancreas and different gut segments were prepared from STZ-induced diabetic, insulin-treated diabetic, and control rats. Fluorescent immunohistochemistry was used to count IL1 $\beta$ -expressing neurons as well as nNOS- and CGRP-immunoreactive (IR) myenteric neurons within this group. Tissue IL1 $\beta$  level was measured by enzyme-linked immunosorbent assay in muscle/myenteric plexus-containing intestinal homogenates. NLRP3 density was measured by immunogold electron microscopy in the myenteric ganglia. IL1 $\beta$  and NLRP3 mRNA levels were detected and quantified in different intestinal wall layers (myenteric ganglia, smooth muscle, mucosa) using RNAscope multiplex fluorescent V2 assay.

In healthy rats, we observed higher baseline levels of the proportion of IL1 $\beta$ -IR myenteric neurons in the colon compared to the small intestine, likely influenced by anaerobic microbial content and higher oxidative stress mechanisms. In diabetics, the proportion of IL1 $\beta$ -IR myenteric neurons was induced by hyperglycaemia in a time-dependent and gut region-specific manner. Duodenal and ileal myenteric neurons showed an early increase in their IL1 $\beta$  immunoreactivity after acute hyperglycaemia, which was sustained during chronic hyperglycaemia. On the other hand, colonic myenteric neurons only developed an induction in IL1 $\beta$  immunoreactivity after chronic hyperglycaemia. This suggests that the colon may have defence mechanisms against short-term hyperglycaemia due to the presence of higher oxidative and pro-inflammatory processes, which could render it less sensitive to further increase in oxidative stress. Immediate insulin treatment prevented the diabetes-induced increase in the proportion of IL1 $\beta$ -IR myenteric neurons.

IL1 $\beta$  expression was specific to different myenteric neuronal subpopulations even in control animals. In diabetics, a strict regional induction of IL1 $\beta$  immunoreactivity was observed in different populations of myenteric neurons. While the proportion of IL1 $\beta$ -nNOS-IR myenteric neurons was elevated only in the colon, the proportion of IL1 $\beta$ -CGRP-IR myenteric neurons was increased in the ileum. An increase in colonic proportion of IL1 $\beta$ -nNOS-IR myenteric neurons may be associated with nitrergic neuropathy in this gut segment. Whereas the induction of IL1 $\beta$ -CGRP-IR myenteric neurons in the ileum could be associated with the previously observed pathogenic

microbial invasion in this particular gut segment. Insulin treatment did not protect against the induction of IL1 $\beta$  immunoreactivity in the nNOS neurons but normalised that in the CGRP neurons. Elevated IL1 $\beta$  levels were also confirmed in tissue homogenates of myenteric plexus and smooth muscle layers. IL1 $\beta$  mRNA levels displayed distinct spatial patterns within the different intestinal wall layers along the intestinal tract of controls. In diabetic rats, a gut segment-specific and layer-dependent increase in IL1 $\beta$  mRNA levels was revealed. While IL1 $\beta$  mRNA expression was increased in the myenteric ganglia of all gut segments, mucosal IL1 $\beta$  mRNA was induced only in the small intestine whereas muscular IL1 $\beta$  mRNA expression was elevated in the duodenum and colon. This proves that the whole enteric nervous system and its environment responds to hyperglycaemia and are sources for inflammatory cytokines like IL1 $\beta$ . Insulin treatment regionally prevented the hyperglycaemia-induced IL1 $\beta$  mRNA expression.

Evaluation of NLRP3 levels in the myenteric ganglia revealed a regional decrease in the density of NLRP3-labelling gold particles in the duodenal and colonic segments of diabetics. Moreover, NLRP3 mRNA levels were reduced specifically in the different compartments of the small intestine which was not prevented by immediate insulin treatment. Similarly, the expression of other inflammasome proteins like NLRP1, NLRP3, and NLRP6 was also decreased in the small intestine of an obesity-induced diabetic animal model. Moreover, another study demonstrated the inhibition of NLRP3 inflammasome by inducing haem oxygenase1 which has been robustly induced in the myenteric neurons of the ileum in our type 1 diabetic rat model. The intestinal wall layers including the myenteric neurons may downregulate the NLRP3 inflammasome protein as a compensatory mechanism to limit further propagation of intestinal inflammation. A downregulated NLRP1 and NLRP3 in the circulatory system was associated with poor prognosis in T1D patients. Therefore, the decrease in NLRP3 inflammasome besides others, may play a role in the disrupted intestinal barrier seen in diabetes and myenteric neuropathy. Additionally, this indicates that IL1 $\beta$  induction may occur through alternative pathways in the diabetic gut, independent of NLRP3 activation.

In conclusion, IL1 $\beta$  is a crucial cytokine expressed by cells in the intestinal tract which displays spatial and segment-specific expressional patterns in healthy rats. Hyperglycaemia causes intestinal region-specific and layer-dependent induction in this cytokine. Specific myenteric neurons react to hyperglycaemia and become a higher source for IL1 $\beta$  production. This highlights the role of IL1 $\beta$  in myenteric subpopulation-specific

neuropathy that can give rise to diabetic dysmotility. Moreover, since NLRP3 is regionally downregulated in chronic hyperglycaemia, it is assumable that hyperglycaemia-related IL1 $\beta$  induction is not mediated through the NLRP3 inflammasome protein rendering it dispensable for IL1 $\beta$  activation in the gut in T1D. Understanding alternative mechanisms involved in hyperglycaemia-induced IL1 $\beta$  activation could provide further insights into new therapeutic strategies for managing diabetic gastrointestinal myenteric neuropathy.

## 10. ÖSSZEFOGLALÁS

A gyomor-bélcsatorna összehangolt működését az enterális idegrendszer szabályozza. Az enterikus neuronok és gliasejtek két fő ganglionált plexusba tömörülnek. A myentericus és submucosus ganglionokban az érző, motoros és interneuronok lokális reflexívek révén szabályozzák a gasztrointesztinális rendszer működését, az abszorpció, szekréció és a bélperisztaltika összehangolását. Az 1-es típusú cukorbetegség gyakran szenvednek különböző gyomor-bélrendszeri tünetektől, mint a bélmotilitási zavarok, puffadás vagy hasi fájdalom, melyek hátterében az entericus neuronok sérülése áll. Korábbi munkánk során bizonyítottuk, hogy streptozotocin (STZ)-indukált diabéteszes állatokban a myentericus nitrerg neuronok bélszakasz-specifikusan sérülnek. Mindehhez a krónikus hiperglikémia következtében fokozódó oxidatív stressz és gyulladási folyamatok is hozzájárulhatnak, a különböző gyulladási kaskádok pedig az interleukin 1 $\beta$  (IL1 $\beta$ ) aktiválódását eredményezik. A sejtekben az IL1 $\beta$  előalakja egy inflammaszóma komplexben a kaspáz-1 enzim segítségével aktiválódik. Az IL1 $\beta$  egy pleiotróp citokin, amely kulcsfontosságú a bél homeosztázisának fenntartásában, s hatással lehet a különböző myentericus neuronpopulációkra is, így hozzájárulhat a nitrerg neuronok diabéteszhez köthető regionális károsodásához. Emellett az IL1 $\beta$  fontos szerepet játszik a kalcitonin gén-rokon peptid (CGRP) jelátviteli útvonalban, így hatással lehet a CGRP-t expresszáló többségükben intrinsic primer afferens neuronokra is.

A NOD-, LRR- és pirin-domén-tartalmú protein 3 (NLRP3) inflammaszóma szerepét széles körben tanulmányozzák a különböző autoimmun és gyulladási betegségekben, köztük az 1-es típusú diabéteszben is. Irodalmi adatok alapján az NLRP3 fontos a bél mikrobióta összetételének fenntartásában, s a gyomor-bélcsatorna homeosztázisában, azonban kevés tanulmány foglalkozik az NLRP3 myentericus neuronokban és a diabéteszes enterikus neuropátia kialakulásában játszott esetleges szerepével. Nemrégiben megfigyeltük, hogy 1-es típusú diabéteszes állatmodellben a Toll-like receptor 4 expressziója bélszakasz-specifikus módon változott a myentericus neuronokban. Mivel a Toll-like receptor 4 fontos az NLRP3 expresszió indukálásában, ezért úgy gondoljuk, hogy az entericus neuronok NLRP3 expresszióját is érdemes megvizsgálni.

Ezért, a doktori munkám elsődleges célja az volt, hogy feltérképezzük, milyen hatása van a hiperglikémiának és az azonnali inzulinkezelésnek az IL1 $\beta$  és az NLRP3 expressziójára a myentericus neuronok különböző populációiban és a bélfal különböző

rétegeiben 1-es típusú diabéteszes patkánymodellben. Egy héttel (akut) vagy tíz héttel (krónikus) a hiperglikémia kiváltást követően mintákat vettünk a kontroll, diabéteszes és inzulin-kezelt diabéteszes állatok különböző bélszakaszaiból és a hasnyálmirigyből. Az IL1 $\beta$ -immunreaktív (IR) myentericus neuronok, valamint az IL1 $\beta$ -IR nNOS illetve CGRP neuronok arányát fluoreszcens immunhisztokémiával követtük nyomon. Az IL1 $\beta$  szöveti kifejeződését enzimhez kötött immunszorbens teszttel határoztuk meg a bél simaizom/myentericus plexusból készült homogenizátumokban. Az NLRP3-t jelölő arany szemcsék denzitását poszt-embedding aranyjelöléses elektronmikroszkópiával a myentericus ganglionokban vizsgáltuk. Az IL1 $\beta$  és az NLRP3 mRNS kifejeződését a bélfal különböző rétegeiben (myentericus ganglionok, simaizom, nyálkahártya) RNAscope multiplex fluoreszcens V2 módszerrel térképeztük fel.

Egészséges állatokban az IL1 $\beta$ -IR myentericus neuronok aránya magasabb volt a vastagbélben, mint a vékonybélben, melyben valószínűleg a colonra jellemző oxidatív körülmények és az anaerob mikrobióta-összetétel is szerepet játszik. A diabéteszes patkányokban az IL1 $\beta$ -IR myentericus neuronok aránya a hiperglikémiás időszak hosszától függően, bélszakasz-specifikus módon növekedett. A duodenumban és az ileumban az IL1 $\beta$ -IR myentericus neuronok aránya már akut hiperglikémát követően megnövekedett, s ez a változás a krónikus hiperglikémia során is fennmaradt. Ezzel szemben a vastagbélben ezeknek a neuronoknak az aránya csak a krónikus hiperglikémiás állapot következtében indukálódott. Mindez arra utal, hogy a vastagbélben uralkodó fokozottabb oxidatív és pro-inflammatórikus folyamatok miatti alapvető mechanizmusok a rövid ideig fennálló hiperglikémiával szemben még elegendő védelmet nyújthatnak. Az azonnali inzulinkezelés sikeresen kivédte az IL1 $\beta$ -IR myentericus neuronok arányának diabéteszes növekedését.

Az IL1 $\beta$  kifejeződése a myentericus neuronok különböző populációiban változatos képet mutatott még kontroll állatokban is. A diabéteszes csoportban az IL1 $\beta$  expressziója bélszakasztól függően indukálódott a vizsgált myentericus neuronpopulációkban. Míg az IL1 $\beta$ -nNOS-IR myentericus neuronok aránya kizárólag a vastagbélben emelkedett, addig az IL1 $\beta$ -CGRP-IR myentericus neuronok aránya az ileumban fokozódott. Az IL1 $\beta$ -IR CGRP-t expresszáló főként szenzoros neuronok arányának növekedése az ileumban korábban megfigyelt patogén mikrobióta invázióval hozható összefüggésbe. Az inzulinkezelés nem védte ki az IL1 $\beta$  immunreaktivitás fokozódását a nNOS neuronokban, viszont helyreállította azt a CGRP neuronokban. Az

IL1 $\beta$  expresszió emelkedett szintjét a myentericus plexust és a bél simaizomrétegét tartalmazó szöveti homogenizátumokban is igazoltuk. Az IL1 $\beta$  mRNS kifejeződése a kontroll patkányok bélfalának különböző rétegeiben eltérő térbeli mintázatot mutatott. Diabéteszes állatokban az IL1 $\beta$  mRNS expressziója bélszakasztól és a bélfal szövettani rétegeitől függően növekedett. Míg az IL1 $\beta$  mRNS szintje minden bélszakasz myentericus ganglionjaiban megemelkedett, addig a nyálkahártya IL1 $\beta$  mRNS szintje csak a vékonybélben indukálódott, a simaizom IL1 $\beta$  mRNS expresszió pedig a duodenumban és a colonban fokozódott. Mindez bizonyítja, hogy nemcsak a bélidegrendszer, hanem az entericus neuronok környezete is reagál a hiperglikémiára, és olyan gyulladáscitokinek forrásai lehetnek, mint az IL1 $\beta$ . Az inzulinkezelés regionálisan akadályozta meg a hiperglikémia által kiváltott IL1 $\beta$  mRNS expressziós változásokat.

Az NLRP3 expressziójának vizsgálata során megállapítottuk, hogy a myentericus ganglionokban az NLRP3-t jelölő aranyzemcsék denzitása csökkent a diabéteszes csoport duodenumában és a colonban. Ezen kívül az NLRP3 mRNS szintje is jelentősen csökkent a vékonybél különböző rétegeiben, melyet az azonnali inzulinkezelés sem akadályozott meg. Ehhez hasonlóan más inflammaszóma proteinek, mint az NLRP1, NLRP3 és NLRP6 expressziója is csökkent elhízás okozta diabéteszes állatok vékonybéljében. Az NLRP3 inflammaszóma gátlásához a hemoxigenáz 1 is hozzájárul, melynek fokozott expresszióját munkacsoportunk 1-es típusú diabéteszes patkányokban korábban igazolta. Az NLRP3 inflammaszóma protein gátlása, mint kompenzációs mechanizmus, mérsékelheti a gyulladáscitokinek előrehaladását. Mindamelllett az NLRP3 expresszió csökkenése szerepet játszhat a bél barrier diabéteszhez köthető károsodásában is. NLRP3 eredményeink arra engednek következtetni, hogy a myentericus ganglionokban és a bélfal más rétegeiben is megfigyelt diabéteszes IL1 $\beta$  indukció nem az NLRP3 inflammaszóma protein közvetítésével, hanem más, alternatív útvonalakon keresztül mehet végbe, melyek további vizsgálatokat igényelnek.

Eredményeinket összefoglalva, megfigyeltük, hogy az IL1 $\beta$  kifejeződése bélszakasztól és a bélfal szövettani rétegeitől függő eltéréseket mutatott a kontroll állatokban. Hiperglikémia hatására az IL1 $\beta$  expressziója minden bélszakaszban és rétegben indukálódott. Bizonyítottuk azt is, hogy az IL1 $\beta$  expresszió fokozódása a myentericus neuronok egyes szubpopulációit különbözően érinti, s ezek is bélszakaszspecifikusan reagálnak a krónikus hiperglikémiára. Ez is azt hangsúlyozza, hogy az IL1 $\beta$ -

nak fontos szerepe lehet a myentericus neuronok populáció-specifikus diabéteszes károsodásában, mely hozzájárul a különböző bélmotilitási zavarok kialakulásához.

## 11. LIST OF PUBLICATIONS

MTMT number: 10074158

Publications related to the thesis:

1. **AL Doghmi A**, Barta BP, Egyed-Kolumbán A, Onhausz B, Kiss S, Balázs J, Szalai Z, Bagyánszki M, Bódi N. Gut Region-Specific Interleukin 1 $\beta$  Induction in Different Myenteric Neuronal Subpopulations of Type 1 Diabetic Rats. *Int J Mol Sci.* 2023 Mar 18;24(6):5804. doi: 10.3390/ijms24065804. IF: 5.6
2. Bódi N, Chandrakumar L, **AL Doghmi A**, Mezei D, Szalai Z, Barta BP, Balázs J, Bagyánszki M. Intestinal Region-Specific and Layer-Dependent Induction of TNF $\alpha$  in Rats with Streptozotocin-Induced Diabetes and after Insulin Replacement. *Cells.* 2021 Sep 13;10(9):2410. doi: 10.3390/cells10092410. IF: 7.43

Other publications:

1. Barta BP, Onhausz B, **AL Doghmi A**, Szalai Z, Balázs J, Bagyánszki M, Bódi N. Gut region-specific TNFR expression: TNFR2 is more affected than TNFR1 in duodenal myenteric ganglia of diabetic rats. *World J Diabetes.* 2023 Jan 15;14(1):48-61. doi: 10.4239/wjd.v14.i1.48. IF: 4.1
2. Bódi N, Egyed-Kolumbán A, Onhausz B, Barta BP, **AL Doghmi A**, Balázs J, Szalai Z, Bagyánszki M. Intestinal Region-Dependent Alterations of Toll-Like Receptor 4 Expression in Myenteric Neurons of Type 1 Diabetic Rats. *Biomedicines.* 2023 Jan 4;11(1):129. doi: 10.3390/biomedicines11010129. IF: 4.7

Cumulative impact factor: 21.83

## CONFERENCES

Conferences related to the thesis:

1. Bódi N, Barta BP, **AL Doghmi A**, Onhausz B, Chandrakumar L, Mezei D, Szalai Z, Balázs J, Bagyánszki M. Intestinal region- and layer-dependent TNF $\alpha$  induction and TNF receptor expression may contribute to myenteric neuroprotection of duodenum in type 1 diabetic rats. 46th FEBS congress, Lisbon, July 9-14, 2022.
2. **AL Doghmi A**, Barta BP, Egyed-Kolumbán A, Onhausz B, Kiss S, Szalai Z, Balázs J, Bagyánszki M, Bódi N. Intestinal segment-specific alterations of interleukin-1 $\beta$  expression in the myenteric neurons of streptozotocin-induced diabetic rats. 30th UEG Week, Vienna, Austria, Oct 9-11, 2022.
3. Bagyánszki M, **AL Doghmi A**, Barta BP, Egyed-Kolumbán A, Onhausz B, Kiss S, Balázs J, Szalai Z, Bódi N. Interleukin 1 $\beta$  expresszió bélszakasz-specifikus indukciója különböző myentericus neuronpopulációkban 1-es típusú diabéteszes patkánymodellben Central European Journal Of Gastroenterology And Hepatology/ Gasztroenterológiai És Hepatológiai Szemle, Siofok, Hungary, June 1-6, 2023.

Other Conferences

1. Bagyánszki M, Barta BP, Onhausz B, **AL Doghmi A**, Balázs J, Szalai Z, Bódi N. Region-dependent alterations of toll-like receptor 4 expression in myenteric neurons of type 1 diabetic rats. 3rd International Conference on Cell and Experimental Biology, (Hybrid), April 18-20, 2022.
2. Barta BP, Onhausz B, **AL Doghmi A**, Egyed-Kolumbán A, Kiss S, Szalai Z, Balázs J, Bagyánszki M, Bódi N. Gut region-specific expression of nuclear factor kappa B p65 in the myenteric ganglia and its microenvironment of streptozotocin-induced diabetic rats. The First International Conference on Antioxidants: Sources, Methods, Health Benefits and Industrial Applications, Barcelona, Spain, May 10-12, 2023.
3. Onhausz B, Barta BP, Egyed-Kolumbán A, **AL Doghmi A**, Szalai Z, Bódi N, Bagyánszki M. Regionally distinct alterations in the proportion of enteric glial cells in myenteric and submucous ganglia of type 1 diabetic rats. The 23rd FEBS Young Scientists' Forum, Pavia, Italy, June 26-29, 2024.